Jabbarzadeh Khoei, Ahmad
M.E.S. 1993

The University of Sydney

## Copyright in relation to this thesis*

Under the Copyright Act 1968 (several provisions of which are referred to below), this thesis must be used only under the normal conditions of scholarly fair dealing for the purposes of research, criticism or review. In particular no results or conclusions should be extracted from it, nor should it be copied or closely paraphrased in whole or in part without the written consent of the author. Proper written acknowledgement should be made for any assistance obtained from this thesis.

Under Section 35(2) of the Copyright Act 1968 'the author of a literary, dramatic, musical or artistic work is the owner of any copyright subsisting in the work'. By virtue of Section 32(1) copyright 'subsists in an original literary, dramatic, musical or artistic work that is unpublished' and of which the author was an Australian citizen, an Australian protected person or a person resident in Australia.

The Act, by Section 36(1) provides: 'Subject to this Act, the copyright in a literary, dramatic, musical or artistic work is infringed by a person who, not being the owner of the copyright and without the licence of the owner of the copyright, does in Australia, or authorises the doing in Australia of, any act comprised in the copyright'.

Section 31(1)(a)(i) provides that copyright includes the exclusive right to 'reproduce the work in a material form'. Thus, copyright is infringed by a person who, not being the owner of the copyright and without the licence of the owner of the copyright, reproduces or authorises the reproduction of a work, or of more than a reasonable part of the work, in a material form, unless the reproduction is a 'fair dealing' with the work 'for the purpose of research or study' as further defined in Sections 40 and 41 of the Act.

Section 51(2) provides that 'Where a manuscript, or a copy, of a thesis or other similar literary work that has not been published is kept in a library of a university or other similar institution or in an archives, the copyright in the thesis or other work is not infringed by the making of a copy of the thesis or other work by or on behalf of the officer in charge of the library or archives if the copy is supplied to a person who satisfies an authorized officer of the library or archives that he requires the copy for the purpose of research or study'.

Keith Jennings
*Registrar and Deputy Principal*

*'Thesis' includes 'treatise', 'dissertation' and other similar productions.

This thesis has been accepted for the award of the degree in the Faculty of Engineering

# THE OPTIMUM TWIST FOR WINDMILLING OPERATION OF A TETHERED ROTORCRAFT

by

AHMAD JABBARZADEH KHOEI

A THESIS SUBMITTED TO
THE UNIVERSITY OF SYDNEY
FOR PARTIAL FULFILMENT OF
MASTER OF ENGINEERING STUDIES DEGREE

DEPARTMENT OF MECHANICAL ENGINEERING

AUGUST 1993

**I wish to dedicate this thesis**
**to my parents from whom I learnt the first word,**
**and to my wife who always supports me.**

# Abstract

The concept of using a tethered flying windmill known as gyromill was introduced several years ago. This machine can produce electricity from the upper atmospheric winds.

The main objective of this thesis is to determine the optimum twist for the rotor blades in windmilling operation. The extended theory of Gessow and Crim has been employed to predict the performance of the rotor. A numerical optimisation was used with the aid of a computer program based on the above theory. The operational variables of $\mu, \theta_1, \theta_0$ and $C_Q$ have been used to examine the effect of twist over a comprehensive range of operation. The numerical results have been used to derive the optimum value of $\theta_1$.

Chapter One gives an introduction to wind energy in general and explainsin particular the concept of a tethered rotorcraft.

In Chapter Two we review the aerodynamic performance of lifting rotor. This chapter leads to a choice of Gessow and Crim extended theory. Chapter Three deals with the performance of the tethered system and introduces some windmill performance parameters.

The computer program and the input data used in the program is introduced in Chapter Four.

Chapter Five examines several optimisation criteria and discuss the relationship between the operational variables and the windmill performance parameters through the use of several charts. The optimum twist is given based on the various criteria. The dependence of optimum twist on $\mu$ is also established. This chapter concludes by recommending that the ultimate twist should be a delicate balance between the lift and output power. In this regard an average optimum twist of 7° to 8° is suggested, though, this value may change depending on the design requirements and the value of $\mu$. Also the minimum wind velocity to keep the system aloft has been determined for some values of twist.

The study also gives some suggestions for optimum operation of the craft.

# Statement of Originality

**I believe that the material presented in this thesis is original except where acknowledgment is given. It has not been submitted for the award of any degree at this or at any other University.**

# Acknowledgments

**I wish to express my highest gratitude to Associate Professor Bryan Roberts for his intelligent supervision and endless support and encouragement during the preparation of this thesis.**

**I wish also to thank my wife for her continual support.**

# *Table of Contents*


| | | |
|---|---|---|
| **Abstract** | | **iii** |
| **Statement of originality** | | **iv** |
| **Acknowledgments** | | **v** |
| **Table of contents** | | **vi** |
| **List of figures** | | **x** |
| **List of Tables** | | **xii** |
| **Nomenclature** | | **xiii** |
| **Chapter One** | **Introduction** | **1** |
| **1.1** | **Wind energy** | **2** |
| **1.2** | **Generating electricity from upper atmospheric winds.** | **3** |
| **1.3** | **Tethered wind generator or " gyromill" concept.** | **5** |
| **1.4** | **An optimisation study relating to the flying wind generator** | **9** |
| **Chapter Two** | **Aerodynamic Performance of The Flying Windmill** | **10** |
| **2.1** | **Evolution of various theories for a lifting rotor** | **11** |
| **2.2** | **A review of a rotor operating under high inflow conditions** | **12** |
| **2.2.1** | **The theory of Gessow and Myers** | **12** |
| **2.2.2** | **Blade element theory** | **14** |
| **2.2.3** | **The rotor thrust** | **17** |
| **2.2.4** | **Expressions for the flapping coefficients** | **18** |
| **2.2.5** | **Expression for the rotor torque** | **19** |

2.3 Wheatley's contribution to the theory 20
2.4 Bailey's contributions 21
2.5 The Gessow and Crim extended theory 22
2.5.1 Calculation of the thrust 23
2.5.2 Expressions for the flapping coefficients 24
2.5.3 The rotor torque 27
2.5.4 Validity and limitations of the theory 29
2.6 Effect of stall on the performance 30

2.7 Choice of an appropriate theory for the current current optimisation 32

Chapter Three Performance Analyses of the Tethered System 33

3.1 Total force from the rotor 33
3.2 The windmill performance parameters 34
3.2.1 Force equilibrium on the system 34
3.2.2 Relationship between helicopter and windmill parameters. 36
3.2.3 Windmill power coefficient 36
3.2.4 Windmill thrust and lift coefficient 37
3.2.5 Windmill torque coefficient 38
3.2.6 Operation at a constant tether angle 39
3.2.7 The optimum twist criterion 40

Chapter Four The Computer Program 42

4.1 Limitation of the theory 43
4.2 Program development 44
4.3 The program's flowchart 45
4.4 Input data used in the analyses 47
4.5 Operational range used in the program 48

**Chapter Five Optimisation Study and Results 49**

5.1 The influence of operational and design variables on windmill power coefficient 49

5.1.1 The effect of control axis angle and tip speed ratio on windmill power coefficient 50

5.1.2 Variation of $C_{PW}$ with collective pitch angle ($\theta_0$) 50

5.1.3 Influence of twist on $C_{PW}$ 54

5.2 The influence of operational variables on the windmill lift coefficient 55

5.2.1 The influence of tip speed ratio and control axis angle 58

5.2.2 The influence of twist 58

5.2.3 Optimum twist using $C_{LW}$ as the criterion 63

5.3 The effect of operational variables on the disk loading to dynamic pressure ratio 65

5.3.1 Maximum operational control axis angle 65

5.3.2 The influence of tip speed ratio on the parameter 67

5.3.3 The influence of twist on the parameter $C_{LWOP}$ 67

5.3.4 Optimum twist using $C_{LWOP}$ as criterion 71

5.3.5 The minimum wind speed 71

5.4 The influence of twist on the windmill torque coefficient 77

5.4.1 Optimum twist using $C_{QW}$ as the criterion 77

5.5 Alternative criteria in the choice of optimum twist 80

5.5.1 The optimum twist using $C_{opt1}$ as the criterion 80

5.5.2 The optimum twist using $C_{opt2}$ as the criterion 82

5.5.3 The optimum twist using $C_{opt3}$ as the criterion 85

5.6 Choice of the ultimate criterion 90

5.7 Proposal for future research 90

5.7.1 Operation at a steady wind velocity 91

5.7.2 Operation at various values of $\mu$ 91

| | | |
|---|---|---|
| **Chapter Six** | **Conclusion** | **94** |
| **6.1** | **Introduction** | **94** |
| **6.2** | **Conclusions in detail** | **95** |
| **References** | | **97** |
| **Appendix A** | | **100** |
| **Appendix B** | | **109** |
| **Appendix C** | | **116** |

# *List of Figures*


| Figure | | Page |
|---|---|---|
| 1.1 | Upper atmospheric wind power density for Australia ( after Atkinson). | 4 |
| 1.2 | The arrangements for a typical gyromill (after Roberts, Blackler and Barratt). | 7 |
| 1.3 | A gyromill in flight conditions. | 8 |
| 2.1 | Velocities at the rotor when acting under high inflow conditions. | 13 |
| 2.2 | Forces and velocities on the blade element. | 15 |
| 2.3 | Velocity distribution in the flapping plane. | 15 |
| 2.4 | Velocities in the plane normal to the control axis. | 16 |
| 3.1 | Thrust and H forces relative to the control axis and tip path plane. | 35 |
| 3.2 | The tethered system. | 35 |
| 5.1 | $C_{PW}$ Vs. control axis angle for a twist of 9°. | 51 |
| 5.2 | Maximum $C_{PW}$ for various tip speed ratios for a twist of 8°. | 52 |
| 5.3 | $C_{PW}$ Vs. collective pitch angle for a twist of 7°. | 53 |
| 5.4 | Maximum $C_{PW}$ at various tip speed ratios Vs. twist angle. | 56 |
| 5.5 | Optimum linear twist for $C_{PW}$ at various tip speed ratios. | 57 |
| 5.6 | $C_{LW}$ Vs. control axis angle for a twist of 4°. | 59 |
| 5.7 | $C_{LW}$ envelope for various tip speed ratios ($\theta_1$ = 8°). | 60 |
| 5.8 | Maximum $C_{LW}$ for various tip speed ratios ($\theta_1$ = 8°). | 61 |
| 5.9 | Maximum $C_{LW}$ for various tip speed ratios Vs. twist. | 62 |
| 5.10 | Optimum linear twist for $C_{LW}$ at various tip speed ratios. | 64 |
| 5.11.a | $C_{LWOP}$ envelope for various tip speed ratios ($\theta_1$ = 8°). | 66 |
| 5.11.b | $C_{LW}$ envelope for various tip speed ratios ($\theta_1$ = 8°) for positive values of $C_{LWOP}$ . | 68 |

| Figure | | Page |
|---|---|---|


| | | |
|---|---|---|
| 5.12 | Maximum $C_{LWOP}$ at various tip speed ratios Vs. control axis angle. | 69 |
| 5.13 | Maximum $C_{LWOP}$ for different tip speed ratios Vs. twist angle. | 70 |
| 5.14 | Optimum linear twist for $C_{LWOP}$ at various tip speed ratios. | 72 |
| 5.15 | Minimum wind speed for remaining aloft at various tip speed ratios ( $\theta_1$ =2°). | 74 |
| 5.16 | Minimum wind speed for remaining aloft at various tip speed ratios,($\theta_1$ = 13° ). | 75 |
| 5.17 | Wind velocity at the autorotation limit for various tip speed ratios. | 76 |
| 5.18 | Maximum $C_{QW}$ for different tip speed ratios Vs. twist angle. | 78 |
| 5.19 | Optimum linear twist for $C_{QW}$ at various tip speed ratios. | 79 |
| 5.20 | Maximum $C_{opt1}$ for different tip speed ratios Vs. twist angle. | 81 |
| 5.21 | Optimum linear twist for $C_{opt1}$ at various tip speed ratios. | 83 |
| 5.22 | Maximum $C_{opt2}$ for different tip speed ratios Vs. twist angle. | 84 |
| 5.23 | Optimum linear twist for $C_{opt2}$ at various tip speed ratios. | 86 |
| 5.24 | Maximum $C_{opt3}$ for different tip speed ratios Vs. twist angle. | 87 |
| 5.25 | Optimum linear twist for $C_{opt3}$ at various tip speed ratios. | 89 |
| 5.26 | Minimum wind speed for remaining aloft at various tip speed ratios ($\theta_1$ = 8°). | 92 |
| 5.27 | $C_{PW}$ envelope for various tip speed ratios ($\theta_1$ = 8°). | 93 |

# *List of Tables*


| Table | | Page |
|---|---|---|
| 1.1 | Leading data for MK3. | 8 |
| 4.1 | The range of operation. | 48 |
| 5.1 | Predicted improvement in $C_{PW}$ using the optimum twist. | 55 |
| 5.2 | Predicted improvement in $C_{LW}$ using the optimum twist. | 63 |
| 5.3 | Predicted improvement in $C_{LWOP}$ using the optimum twist. | 71 |
| 5.4 | Predicted improvement in $V_{min}$ using the optimum twist. | 73 |
| 5.5 | Predicted improvement in $C_{QW}$ using the optimum twist. | 77 |
| 5.6 | Predicted improvement in $C_{opt1}$ using the optimum twist. | 82 |
| 5.7 | Predicted improvement in $C_{opt2}$ using the optimum twist. | 85 |
| 5.1 | Predicted improvement in $C_{opt3}$ using the optimum twist. | 88 |

# Nomenclature

| Symbols | | Units |
|---|---|---|
| $a$ | Slope of curve of section lift coefficient | [rad$^{-1}$] |
| $a_0$ | The rotor coning angle | [rad] |
| $a_1$ | Rotor backward tilt angle | [rad] |
| $a_2$ | Coefficient of cos $2\psi$ in fourier series for $\beta$ | [rad] |
| $B$ | Tip loss factor | |
| $b$ | number of blades | |
| $b_1$ | Coefficient of sin$\psi$ in fourier series for $\beta$ | [rad] |
| $b_2$ | Coefficient of sin$2\psi$ in fourier series for $\beta$ | [rad] |
| $c$ | Blade section chord | [ m ] |
| $C_{d0}$ | Section profile drag coefficient | |
| $\overline{C}_{d_r}$ | Average section profile drag coefficient in the reversed velocity region | |
| $\overline{C}_l$ | Average section lift coefficient in the reversed velocity region | |
| $C_l$ | Section lift coefficient | |
| $C_{LW}$ | Windmill lift coefficient $\left(\frac{L}{\frac{1}{2}\pi R^2 \rho V^2}\right)$ | |
| $C_{LWOP}$ | Disk loading to dynamic pressure ratio in windmill terminology | |
| $C_P$ | Rotor's power coefficient $\left(\frac{P}{\pi R^2 \rho (\Omega R)^3}\right)$ | |
| $C_{PW}$ | Windmill power coefficient $\left(\frac{P}{\frac{1}{2}\pi R^2 \rho V^3}\right)$ | |
| $C_Q$ | Rotor's torque coefficient $\left(\frac{Q}{\pi R^2 \rho (\Omega R)^2 R}\right)$ | |

| Symbols | | Units |
|---|---|---|
| $C_{Q0}$ | Profile torque coefficient | |
| $C_{Qi}$ | Induced torque coefficient | |
| $C_{QW}$ | Windmill torque coefficient $\left(\frac{Q}{\frac{1}{2}\pi R^3 \rho V^2}\right)$ | |
| $C_{opt1}$ | First optimisation criterion ( $C_{LW} \times C_{PW}$ ) | |
| $C_{opt2}$ | Second optimisation criterion ( $C_{LWOP} \times C_{PW}$ ) | |
| $C_{opt3}$ | Third optimisation criterion ( $C_{LWOP} \times C_{QW}$ ) | |
| D | Total rotor drag | [ N] |
| H | H force | [ N ] |
| $H_D$ | H force ( using tip path plane axis as the reference) | [ N ] |
| $h_{CD}$ | H force coefficient ( using tip path plane axis as the reference) | |
| $I_1$ | Mass moment of inertia of a blade about the flapping hinge | [ kg/m$^2$ ] |
| P | Rotor shaft profile drag power | [ N ] |
| Q | Rotor shaft torque | [ N.m ] |
| $Q_0$ | Profile torque | [ N.m ] |
| $Q_i$ | Induced torque | [ N.m ] |
| R | Rotor blade radius | [ m ] |
| r | Radial distance to blade element | [ m ] |
| T | Thrust | [ N ] |
| $T_C$ | Tether tension | [ N ] |
| $T_D$ | Thrust( using tip path plane axis as the reference) | [ N ] |
| $T_f$ | Thrust developed in forward velocity region | [ N ] |
| $T_{rd}$ | Thrust developed in reversed velocity region due to drag vector | [ N ] |
| $T_{rl}$ | Thrust developed in reversed velocity region due to lift vector | [ N ] |
| $t_{CD}$ | Thrust coefficient ( using tip path plane axis as the reference) | |
| U | Resultant velocity at the blade element | [ m/s ] |
| $U_P$ | Component of resultant velocity at the blade element parallel to control axis | [ m/s ] |

| Symbols | | Units |
|---|---|---|
| $U_T$ | Component of resultant velocity at the blade element perpendicular to control axis | [ m/s ] |
| $u_T$ | Nondimensional component of resultant velocity at blade element | [ m/s ] |
| $V$ | Wind velocity in windmill terminology or flight speed in helicopter terminology | [ m/s ] |
| $v$ | Induced inflow velocity at rotor | [ m/s ] |
| $V'$ | Resultant velocity at the rotor | [ m/s ] |
| $V_{min}$ | Minimum wind velocity in order to remain aloft | [ m/s ] |
| $x$ | Ratio of blade element radial distance to rotor blade radius | |
| $\alpha_C$ | Control axis angle | [ rad ] |
| $\alpha_r$ | Blade element angle of attack | [ rad ] |
| $\alpha_{(1.0)(270°)}$ | Maximum blade element angle of attack near the tip | [ rad ] |
| $\alpha_{(0.4)(270°)}$ | Maximum blade element angle of attack near the root | [ rad ] |
| $\alpha_{r,max}$ | Maximum blade element angle of attack | [ rad ] |
| $\beta$ | Blade flapping angle | [ rad ] |
| $\beta'$ | Tether angle to the horizon | [ rad ] |
| $\delta$ | Average blade element drag coefficient | |
| $\delta_0,\delta_1,\delta_2$ | Coefficients in power series expressing $C_{d0}$ as a function of $\alpha_r$ | |
| $\phi$ | Inflow angle | [ rad ] |
| $\gamma$ | Lock number | |
| $\lambda$ | Inflow ratio | |
| $\lambda_D$ | Inflow ratio( using tip path plane axis as the reference) | |
| $\mu$ | Tip speed ratio | |
| $\theta$ | Blade element pitch angle | [ rad ] |
| $\theta_0$ | Blade pitch angle at hub (collective pitch) | [ rad ] |
| $\theta_1$ | Blade twist( difference between hub and tip pitch angles) | [ rad ] |
| $\rho$ | Air density | [ kg/m$^3$ ] |
| $\sigma$ | Rotor solidity | |
| $\psi$ | Blade azimuth angle ( measured from downwind position in direction of rotation ) | [ rad ] |

# *CHAPTER ONE*

## *Introduction*

It was during the 70's that fuel shortage and several oil prices shocks struck the industrial world. In recent years, the excessive use of fossil fuels, such as oil and coal, has lead to extreme environmental and pollution problems. The excessive emission of carbon dioxide and other gases has caused global warming well known as " greenhouse effect " and degradation to the ozone layer.

The above problems have motivated some researchers to find solutions. In doing so, there are continuing efforts directed forwards finding new and alternative sources of energy. Nuclear, solar, geothermal and tidal means have been suggested. However, any new source of energy has to posses at least three characteristic, namely be economical, practical and safe.

## 1.1 Wind Energy

One of the more promising alternative sources of energy is wind.
While some researchers believe that the Chinese used simple windmills for irrigation purposes as long ago as 2000 B.C. [7], others believe that the Persians (Iranians) first developed large scale windmills between 100 BC and 700 AD. [7]

In the first instance, the windmills converted wind energy to useful mechanical energy. For example, in Europe the Netherlands has been famous for its windmills. Here, windmills are widely used for pumping sea water off the land and for many other applications. In America there are many signs of water-pumping windmills which were developed and manufactured in their thousands in the 1860's.
It was in the early 20th century that wind energy was first used for generating electricity. Small wind turbines brought light and power to rural areas of the United States.

After the first world war scientists in France, Germany and Russia developed the modern theory for windmills. This was the result of the new theory of propellers. Scientists such as Jaukawsky, Drzewiecki, Krassavsky and Sabbinin worked in Russia, Prandtl and Betz in Germany and Canstantin and Eiffel in France [8] (p.98). Betz showed that no windmill could have an efficiency greater than 16/27.

The new theories brought engineers to the design of large scale wind generators. The Russians built a 100 kW DC wind generator of 100 foot diameter near Yalta on the Black Sea in 1931. America's largest wind

generator, the Smith-Putnam wind turbine, was built in 1941 and it produced 1250 kilowatts nominal output. In the same year the Smith-Putnam machine was connected to the local AC network.

Since that time there have been many efforts to develop new, practical and more efficient wind turbines. However, in all these applications the speed of the air entering the turbine is severely limited. This is because the rotor is mounted in close proximity to the ground.

## 1.2 Generating Electricity from Upper Atmospheric Wind

The higher speed and persistence of the wind at altitude has attracted several researchers around the world. These upper atmospheric winds are often called jet stream winds . They were first discovered by pilots during world war II.They extend thousands of kilometres. The jet streams have velocities up to 500 Km per hour at their centres. But this speed drops rapidly both laterally and vertically from the core. So that the high speeds are limited to a narrow band in the very low stratosphere and upper troposphere [16].

The kinetic energy in the jet stream is the result of the movement of warm air from the equator to the poles, where the air is much cooler. The jet streams surround the earth and change their position and speed with seasons. It is found that there are three major jet streams in each hemisphere. [16].

Atkinson et al [14] in Australia and O'Dorhety and Robert [15] in America found from known weather records that the average power density in both continents can be as high as 16 to 20 $kw/m^2$. Figure (1.1) shows the average power density isoplets for Australia.

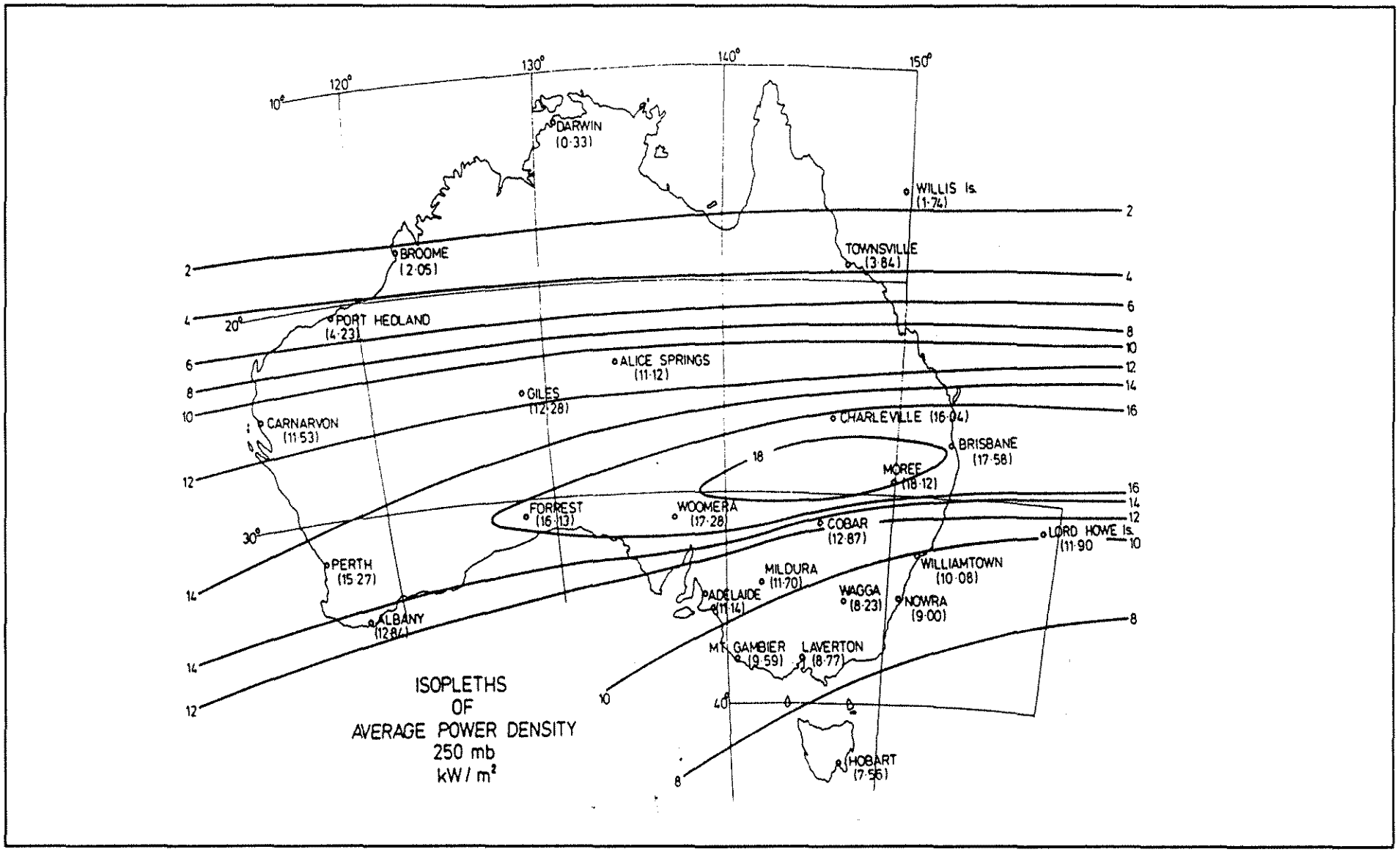


Fig (1.1) Upper atmospheric wind power density for Australia (after Atkinson, *et al*)

To utilise this high source of energy it is necessary that an aerodynamics platform be suitably located to convert the wind's kinetic energy to useful energy. Several proposals have been suggested for such an aerodynamic platform. Fletcher and Roberts [9] investigated ducted turbines mounted on a monoplane to develop the lift forces. Roberts and Blackler [1] consider three other concepts for this platform:

1. Airship concept
2. The open - rotor type turbine in a monoplane concept
3. Rotary wing concept

Among the concepts mentioned above the ducted turbines and the open rotor concepts involve a fixed wing airframe. However, fixed wing platforms need adequate winds to remain aloft and avoid stall.
The airship concept, although it has no stall limits, suffers from the fact that it produces a large amount of drag and involves great expense through the use of helium.

For the above mentioned reasons Roberts and Blackler [1] (p.73) suggested that a tethered rotary wing concept is the most pragmatic configuration for the platform.

## 1.3 Tethered Wind Generator or " Gyromill " Concept

The tethered rotary wing generator preferably has an even number of rotors with suitable pairs in contra rotation. These rotors should be mounted on a light airframe. Each rotor is coupled directly, or through gearboxes, to one or more generators / motors. The whole structure is constrained by tethers. One end of each tether is attached to the machine and the other end is firmly

attached to the ground. It should be pointed out that the tethers could ideally be made of kevlar, containing aluminium conductors. The transmission of electricity from or to the machine is made through these cables. The drag in combination with the lift, is reacted by the tether system.

The machine is able to operate in three different modes, namely

1. Generation mode as a gyromill

When the wind speed is high enough the machine can generate sufficient lift to keep the structure aloft as well as produce enough torque to generate an electric output.

2. Autorotation mode as a autogyro

In light wind the machine does not produce electricity. However, it is still possible to develop sufficient lift, using the well known autorotation principle.

3. Hovering mode as a helicopter

In calm conditions, or when the wind speed is below the autorotation limit, it is possible to supply electricity to the system with the generators acting as motors. This can keep the machine aloft. It is evident that if this calm periods lasts for a reasonable length of time the machine may be landed. Then it is possible for the machine to take - off again and climb, under power, to an appropriate generating altitude.

The advantages of the flying wind generator or gyromill is that it has the flexibility to be landed in any unfavourable atmospheric condition or in storm conditions. Furthermore, it does not have the landing and stalling disadvantages of the fixed wing concepts.

Fig. (1.2) shows the arrangement for a typical gyromill,(MK2). Fig( 1.3) shows this machine in flight condition. Table (1.1) shows the leading data of MK.3. Both MK2 and MK3 have been designed and built within the Department of Mechanical Engineering in the University of Sydney.

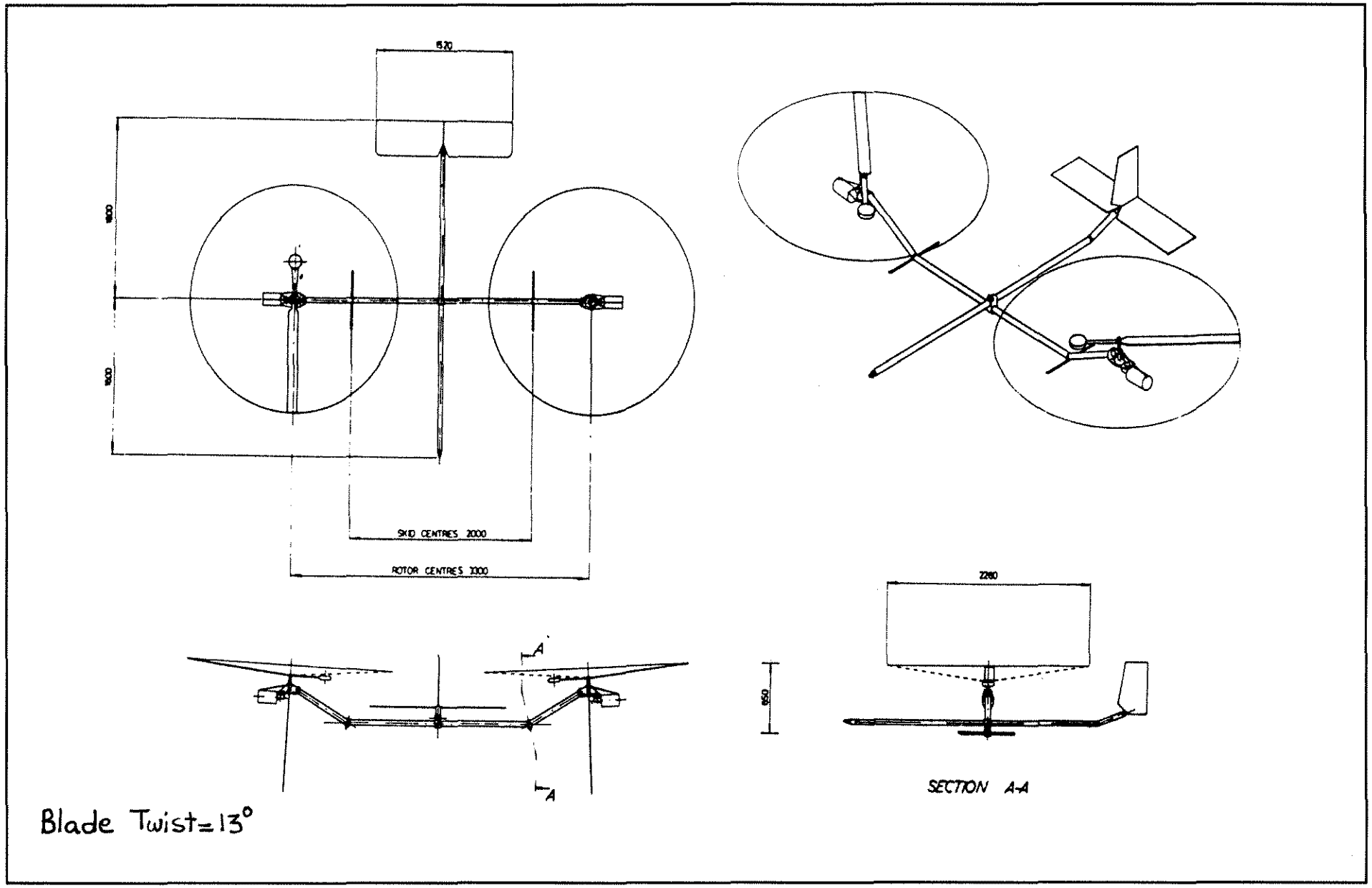


Fig (1.2) The arrangement for a typical gyromill ( after Roberts, Blackler and Barratt ).

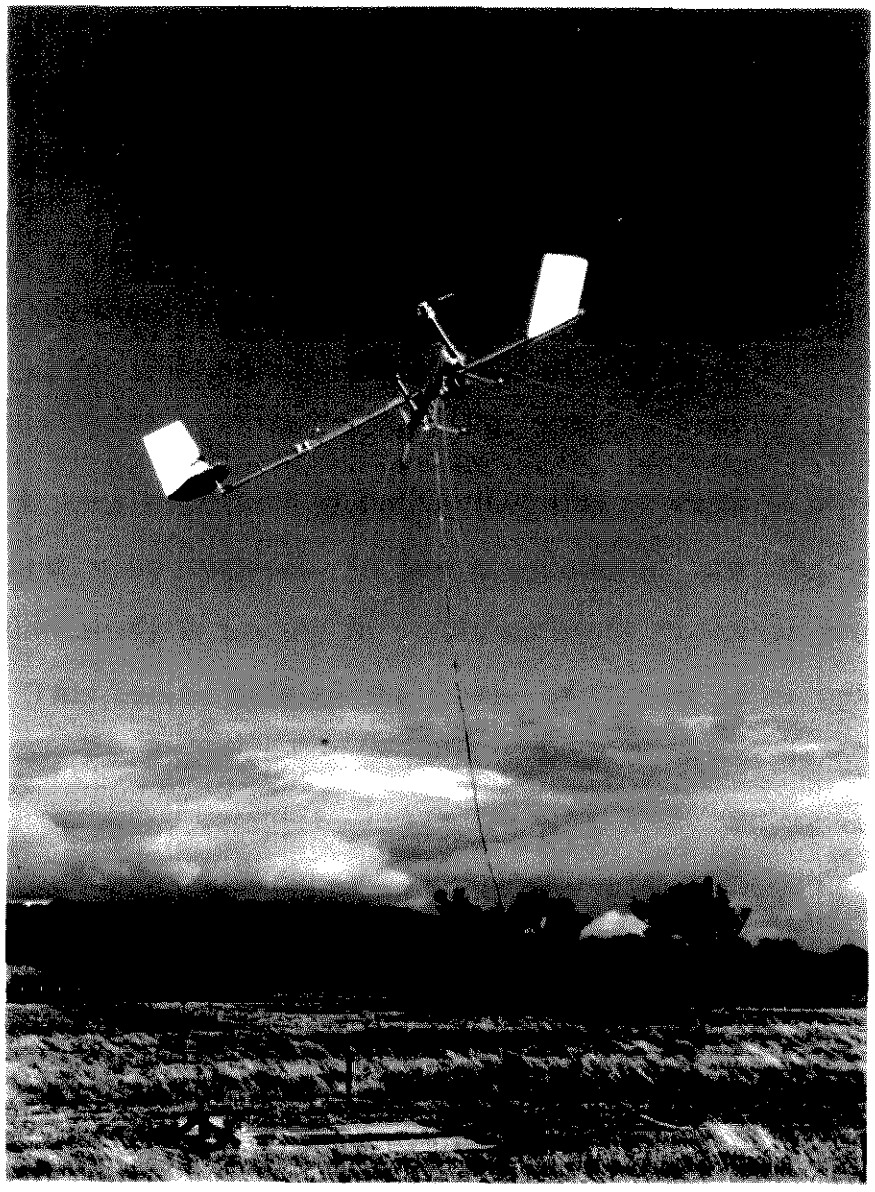

**Fig 1.3 A gyromill,(MK2), in flight.**

**Table (1.1) Leading data for Mk.3**

| Rotor | | Motor/ Generator | | General |
|---|---|---|---|---|
| Configuration: Twin , Side by side | | No. of units | 2 | Total weight: |
| Diameter (m) | 1.22 | Nominated rate | 1000(W) | |
| Root solidity | 0.05 | Armature: DC , Seperately excited 0 to 200 Volts | | 10 kg |
| Lock number | 10 | | | Tethers No |
| Speed (RPM) | 0-2000 | Field: DC, seperately excited 0 to 200 Volts | | 3 |
| Blade section | NACA 0012 | | | |
| Blade Twist | 0° | | | |

## 1.4 An Optimisation Study Relating to the Flying Wind Generator

The main objective of this thesis to determine the optimum linear twist of the rotor blades for windmill operation of the wind generator.

It is very important to realise that this machine is different from the conventional wind turbines. In the conventional case the objective of an optimisation study is usually to obtain as much power as possible from the machine. This means holding the power coefficient at or near a maximum value. Such an optimisation study has been undertaken for conventional windmills by many researchers. [11, 12, 13]. They mostly use the Glauert blade element model applied to propeller type windmills.

For the current wind generator optimisation study, Gluaert's model is not the most appropriate theory.The current optimisation study is a delicate balance between power output and lift. The ultimate goal is to generate as much power as possible while simultaneously generating sufficient lift to keep the system aloft. The question of optimum twist will be paramount. An alternative issue is to examine the amount of twist required in order to maintaining the system aloft with a minimum autorotative wind speed.

# *CHAPTER TWO*

## Aerodynamic Performance of the Flying Windmill

The performance study of the gyromill is not unrelated to helicopter performance. We should also realise that there is a direct relationship between the windmill performance parameters and the relevant helicopter performance parameters.

Furthermore, Gessow & Myers [2] state that " Windmilling implies blade settings which produce maximum of torque regardless of the thrust produced and autorotation implies blade settings that produce maximum axial resistance to the wind at zero torque ".

It is important to realise that a rotorcraft, whether it be in its helicopter, autorotation or windmill state can be analysed according to the methods review below.

## 2.1 Evolution of Various Theories for a Lifting Rotor

Several researchers have developed theories to evaluate the performance of a lifting rotor. These theories are mostly based on a combination of momentum theory and blade element theory.

In 1926 Glauert developed the theory of the autogyro. Since that time most aerodynamic analyses for the lifting rotor have been based on the original work of Glauert. Glauert used many assumptions to simplify the complexity of his equations. Other researchers reduced the number of assumptions used by Glauert.

Their work added to the accuracy of the theories. Researchers such as Sissingh, Lock and Wheatly made great contributions. Although their work was significant, their expression were not satisfactory for engineering applications because of the complexity of equations.

It was Bailey [3] who derived performance equations of the lifting rotor that were practical for engineering calculations. The significant part of Bailey's work was that he reduced all his expression to be functions of three basic parameters.These three are tip speed ratio ($\mu$), the inflow velocity ratio ($\lambda$) and the blade pitch ($\theta$).

Gessow in Ref. 2 reported on the previous theories and simplified them as a first step in understanding the more comprehensive theories. This was further extended by Gessow and Crim [4] in their work " An extension of lifting rotor theory to cover operation at large angles of attack and higher inflow conditions " [4]. They also removed some assumptions from Bailey's work. Their work gives analytical expressions for the flapping coefficients, thrust, torque and the profile drag power of the lifting rotor without any limitations on the blade section inflow angles and reversed velocity region. In the next section we will review some of the above mentioned theories in some detail. The theory of Gessow and Crim will be

subsequently chosen for a detailed analysis of the gyromill.

## 2.2 A Review of a Rotor Operating Under High Inflow Conditions

The rotor used in the tethered wind generator concept essentially operates under high positive values of the inflow parameter, $\lambda$. This inflow parameter is formally defined below. The tethered windmill evokes the windmill brake state and this will now be examined in some detail. For the moment we will follow the standard analysis of Gessow and Myers [2].

### 2.2.1 The Theory Review of Gessow and Myers

This analysis first made the following assumptions and then removed some of them in a more refined approach.

- The blades are untwisted and untapered
- The radial velocity on blade elements is negligible.
- The induced velocity through the rotor is constant.
- The inflow angle $\phi$ and flapping angle $\beta$ are small.
- In the fourier series for $\beta$, the harmonics higher than the first are neglected.
- The effect of the reversed velocity region is neglected .
- The profile drag coefficient and section lift curve slope are both constant.
- Tip losses are neglected.
- Torsional and bending deflections of blade are neglected.

Fig (2.1) shows a rotor under high inflow conditions and the following parameters can be defined.

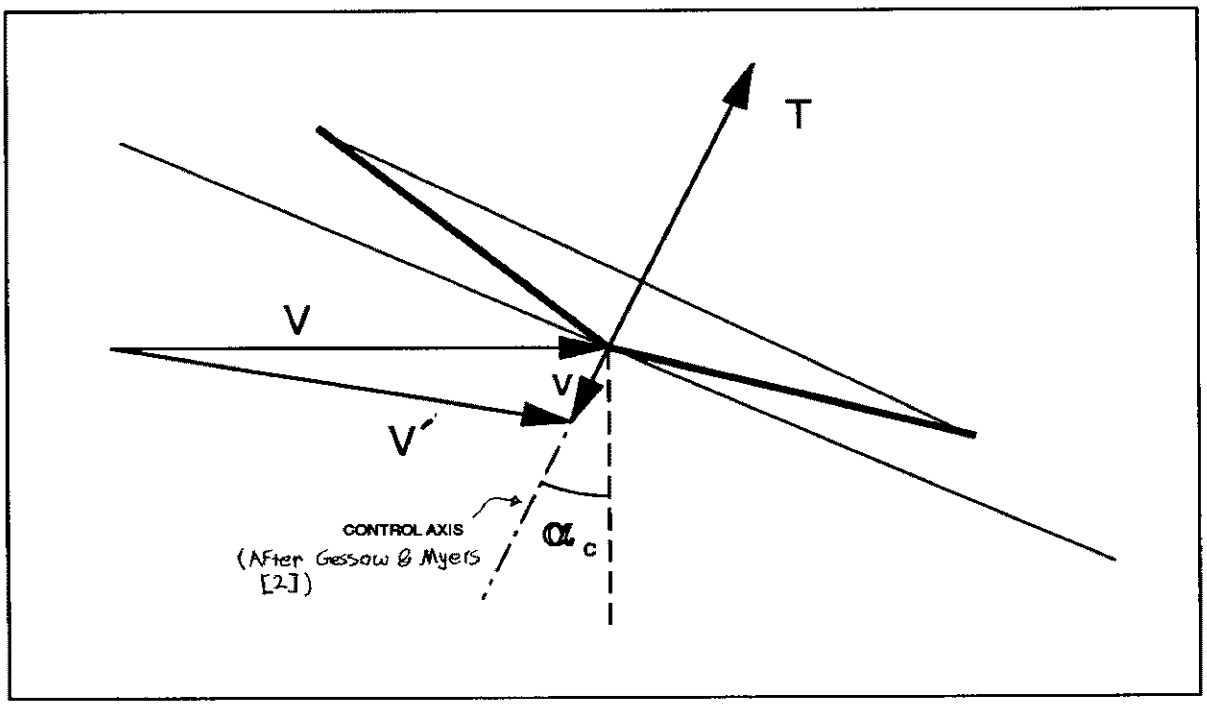


**Figure (2.1) Velocities at the rotor when acting under high inflow conditions**

- **V Wind speed of the flow approaching the wind generator, or for the helicopter this is the forward flight speed.**
- **v Induced velocity**
- **$V'$ Resultant velocity at the rotor**
- **$\alpha_c$ Control axis angle**

**Two dimensionless parameters can be defined.**

**. Inflow ratio is defined as**

$$\lambda = \frac{V \sin \alpha_c - v}{\Omega R} \qquad (2.1)$$

**. Tip speed ratio is defined as**

$$\mu = \frac{V \cos \alpha_c}{\Omega R} \qquad (2.2)$$

**where R is the rotor radius and Ω is the rotational speed.**

By application of the momentum theory it follows that the thrust can be expressed as:[2]

$$T=(\pi R^2 \rho V')2v = C_T \ \pi R^2 \rho (\Omega R)^2 \quad * \qquad (2.3)$$

It can also be shown that [2] p 185-186

$$\tan\alpha_c = \frac{\lambda}{\mu} + \frac{C_T}{2\mu(\mu^2+\lambda^2)^{\frac{1}{2}}} \qquad (2.4)$$

### 2.2.2 Blade Element Analysis

To calculate the elemental lift, drag and thrust, the resultant velocity at the blade element should be evaluated.

Fig (2.2) shows the elemental velocity distribution and the forces acting on the blade element. Here U is total velocity acting on the element. $U_P$ and $U_T$ are the resultant velocity components along and perpendicular to the control axis.

Fig (2.3) shows velocities in the flapping plane . Also, Fig (2.4) shows the distribution of velocity in a plane perpendicular to the control axis.

---

* Following the Gessow's , Bailey's and Weathly's works throughout this thesis it is assumed that the induced velocity is uniform over the rotor disk.

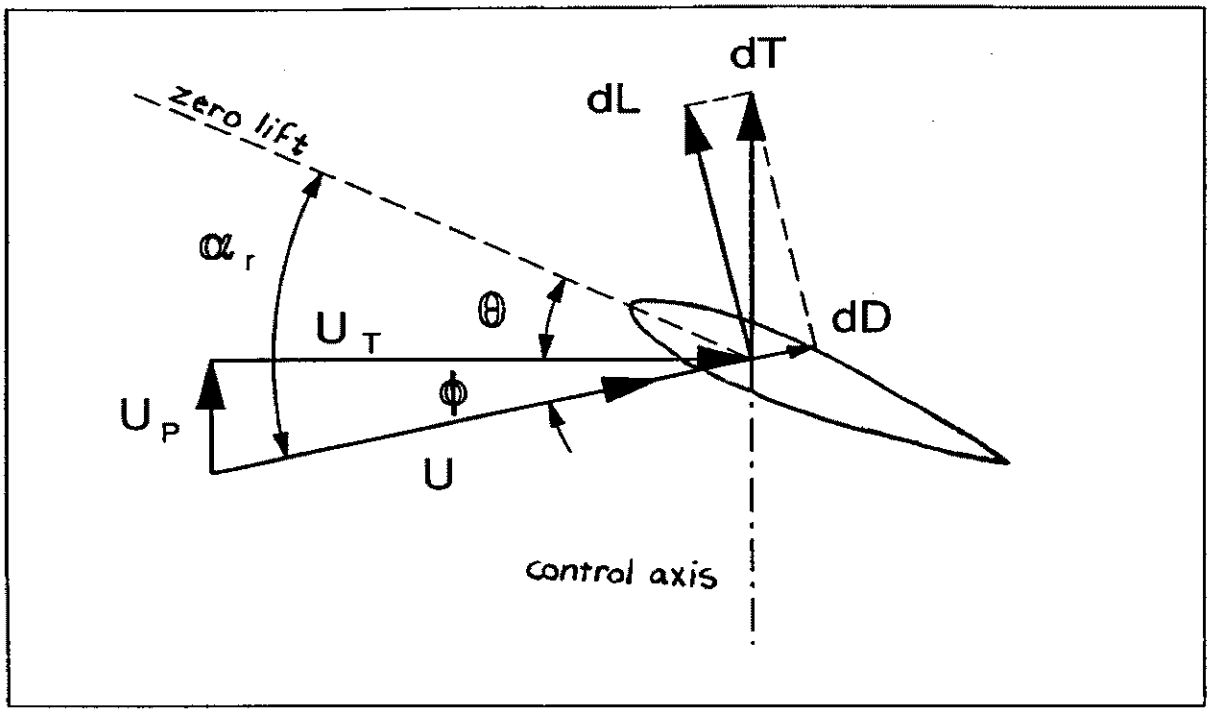


**Figure (2.2) Forces and velocities on the blade element.** [2]

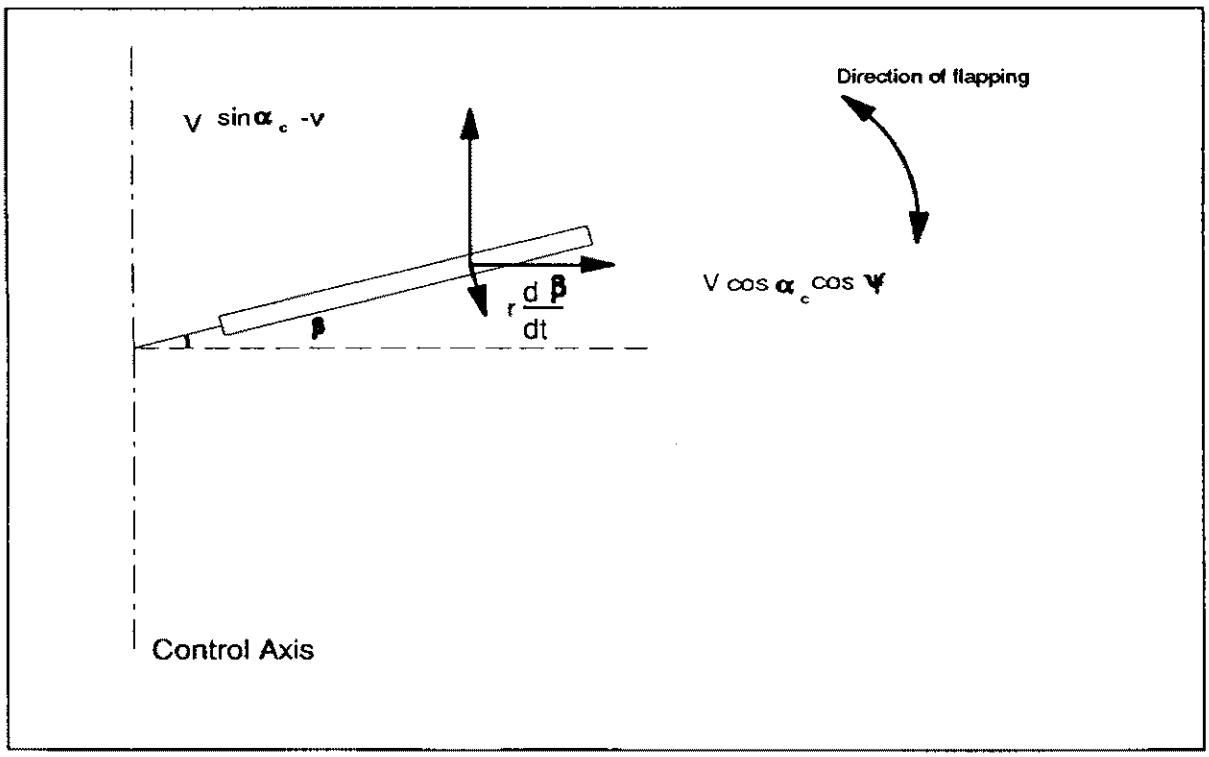


**Figure (2.3) Velocity distribution in the flapping plane**

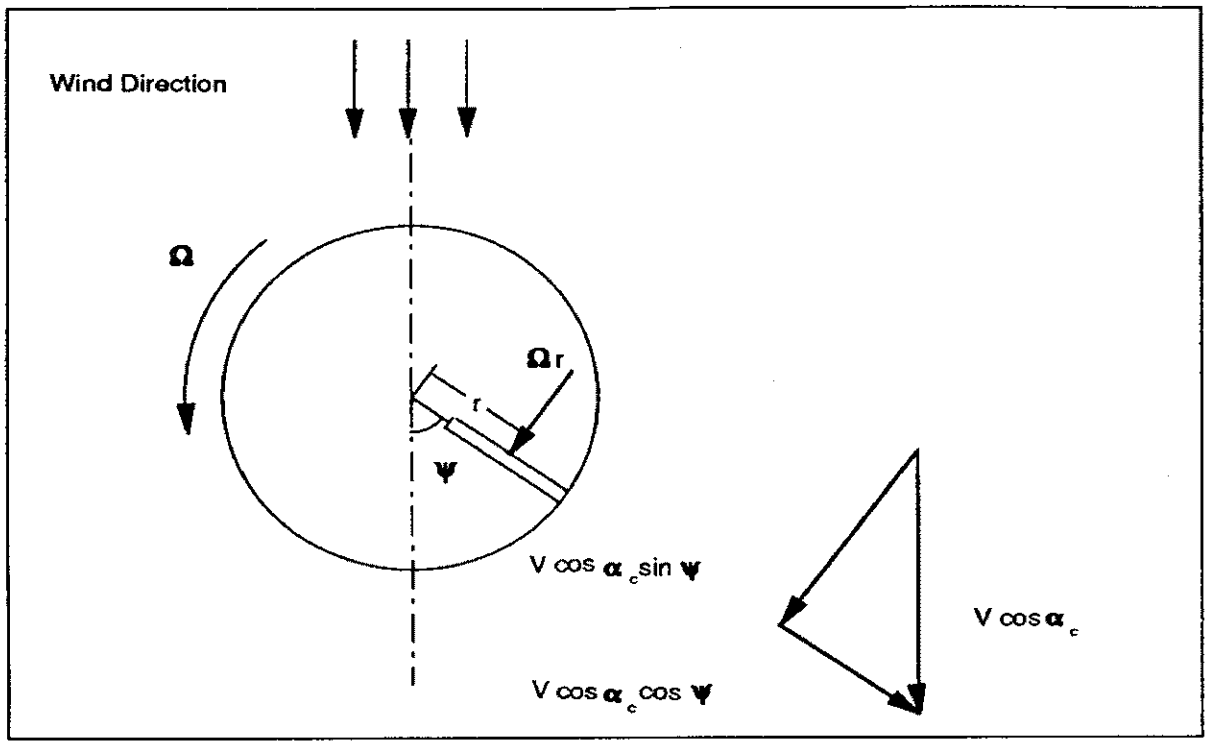


**Figure (2.4) Velocities in the plane normal to the control axis.**[2]

**from figures (2.2), (2.3) and (2.4) it can be readily shown**

$$U_P = (V\sin\alpha_C - v)\cos\beta - r\frac{d\beta}{dt} - V\cos\alpha_C\cos\psi\sin\beta \qquad (2.5)$$

$$U_T = \Omega r + V\cos\alpha_C\sin\psi \qquad (2.6)$$

**It is assumed that ß is a small angle. So that cos ß = 1 and sin ß = ß. Substituting eqs. (2.1), (2.2) in the equations for $U_P$ , $U_T$ gives**

$$U_T = \Omega r + \mu\Omega R\sin\psi \qquad (2.7)$$

$$U_P = \lambda\Omega R - r\frac{d\beta}{dt} - \mu\Omega R\beta\cos\psi \qquad (2.8)$$

**We will assume $\phi$ is small, so it immediately follows form fig (2.2) that**

$$\alpha_r = \theta + \phi = \theta + \frac{U_P}{U_T} \qquad (2.9)$$

### 2.2.3 The Rotor Thrust

In calculating the thrust it is assumed throughout that the angle $\phi$ is small. Thus it immediately follows that

$U \cong U_T$ and $dT \cong dL$.

The following expression can be derived for the elemental thrust

$$dT = \frac{1}{2}\rho a(\theta U_T^2 + U_P U_T)c\, dr \qquad (2.10)$$

where a is the slope of the section lift coefficient curve against $\alpha_r$, ($c_l = a\ \alpha_r$). Integration of the differential thrust along the blade and around the azimuth for a rotor with b blades, gives the total thrust as

$$T = \frac{b}{2\pi}\int_0^{2\pi}\int_0^R \frac{dT}{dr}\, dr\, d\psi \qquad (2.11)$$

It is assumed that blade is untwisted with a constant chord. So that

$$T = \frac{1}{2}\rho abc\Omega^2 R^3[\theta/3 + \frac{\mu^2\theta}{2} + \frac{\lambda}{2}] \qquad (2.12)$$

In nondimensional from

$$C_T = \frac{1}{2}a\sigma[\frac{\theta}{3} + \frac{\mu^2\theta}{2} + \frac{\lambda}{2}] \qquad (2.13)$$

Here $\sigma$ is the solidity ratio defined by

$$\sigma = \frac{bc}{\pi R} \qquad (2.14)$$

### 2.2.4 Expressions for the Flapping Coefficients

The flapping angle is defined as the angle between the blade span axis and the plane perpendicular to the control axis. This angle can be expressed as a fourier expansion of the azimuth angle $\psi$.

$$\beta = a_0 - a_1\cos\psi - b_1\sin\psi - a_2\cos 2\psi - b_2\sin 2\psi - \ldots \qquad (2.15)$$

Harmonics higher than the second will be neglected. In the above equation $a_0$, $a_1$, $b_1$ are the coning angle and flapping coefficients. Following Gessow and Myers [2] and noting the fact that the moment of all forces* acting on the blade about the flapping hinge should sum to zero then it follows that

$$a_0 = \frac{1}{2}\gamma[\frac{\theta}{4}(1+\mu^2) + \frac{\lambda}{3}] - \frac{M_w}{I_1\Omega^2} \qquad (2.16)$$

$$a_1 = \frac{\mu(\frac{8}{3}\theta + 2\lambda)}{1-\mu^2/2} \qquad (2.17)$$

$$b_1 = \frac{4\mu a_0}{3(1+\mu^2/2)} \qquad (2.18)$$

Where $\gamma$ is the Lock number. This number can be defined as

$$\gamma = \frac{C\rho a R^4}{I_1} \qquad (2.19)$$

where $I_1$ is the moment of inertia of the blade about the flapping hinge.

* These are aerodynamic, dynamic and gravity forces.

### 2.2.5 Expression for the Rotor Torque

Considering fig (2.2) the following equation gives the differential torque at the blade element[2] as

$$dQ = r(dD\cos\phi - dL\sin\phi) \qquad (2.20)$$

According to the small $\phi$ assumption and assuming a constant profile drag coefficient along the blade, equal to $\delta$ it can be readily seen that

$$dQ = \frac{1}{2}\rho U_T^2 \delta c r dr - \frac{1}{2}\rho U_T^2 \phi C_l c r dr \qquad (2.21)$$

The first term in the equation (2.21) is the elemental profile torque and the second term is the elemental induced torque. The total torque can be derived by integrating eq.(2.21) to give

$$\overset{*}{Q} = Q_0 + Q_i = \frac{b}{2\pi}\int_0^R\int_0^{2\pi}\frac{1}{2}\rho U_T^2 \delta c r d\psi dr + \frac{b}{2\pi}\int_0^R\int_0^{2\pi}\frac{1}{2}\rho U_T^2 \phi C_l c r d\psi dr \qquad (2.22)$$

After simplification it can be shown that

$$Q = \frac{1}{2}\rho abc\Omega^2 R^4[\frac{\delta}{4a}(1+\mu^2) - \frac{1}{3}\lambda\theta - \frac{1}{2}\lambda^2 - \frac{(a_1^2+b_1^2)}{8} - \frac{1}{2}\mu^2(\frac{a_0^2}{2} + \frac{3a_1^2}{8} + \frac{b_1^2}{8}) - \frac{1}{2}\mu\lambda a_1 + \frac{1}{3}\mu a_0 b_1]$$

$$(2.23)$$

In nondimensional form

$$C_Q = \frac{\sigma a}{2}[\frac{\sigma}{4a}(1+\mu^2) - \frac{1}{3}\lambda\theta - \frac{1}{2}\lambda^2 - \frac{1}{8}\mu a_0 b_1 - \frac{\mu^2}{2}(\frac{a_0^2}{2} + \frac{3a_1^2}{8} + \frac{b_1^2}{8}) - \frac{\mu\lambda a_1}{2} + \frac{\mu a_0 b_1}{3}]$$

$$(2.24)$$

---

* In this text the power and torque positive sign will mean output and negative sign will mean input.

## 2.3 Wheatley's Contribution to the Theory

Wheatley in 1930's removed several assumptions and limitations from the Glauert's theory namely

. The limitation for untwisted blades was removed by introducing a linear twist applied to blade elements of

$$\theta = \theta_0 + \theta_1 \left(\frac{r}{R}\right) \qquad (2.25)$$

where $\Theta_0$ is the blade pitch at the root and $\Theta_1$ is the difference between the tip and root pitch angles. The $\Theta_1$ angle is well known as the linear twist.

- A method was introduced for approximation of the tip losses. A tip loss factor of B = 0.97 is suggested. It is applied by simply integrating thrust and torque from r = 0 to r = 0. 97R.
- The second harmonics in the flapping angle and powers of μ up to the fourth were retained.
- The effect of reversed velocity region was considered.

Reversed flow occurs on the in board part of retreating blade where the forward flight velocity* is greater than the local rotational velocity. This phenomenon causes a flow from the trailing edge of the blade to the leading edge. This region is called the reversed velocity region. The area of this region increases with increasing tip speed ratio.

Inclusion of the reversed velocity effect was undertaken by integrating thrust and torque in several parts.

Hence thrust can be written as

---

*This is the component of forward flight velocity normal to the blade span.

$$T = \frac{b}{2\pi}\int_0^{2\pi} d\psi \int_0^{BR} \frac{1}{2}\rho c a U^2 C_l dr = \frac{b}{2\pi}[\int_0^{\pi} d\psi \int_0^{BR} \frac{1}{2}\rho c a U^2 (\theta_0 + \theta_1 \frac{r}{R} + \phi) dr +$$

$$\int_{\pi}^{2\pi} d\psi \int_{-\mu R \sin\psi}^{BR} \frac{1}{2}\rho a c U^2 (\theta_0 + \theta_1 \frac{r}{R} + \phi) dr + \int_{\pi}^{2\pi} d\psi \int_0^{-\mu R \sin\psi} \frac{1}{2}\rho a c U^2 (-\theta_0 - \theta_1 \frac{r}{R} - \phi) dr]$$

( 2.26 )

**The onset of the reverse flow region is defined by**

$$U_T = \Omega r + \mu \Omega R \sin \psi = 0$$

**This immediately defines the extent of reversed velocity region as where the r value lies between the limits**

$$-\mu R \sin \psi < r < 0 .$$

**In the above integrations the first integration in the brackets is for the advancing blade ( $0 < \phi < \pi$ ), while the second integration is for that part of the retreating blade which acts conventially. The third part is for the retreating blade under reversed velocity conditions.**

## 2.4 Bailey's Contributions

**Bailey extended Wheatly's work by defining a relationship between blade angle of attack and the section profile drag.**

**In mathematical form, Bailey defined the profile drag coefficient as**

$$C_{d_0} = \delta_0 + \delta_1 \alpha_r + \delta_2 \alpha_r^2 \qquad (2.27)$$

**He also developed a method to assign appropriate values for $\delta_0$, $\delta_1$, $\delta_2$ at any Reynolds number.**

**Bailey also tabulated equations for thrust, torque and flapping coefficients as a function of $\mu$, $\lambda$, $\Theta$.**

**He introduced the drag to lift ratio ( D / L ) as a function of $\lambda$, $\Theta_0$, $\Theta_1$, $\mu$.**

## 2.5 The Gessow and Crim Extended Theory

Gessow and Crim extended Bailey and Wheatly's work in 1952. This extension made it possible to examine operational conditions at high inflows and large angles of attack. Gessow and Crim removed the assumption that the blade section inflow angle $\phi$ be small.
Hence the restriction of $\cos \phi = \phi$ is also removed. The extended theory also covers the effects of a reversed flow region.

The following review is a summary of Gessow and Crim's extended theory given in reference [4].

1. In the forward velocity region the elemental thrust is considered to be the projection of the elemental lift onto the control axis. This is used for deriving the thrust and the thrust moment expressions.

In the reverse velocity region the component of elemental drag in the thrust direction is also considered. The torque equation use similar components of lift and drag.

2. The resultant velocity (U) is used for calculating the elemental lift and drag forces, instead of $U_T$

3. In considering the effect of stalled flow in the reversed velocity region, a typical value of blade section angle of attack equal to $60^0$is assumed. The section lift and drag coefficients are also assumed to be constant for this region at 1.2 and 1.0 respectively.

4. In order to reduce the complexity of equations it was assumed that

$$\alpha_r = \sin \alpha_r$$

### 2.5.1 Calculation of the Thrust

From fig (2.4) we can write the elemental thrust as

$$dT = dL\cos\phi \qquad (2.28)$$

neglecting the drag component

and

$$C_l = a\sin\alpha_r = a\sin(\theta_0 + x\theta_1 + \phi) \qquad (2.29)$$

After some algebraic work Gessow and Crim [4] show that

$$\frac{dT}{dr} = \frac{1}{2}\rho ac[(\sin\theta_0\cos x\theta_1 + \cos\theta_0\sin x\theta_1)U_T^2 + (\cos\theta_0\cos x\theta_1 - \sin\theta_0\sin x\theta_1)U_T U_P]$$

$$(2.30)$$

The total thrust in the forward velocity region is

$$T_f = \frac{b}{2\pi}\int_0^{2\pi}\int_0^{BR}\frac{dT}{dr}dr\,d\psi - \frac{b}{2\pi}\int_\pi^{2\pi}\int_0^{-\mu R\sin\psi}\frac{dT}{dr}dr\,d\psi \qquad (2.31)$$

Next the, total thrust is the algebraic sum of the

1. The thrust in the forward velocity region due to lift on the blade elements, $T_f$.
2. The thrust in the reversed velocity region due to the lift, $T_{rl}$.
3. The thrust in the reversed velocity region due to the drag ,$T_{rd}$ .

Then it follows that

$$T = T_f + T_{r_1} + T_{r_2} \tag{2.32}$$

Or in nondimensional form

$$\frac{2C_T}{\sigma a} = \left(\frac{2C_T}{\sigma a}\right)_f + \left(\frac{2C_T}{\sigma a}\right)_{r_1} + \left(\frac{2C_T}{\sigma a}\right)_{r_2} \tag{2.33}$$

**The terms in eq. (2.33) are given reference [4] as**

$$\begin{aligned}\left(\frac{2C_T}{\sigma a}\right)_f = \sin\theta_0 [ & \frac{B^3}{3} + \mu^3 \frac{B}{2} - \frac{2\mu^3}{9\pi} - \theta_1 \left(\lambda \frac{B^3}{3} + \frac{\mu^3 \lambda}{9\pi}\right) \\ & - \theta_1^2 \left(\frac{B^5}{10} + \frac{\mu^2 B^2}{12}\right) + \theta_1^3 \lambda \frac{B^5}{30} + \theta_1^4 \frac{B^7}{168}] \\ & + \cos\theta_0 [\lambda \frac{B^2}{2} + \mu^2 b_2 \frac{B}{4} + \frac{\mu^2 \lambda}{8} + \frac{\mu^3 a_1}{16} + \theta_1 \left(\frac{B^4}{4} + \frac{\mu^2 B^2}{4} - \frac{\mu^4}{64}\right) \\ & + \theta_1^2 \left(\frac{\mu^4}{128}\lambda - \frac{B^4 \lambda}{8}\right) - \theta_1^3 \left(\frac{B^6}{36} + \mu^2 \frac{B^4}{48}\right)]\end{aligned} \tag{2.34}$$

$$\left(\frac{2C_T}{\sigma a}\right)_{r_1} = \frac{\overline{C}_l}{a} \left[\frac{1}{8}\mu^2 |\lambda| \left(1 - \frac{\mu}{2}\right) + \frac{\mu^3}{9\pi}\right] \tag{2.35}$$

$$\left(\frac{2C_T}{\sigma a}\right)_{r_2} = \frac{\overline{C}_{d_0}}{a} \left[\frac{\mu}{\pi}\lambda |\lambda| \left(1 - \frac{\mu}{2}\right) + \frac{\mu^2 \lambda}{16}\right] \left(1 - \frac{\mu}{2}\right) \tag{2.36}$$

## 2.5.2 Expressions for the Flapping Coefficients

**In calculating the flapping angle harmonics higher than the second are neglected , so that it follows**

$$\beta = a_0 - a_1 \cos\psi - b_1 \sin\psi - a_2 \cos 2\psi - b_2 \sin 2\psi \tag{2.37}$$

The sum of all the moments about the flapping hinge is equal to zero. Hence the equation can be found for the flapping coefficients. These equations should be solved simultaneously to find $a_0$, $a_1$, $b_1$, $a_2$, $b_2$.

These equation are as follow

$$a_0 = \frac{\gamma}{2}\{ \cos\theta_0[\frac{B^3}{3}\lambda + \frac{1}{8}\mu^2 b_2 B^2 + 0.0398\lambda\mu^3 + 0.033 a_1\mu^4$$

$$+ \theta_1(\frac{B^5}{5} + \frac{1}{6}\mu^2 B^3) - \frac{\theta_1^2}{2}(\frac{B^5}{5}\lambda) - \frac{\theta_1^3 B^7}{42}] +$$

$$\sin\theta_0[\frac{B^4}{4} + \frac{B^2}{4}\mu^2 - \frac{\mu^4}{64} - \theta_1(\lambda\frac{B^4}{4} + \frac{1}{64}\lambda\mu^4)$$

$$- \frac{\theta_1^2}{4}(\frac{B^6}{3} + \frac{B^4}{4}\mu^2) + \frac{\theta_1^3 B^6\lambda}{36} + \frac{\theta_1^4 B^8}{192}] +$$

$$\frac{\mu^4 \overline{C}_l}{128a} + \frac{|\lambda|\lambda\mu^2}{8a}(1 - \frac{\mu}{2})^2\overline{C}_{d_e} + \frac{0.0398}{a}\mu^3|\lambda|(1-\frac{\mu}{2})\overline{C}_l$$

$$+ \frac{0.0199}{a}\lambda(1-\frac{\mu}{2})\mu^3\overline{C}_{d_e}\} \qquad (2.38)$$

$$0 = \cos\theta_0[-\frac{\mu B^3 a_0}{3} + \frac{b_1 B^4}{4} + \frac{\mu^2 b_1 B^2}{8} - 0.05 a_2\mu^4 - \frac{\mu B^3 a_2}{6} - \frac{\theta_1^2}{2}(-\frac{\mu B^5 a_0}{5} + \frac{b_1 B^6}{6})]$$

$$-\sin\theta_0[\theta_1(\frac{-\mu B^4 a_0}{4} + \frac{b_1 B^5}{5} + \frac{\mu^2 b_1 B^3}{12} - \frac{\mu B^4 a_2}{8}) - \frac{\theta_1^3 b_1 B^7}{42}] \qquad (2.39)$$

$$0=\sin\theta_0[\frac{2\mu B^3}{3}+0.0265\mu^4-\theta_1(\mu\lambda\frac{B^3}{3}-\frac{a_1B^5}{5}+\frac{\mu^2a_1B^3}{12}-\frac{\mu b_2B^4}{8}-0.0265\lambda\mu^4)$$

$$-\frac{\theta_1^2\mu B^5}{5}-\theta_1^3(\frac{a_1B^7}{42}-\frac{\mu^2a_1B^5}{120})]$$

$$+\cos\theta_0[\frac{\mu\lambda B^2}{2}-\frac{a_1B^4}{4}+\frac{\mu^2a_1B^2}{8}-\frac{\mu B^3b_2}{6}-\frac{1}{32}a_1\mu^4-\frac{\lambda\mu^3}{16}+\frac{\theta_1\mu B^4}{2}$$

$$-\frac{\theta_1^2}{2}(\frac{\mu\lambda B^4}{4}-\frac{a_1B^6}{6}+\frac{\mu^2a_1B^4}{16})-\frac{\theta_1^3\mu B^6}{18}-\frac{\theta_1^4a_1B^8}{192}]$$

$$-0.01325\mu^4\frac{\overline{C}_l}{a}-0.2123\lambda|\lambda|\mu^2(1-\frac{\mu}{2})^2\frac{\overline{C}_{d_0}}{a}-\frac{\mu^3|\lambda|}{16}(1-\frac{\mu}{2})\frac{\overline{C}_l}{a}-\frac{\lambda}{32}(1-\frac{\mu}{2})\mu^3\frac{\overline{C}_{d_0}}{a}$$

( 2.40 )

$$a_2=\frac{\gamma}{6}\{\sin\theta_0[-\frac{\mu^2B^2}{4}+\frac{\mu^4}{64}-\theta_1(\frac{\mu a_1B^4}{4}+\frac{2b_2B^5}{5})+\frac{\theta_1^2}{2}(\frac{\mu^2B^4}{8})]+$$

$$\cos\theta_0[\frac{\mu B^3a_1}{3}+\frac{B^4b^2}{2}+0.0265\lambda\mu^3+0.015a_1\mu^4-\frac{\theta_1\mu^2B^3}{6}-\frac{\theta_1^2}{2}(\frac{\mu B^5a_1}{5}+\frac{B^6b_2}{3})]$$

$$-\frac{\mu^4\overline{C}_l}{128a}-\frac{|\lambda|\lambda\mu^2}{8a}(1-\frac{\mu}{2})^2\overline{C}_{d_0}+\frac{0.0265}{a}\mu^3|\lambda|(1-\frac{\mu}{2})\overline{C}_l+\frac{0.01327}{a}\lambda(1-\frac{\mu}{2})\mu^3\overline{C}_{d_0}\}$$

( 2.41 )

$$b_2=\frac{\gamma}{6}\{\cos\theta_0[-\frac{\mu^2a_0B^2}{4}+\frac{\mu B^3b_1}{3}-\frac{a_2B^4}{2}+\frac{a_2\mu^4}{16}+\frac{\theta_1^2}{2}(\frac{\mu B^5b_1}{5}-\frac{a_2B^6}{3})]$$

$$-\sin\theta_0[\theta_1(-\frac{\mu^2a_0B^3}{6}+\frac{\mu b_1B^4}{4}-\frac{2a_2B^5}{5})]\}\qquad(2.42)$$

### 2.5.3 The Rotor Torque

The torque on the rotor is a combination of the induced or accelerating torque ($Q_i$) and the profile or decelerating torque ($Q_0$). $Q_i$ and $Q_0$ should be evaluated for the forward velocity and reversed velocity regions. In a nondimensional form the torque can be presented as

$$\frac{2C_Q}{\sigma} = \left(\frac{2C_{Q_i}}{\sigma}\right)_f + \left(\frac{2C_{Q_i}}{\sigma}\right)_r + \left(\frac{2C_{Q_0}}{\sigma}\right)_f + \left(\frac{2C_{Q_0}}{\sigma}\right)_r \qquad (2.43)$$

where the subscripts f,r refer to the forward and reversed velocity regions. The analysis given previously in section (2.2.5) can now be used to evaluate the terms in eq (2.43). The normal approximation for the section profile drag will be used. This approximation can be written as

$$C_{d0} = \delta_0 + \delta_1 \alpha_r + \delta_2 \alpha_r^2$$

where $\alpha_r$ is the blade angle of attack. This procedure is given

in reference [4]. It then follows that

$$(\frac{2C_{Q_i}}{\sigma a})_f = \sin\theta_0 [\frac{\lambda}{3}B^3 + \frac{\mu^2 b_2 B^2}{8} - \frac{\theta_1^2 \lambda B^5}{10} + \frac{\mu^3 \lambda}{9\pi} + C_1(\frac{\theta_1^3 B^5}{30} - \frac{\theta_1 B^3}{3})$$

$$+ C_2(\frac{-\theta_1 B^4}{4}) + C_3(\frac{-\theta_1 B^5}{5})] +$$

$$\cos\theta_0 [\ \theta_1(\frac{\lambda B^4}{4} + \frac{\mu^2 b_2 B^3}{12}) - \frac{\theta_1^3 \lambda B^6}{36} + C_1(\frac{B^2}{2} - \frac{\theta_1^2 B^4}{8})$$

$$+ \frac{C_2 B^3}{3} + C_3(\frac{B^4}{4} - \frac{\theta_1^2 B^6}{12}) - \frac{\mu^2 \lambda^2}{8} - \frac{3\mu^3 a_1 \lambda}{16}] \quad (2.44)$$

$$(\frac{2C_{Q_i}}{\sigma a})_r = -\frac{\overline{C}_I}{8a}\mu^2 \lambda |\lambda| (1 - \frac{\mu}{2})^2 \quad (2.45)$$

$$(\frac{2C_{Q_0}}{\sigma})_r = -\overline{C}_{4_0}[\frac{\mu^3}{9\pi}|\lambda|(1 - \frac{\mu}{2}) + \frac{\mu^4}{128}] \quad (2.46)$$

$$
\begin{aligned}
\left(\frac{2C_{Q_0}}{\sigma}\right)_f = {} & K_1\left(\frac{1}{4}+\frac{\mu^4}{4}\right)+K_2\left(\frac{1}{5}+\frac{\mu^2}{6}\right)+K_3\left(\frac{1}{6}+\frac{\mu^2}{8}\right)+K_4\left(\frac{1}{7}+\frac{\mu^2}{10}\right)+K_5\left(\frac{1}{8}+\frac{\mu^2}{12}\right) \\
& +K_6\left(\frac{1}{9}+\frac{\mu^2}{14}\right)+k_7\left(\frac{\lambda}{3}+\frac{\mu^2 b_2}{8}\right)+K_8\left(\frac{\lambda}{4}+\frac{\mu^2 b_2}{12}\right)+K_9\left(\frac{\lambda}{5}+\frac{\mu^2 b_2}{16}\right)+K_{10}\left(\frac{\lambda}{6}+\frac{\mu^2 b_2}{20}\right) \\
& +K_{11}\left(\frac{\lambda}{7}+\frac{\mu^2 b_2}{24}\right)+K_{12}\left(\frac{\lambda}{8}+\frac{\mu^2 b_2}{28}\right)+C_1\left(\frac{K_{13}}{2}+\frac{K_{14}}{3}+\frac{K_{15}}{4}+\frac{K_{16}}{5}+\frac{K_{17}}{6}+\frac{K_{18}}{7}\right) \\
& + C_2\left(\frac{K_{13}}{3}+\frac{K_{14}}{4}+\frac{K_{15}}{5}+\frac{K_{16}}{6}+\frac{K_{17}}{7}+\frac{K_{18}}{8}\right) + C_3\left(\frac{K_{13}}{4}+\frac{K_{14}}{5}+\frac{K_{15}}{6}+\frac{K_{16}}{7}+\frac{K_{17}}{8}+\frac{K_{18}}{9}\right) \\
& - C_4\frac{K_{13}}{2}-K_1\frac{\mu^4}{64}+K_7\frac{\mu^3\lambda}{9\pi}+K_8\frac{\mu^4\lambda}{64} \qquad (2.47)
\end{aligned}
$$

The interested reader may find expressions for coefficients $C_1$, $C_2$, $C_3$, $C_4$, $K_1$, $K_2$, $K_3$, $K_4$, $K_5$, $K_6$, $K_7$, $K_8$, $K_9$, $K_{10}$, $K_{11}$, $K_{12}$, $K_{13}$, $K_{14}$, $K_{15}$, $K_{16}$, $K_{17}$, $K_{18}$ in reference [4] .

### 2.5.4 Validity and Limitations of the Theory

Gessow and Crim suggested that for forward velocities the extended and standard theories should give substantially the same results. However, for high forward speeds, or for large angles of rotor incidence, then different results can be expected.

The extended theory is only valid below the stall conditions outside the reversed flow region. Compressibility effects are also neglected in the theory.

## 2.6 Effect of Stall* on the Performance

The distribution of the angle of attack along the blade is a function of the inflow velocity's direction and magnitude. In autorotation and windmilling states the stall begins at the edge of the reversed flow region and spreads outboard, as the speed increases. Furthermore, the area of the rotor affected by the stall depends upon the airfoil's stall limit. When some part of the blade operates at the stall condition, then the profile drag rapidly increases, while profile lift falls dramatically. In these circumstances, the assumptions made for estimating the profile drag and lift coefficients become optimistic so that the performance predictions give unrealistic results.

In any analysis it should be verified that the blade element angle of attack does not exceed the stall limit.

To perform the above, Bailey developed a method of calculating the element angle of attack. He assumed that the rotor had infinitely heavy blades and thus obtained the following expression for the angle of attack [18] .

$$\alpha_r = \theta_0 + \theta_1 U_T - \theta_1 \mu \sin\psi - a_1 \sin\psi + \frac{\lambda}{u_T} + \frac{\mu a_1}{u_T} \qquad (2.48)$$

The azimuth angle at which the maximum angle of attack occurs, can be found from the following expression

$$\frac{d\alpha_r}{d\psi} = -\theta_1 \mu \cos\psi - a_1 \cos\psi = 0 \qquad (2.49)$$

This gives

$$\alpha_{r_{max}} \quad @ \quad \psi = 270^0 \qquad\qquad \alpha_{r_{min}} \quad @ \quad \psi = 90^0$$

* See next page.

Substitution of $\psi = 270^0$ in eq (2.48) gives the expression for $\alpha_{r,max}$ as a function of twist, collective pitch, tip speed ratio and $a_1$ as

$$\alpha_{r_{max}} = \theta_0 + \theta_1(u_T + \mu) + \frac{\lambda}{u_T} + (1 + \frac{\mu}{u_T})a_1 \qquad (2.50)$$

where $u_T$ is the dimensionless tangential velocity at the blade section. This velocity is given by

$$u_T = \frac{U_T}{\Omega R} = x + \mu \sin\psi \qquad (2.51)$$

---

* The word "stall" in this context implies that the angle of attack has reached a nominal limit. This limit has been chosen herein to be 13°. which is somewhat less than the classical stall limit for NACA 0012 section in two dimensional flow. The angle of attack of 13° is suggested as a practical limit for $\alpha_r$ in a rotorcraft context. Therefore. the word stall is used solely in the current context to refer to this arbitrary, nominal value.

## 2.7 Choice of an Appropriate Theory for the Current Optimisation

The review of different theories in the previous sections reveals that the extended theory of Gessow and Crim is the only real choice for the current optimisation study because

- Small angle assumptions for $\phi$ are made in all other theories. These assumptions have been removed by Gessow and Crim.

- The theory is appropriate for high disk incidences likely to be encountered in operation of the current gyromill.

- The theory is appropriate to high tip speed ratios.

- A reversed flow region is considered in Gessow and Crim's theory and as a result the predictions are likely to approximate the real situation.

- Ho [6] previously showed that despite the limitations Bailey's theory compares favourably with Gessow and Crim's theory provided the tip speed ratio is less than 0.2. To avoid this tip speed ratio limitation we will adopt Gessow and Crim's extended theory throughout the remainder of this thesis.

# CHAPTER THREE

## Performance Analyses of The Tethered System

As mentioned before the main objective of this thesis is to find the optimum twist for windmill operation of a gyromill. In doing so the relationship between the performance parameters such as power coefficient, torque coefficient and lift coefficient needs be established as a function of $\mu$, $\alpha_c$ and $\beta'$ . The second step is to find the effect of the geometrical variables, in particular twist, on the above performance parameters. Then the different possible criteria for choosing the optimum twist can be discussed and the desired optimum established.

### 3.1 Total Force of the Rotor

The resultant force of the rotor can be resolved into three main components. We may choose any reference axis for the analysis such as axis of no feathering (control axis), tip path axis or shaft axis. In all these cases the component of the resultant force along the axis is the thrust. The component perpendicular to the axis and pointing rearward is the H force and the

component pointing sideward and normal to axis is Y force. The Y force magnitude is always small so that it is neglected in the analysis.

Calculation and experimental measurements reveal that the rotor resultant force is about normal to tip path plane with a small backward angle.

Fig ( 3.1 ) shows thrust and H forces relative to the no feathering axis and tip path plane. Subscript D refers to the tip path plane. Since there is only a small angle between $T_D$ and T (this angle is $a_1$ ) the magnitudes of T and $T_D$ are almost equal.

Bramwell [18] shows that thrust coefficient and H force coefficient relative to tip path plane axis are

$$t_{c_D} = C_T = \frac{a}{4}\left[\frac{2}{3}\theta_0\left(1+3\mu^2/2\right)+\lambda_D-\mu\, a_1\right] \qquad (3.1)$$

$$h_{c_D} = \frac{1}{4}\mu\delta + \frac{a\mu\lambda_D}{4}\left[\frac{(\theta_0/3)(1-9\mu^2/2)}{1+3\mu^2/2} + \frac{\lambda_d}{1+3\mu^2/2}\right] \qquad (3.2)$$

Comparing equations 3.1 and 3.2, Bramwell suggests $T_D >> H_D$. Therefore, $H_D$ will be neglected here so that T is then normal to the tip path plane.

## 3.2 The Windmill Performance Parameters

### 3.2.1 Force equilibrium on the Rotorcraft

To define the windmill performance parameters of the gyromill it is helpful to describe the forces which act on the gyromill.

Fig ( 3.2 ) shows the tethered system. The forces involved are thrust, machine weight, and the tension force of the tether. It will be assumed that the tether is weightless and completely straight under tension. $\beta'$ is the angle between the tether and the horizon and this is called the tether angle.

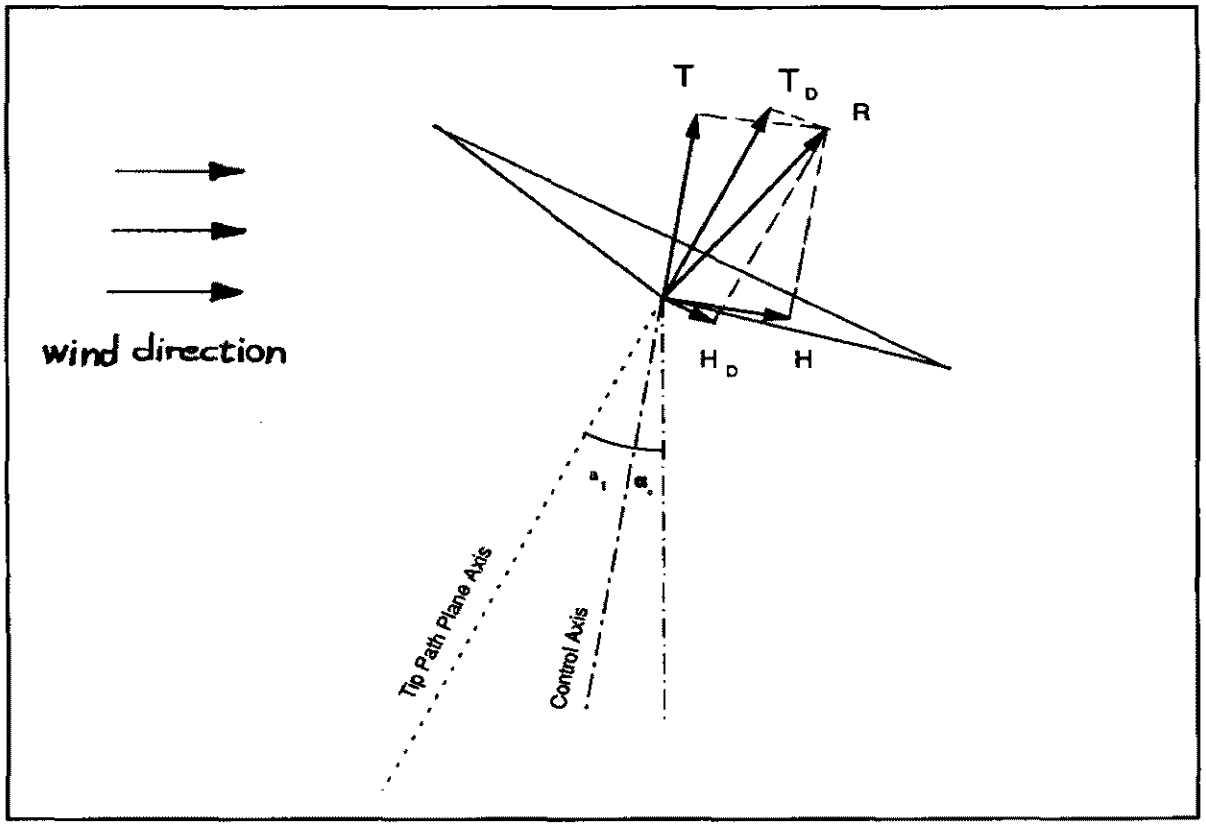


**Fig (3.1) Thrust and H forces relative to the control axis and tip path plane.**

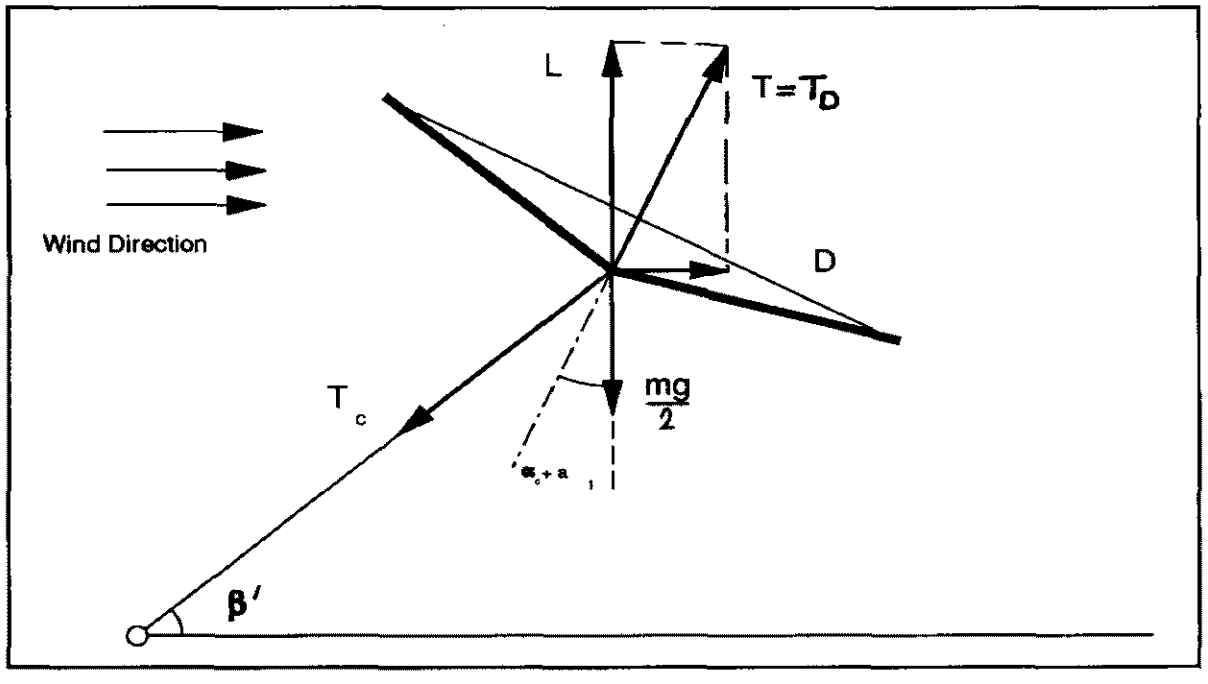


**Fig (3.2) The tethered system**

### 3.2.2 Relationship Between Helicopter and Windmill Parameters

It is useful to compare the thrust and power coefficients when defined from helicopter theory compared to windmill theory. The windmill parameters then can be linked to the helicopter parameters, such as $C_T$, $C_Q$, $C_P$ by the following analyses.

### 3.2.3 Windmill Power Coefficient

Windmill power coefficient is defined as the power available at the shaft of the rotor divided by the kinetic energy in the oncoming cylinder of air of cross-section equal to the rotor disk area. So it follows that

$$C_{PW} = \frac{C_p \rho \pi R^2 (\Omega R)^3}{\frac{1}{2}\rho V^3 \pi R^2} = 2C_p\left(\frac{\Omega R}{V}\right)^3 \qquad (3.3)$$

Nothing that in the helicopter terminology $C_P = C_Q$ and considering eq.( 2.2) one obtains

$$\frac{\Omega R}{V} = \frac{\cos\alpha_c}{\mu} \qquad (3.4)$$

Hence it follows that

$$C_{PW} = 2C_Q\left(\frac{\cos\alpha_c}{\mu}\right)^3 \qquad (3.5)$$

### 3.2.4 Windmill Thrust and Lift Coefficients

In helicopter theory the thrust coefficient is defined as

$$C_T = \frac{T}{\rho \pi R^2 (\Omega R)^2} \qquad (3.6)$$

For a conventional windmill the definition of thrust coefficient is

$$C_{TW} = \frac{T}{\frac{1}{2} \rho \pi R^2 V^2} \qquad (3.7)$$

Divide eq. ( 3.6 ) by ( 3.5 ) and combine with eq. ( 3.4 ) gives

$$C_{TW} = 2 C_T \left(\frac{\cos\alpha_C}{\mu}\right)^2 \qquad (3.8)$$

where $C_{TW}$ is the windmill thrust coefficient.

From fig ( 3.2 ) it can be seen that

$$L = T \cos(\alpha_C + a_1) \qquad (3.9)$$

or in nondimensional from

$$C_{LW} = C_{TW} \cos(\alpha_C + a_1) \qquad (3.10)$$

Substitute ( 3.8 ) in ( 3.10 ) to give

$$C_{LW}=2C_T\left(\frac{\cos\alpha_C}{\mu}\right)^2\cos(\alpha_C+a_1) \qquad (3.11)$$

where $C_{LW}$ is the windmill lift coefficient.

### 3.2.5 Windmill Torque Coefficient

Form the definition of windmill power coefficient we can write

$$C_{PW}=\frac{P}{\frac{1}{2}\rho V^3\pi R^2} \qquad (3.12)$$

since

$$P = Q\,\Omega$$

It follows that

$$C_{PW}=\frac{Q\Omega}{\frac{1}{2}\rho V^3\pi R^2}=\left(\frac{\Omega R}{V}\right)\left(\frac{Q}{\frac{1}{2}\rho\pi R^3V^2}\right)=\left(\frac{\cos\alpha_C}{\mu}\right)C_{QW} \qquad (3.13)$$

and the expression for the windmill torque coefficient is

$$C_{QW}=C_{PW}\left(\frac{\mu}{\cos\alpha_C}\right) \qquad (3.14)$$

### 3.2.6 Operation at a Constant Tether Angle ( $\beta'$ )

**In this thesis it will be assumed that the angle between the tether and the ground is constant during any particular trimmed operation. As a result the forces acting on the rotor in fig ( 3.2 ) will be in equilibrium.**

**Hence**

$$\sum F_X = 0 \quad , \quad \sum F_Y = 0$$

Assume only half the weight is supported by each rotor

$$L - \frac{mg}{2} - T_C \sin\beta' = 0 \qquad (3.15)$$

$$T \sin(\alpha_C + a_1) - T_C \cos\beta' = 0 \qquad (3.16)$$

**Using windmill parameters these can be rewritten as**

$$\frac{1}{2} C_{LW} \rho V^2 \pi R^2 - \frac{mg}{2} - T_C \sin\beta' = 0 \qquad (3.17)$$

$$\frac{1}{2} \tan(\alpha_C + a_1) C_{LW} \rho V^2 \pi R^2 - T_C \cos\beta' = 0 \qquad (3.18)$$

**Solve ( 3.18 ) for $T_c$ and substitute in ( 3.17 ) give**

$$C_{LW} \left(1 - \tan(\alpha_C + a_1) \tan\beta'\right) = \frac{\dfrac{mg}{2\pi R^2}}{\dfrac{1}{2}\rho V^2} \qquad (3.19)$$

In eq. ( 3.19 ) mg /$2\pi R^2$ is the disk loading and $1/2\rho V^2$ represents the dynamic pressure of the on coming flow. The left hand side of eq. ( 3.19 ) is an important function. Its value is the disk loading to the dynamic pressure ratio.

From fig ( 3.2 ) it can be seen that when the thrust vector and the tether tension vector are parallel then

$$\tan(\alpha_c + a_1)\tan\beta' = 1 \qquad (3.20)$$

or

$$\alpha_c + a_1 = 90° - \beta' \qquad (3.21)$$

In these circumstances the left hand side of eq. ( 3.19 ) will be zero. This condition represents maximum possible tip path incidence angle ( $\alpha_c + a_1$ ), beyond which operation is not possible. This is because that equation ( 3.19 ) will be negative if ($\alpha_c + a_1$) is greater than $90° - \beta'$ . In practice the disk loading to dynamic pressure ratio which is given in eq. ( 3.19 ) should be well above zero. Therefore the practical operational incidence angle,($\alpha_C + a_1$), should be lower than the value given by eq. ( 3.21 ) .

It is evident that if the rotorcraft is designed to give higher values for the left hand side of eq. ( 3.19 ), we will be able to keep the system aloft in lower wind speedsfor a given weight.

### 3.2.7 The Optimum Twist Criterion

Firstly this optimum condition should be defined. Then the best twist can be selected to satisfy this optimum condition. Analytical optimisation is complicated because of the complexity of the performance equations. So that it has been decided to formulate a numerical optimisation scheme.

This scheme will be based on the Gessow and Crim extended rotor theory.

In future chapters the relative effects of the operational variables on the performance parameters will be discussed, and then the best linear twist criterion will be decided.

It should also be pointed out that in this thesis the term twist means linear twist. However, the ideal twist might will be of a non-linear form and then the manufacture will be difficult and costly. A matter of future interest might be to consider an optimum twist distribution.

# CHAPTER FOUR

## The Computer Program

As stated before, the extended theory developed by Gessow and Crim is the most appropriate theory to be used here. It can be readily applied in our optimisation study for the aerodynamic performance of the gyromill.

This theory is coded as a computer program[1] to determine the performance characteristic of the gyromill.

The theory behind the program was fully discussed in chapter two. To use this program here its logic should be fully understood. Then it can be modified to cover the aspects discussed in chapter 3 and those in the coming sections. The results will cover operational conditions for windmilling and autorotation states.

---

[1]*The current program is a development of an original program by Ho and Roberts.*

## 4.1 Limitations of the Theory

At high tip speed ratios and large incidence angles the stall conditions can be significant. As discussed in section 2.6, the results predicted by the theory become very optimistic when the angle of attack ( $\alpha_r$ ) on the retreating blade goes beyond the stall limit. The stall limit depends upon the type of airfoil and can be between 12° to 16° as suggested by Gessow for NACA 0012 airfoils [12] ( p. 257 ). Roberts and Blackler [1] suggest that the stall limit can be around 15° for some airfoils. The limit will be taken as 13° for this study. Dynamic stall effects are not considered.
In the autorotation and windmill states the stall often begins at the edge of the reversed flow region and spreads outboard.

The angle of attack will be evaluated at two representative stations along the blade. This ensures that these angles of attack are both at or lower than the stall limit. These sections are chosen arbitrarily at stations where $U_T/\Omega R$ = 0.4 and 1.0, namely one inboard and one outboard. The method described in section 2.6 will be used to evaluate the blade element angle of attack at these section. From eq. (2.50) it can be shown that after Bailey

$$\alpha_{(1.0)(270°)} = \theta_0 + \theta_1(1+\mu) + \frac{\lambda}{1} + (1+\mu)a_1 \qquad (4.1)^*$$

$$\alpha_{(0.4)(270°)} = \theta_0 + \theta_1(0.4+\mu) + \frac{\lambda}{0.4} + (1+\frac{\mu}{0.4})a_1 \qquad (4.2)$$

* Eq. (4.1) is used throughout this thesis as a mathematical means by which to apply the condition $\alpha_{(1.0)(270°)} \leqslant 13°$ using Bailey's theory. It should be remembered that this condition gives an $x$ value greater than unity where $\psi = 270°$, which is a station off the end of the blade tip. ( $\alpha_{(1.0)(270°)}$ is $\alpha_{(u_T=1,\ \psi=270°)}$ )

where $\alpha_{(1.0)(270°)}$ is the angle of attack at 270° azimuth where the tangential velocity is equal to the rotational velocity. This station is physically

somewhere near the tip. By the same definition $\alpha_{(0.4)(270°)}$ is the angle of attack at $\psi = 270^0$ where tangential velocity is four tenths of the rotational velocity. Similarly this station is somewhere near the root of the blade.
Again it is emphasised that $\alpha_{(1.0)(270°)}$ and $\alpha_{(0.4)(270°)}$ should both be less than the chosen stall limit of 13°.

## 4.2 Program Development

The following developments have been added to the program

1. An iteration counter was used to terminate the iteration in the absence of convergence.
2. An error control procedure was added to ensure the accuracy of the results.
3. The solution will not converge for negative or unreal values of $\lambda$. A check point was used to stop the iteration in any of the above conditions.
4. The program was enhanced to calculate two positive values of $\lambda$ if they existed.
5. The angle of attack at two blade stations was compared to the stall limit value discussed above.
6. The program covered all possible ranges of operation of tip speed ratio, collective pitch, torque coefficient and twist.
7. The program calculated some of the parameters defined in chapter 3.
8. A subroutine was added to sort the results based on a variable defined within the call statement.

9. A subroutine was added to evaluate the maximum value of a variable which was stored in an array.
10. The program was also enhanced to select optimum values of certain variables.

## 4.3 The Program's Flowchart

The following steps are undertaken to evaluate the performance parameters.

1. Acquisition of rotor geometry, blade profile characteristics, tether angle and some design variables including
   a, B, $\bar{C}_l$ , $\bar{C}_{d_0}$ ,$\sigma$ , $\delta_0$, $\delta_1$, $\delta_2$, $\beta'$ , stall limit.
2. Acquisition of the operational variables such as $C_Q/\sigma$, $\mu$,$\theta_0$, $\theta_1$.
3. Initial values of $a_0$, $a_1$, $a_2$, $b_1$, $b_2$, $\lambda$ as chosen for the iteration process.
4. Equation ( 2.43 ) can be rearranged as a second order equation in $\lambda$ as*
   $$AA\,\lambda^2 + BB\,\lambda + CC = 0$$
5. Solve for $\lambda$ and choose the positive value as the solution. Note that $\lambda$ is positive for the windmill and autorotation states.
6. Terminate the iteration if there is no positive real solution for $\lambda$.
7. Check if the above value of $\lambda$ is the same as that which it was for the previous iteration. If yes, go to step 9.
8. Substitute $\lambda$ in eqs. ( 2.38 ) to ( 2.42 ) and solve these five equations simultaneously for $a_0$, $a_1$, $a_2$, $b_1$, $b_2$.
9. Repeat steps 4 to 8 unless step 7 is true.
10. Calculate $\alpha_{(1.0)\,(270°)}$, $\alpha_{(0.4)\,(270°)}$
11. Check if $\alpha_{(1.0)\,(270°)}$ and $\alpha_{(0.4)\,(270°)}$ are less than the stall limit. Ascertain if $\alpha_{(1.0)\,(270°)}$ or $\alpha_{(0.4)\,(270°)}$ are very close to stall limit.
12. Go to step 2 if 11 is not true.

* AA, BB, CC are the coefficients of quadratic equation in $\lambda$.

13. Calculate the following parameters and store them in arrays if step 11 is true:[2]

$C_T$, $C_Q$ , $C_{TW}$ , $C_{LW}$ , $C_{PW}$ , $C_{QW}$ , $C_{LWOP}$ , $\alpha_C$

$C_{LW} \times C_{PW}$ , $C_{LWOP} \times C_{PW}$ , $C_{LWOP} \times C_{QW}$

13. Write the results to the output file with an appropriate format.

There are two subroutines which were added to the program, namely

1. SUBROUTINE SORT

This subroutine sorts the data stored in the arrays based on a variable defined in the CALL statement.

2. SUBROUTINE MAX

This subroutine finds the maximum value in an array and stores it into another array.

These two subroutines are used in conjunction with the main program to compare data and to determine the optimum values.

[2] *$C_{LWOP}$ is defined as the disk loading to dynamic pressure ratio, See eq. (3.19).*

## 4.4 Input Data Used in the Analyses

**Input data used for the current optimisation calculations relate to the latest machine namely, gyromill MK3.**

- **The blade airfoil is NACA 0012. For this airfoil the values of section profile drag and lift coefficient are given in reference [4] as**

  $C_l = 5.73\ \alpha_r$

  $C_{d0} = 0.0087 - 0.0216\ \alpha_r + 0.4\ \alpha_r^2$

  **therefore it follows that**

  $a = 5.73,\ \ \delta_0 = 0.0087,\ \ \delta_1 = -0.0216,\ \ \delta_2 = 0.4$

- **The average lift and drag coefficients for the reversed velocity region are also suggested in reference [4] as**

  $\overline{C}_l = 1.2\ ,\quad \overline{C}_{d0} = 1.1$

- **A lock number of 10 is used.**

- **The solidity ratio , $\sigma = 0.05$ is used.**

- **Tip loss factor, B = 0.97, as suggested in the bulk of the literature.**

- **It is assumed that the tether angle to the ground is constant at a typical value of 40°.**

- **Blade element stall limit of 13° is used.**

## 4.5 Operational Range Considered in the Program

The computer program is used to calculate the performance of the rotor during windmill and autorotation modes. In a comprehensive manner it is possible to cover all values of operation for a specific twist.

The table below shows the full extent, step size and the total number of the main variables.

Table 4.1 Range of Operation

| Variable | Range of Variation | Size of each step | Total number of steps |
|---|---|---|---|
| Twist $\theta_1$ | $0 < \theta_1 < 24$ | 1° | 24 |
| Tip speed Ratio $\mu$ | $0.05 < \mu < 0.2$ | 0.0025 | 60 |
| Torque coefficient $C_Q$ | $0 < C_Q < 1.0973 \times 10^{-3}$ | 0.000625 | 35 |
| Collective pitch $\theta_0$ | $-40° < \theta_0 < 10°$ | 0.1 | 500 |

It should be appreciated that the above table represent about 25 million cases ranging form autorotation to extensive windmilling operations. This was a time consuming task but it ensured a full coverage of the twist effect.

# CHAPTER FIVE

## Optimisation Study and Results

The numerical data obtained for various operational conditions will be analysed in this chapter. The effect of the operational and design variables on the performance parameters can be understood by preparing the appropriate charts. Different criteria will be examined to determine the optimum twist.

## 5.1 The Influence of Operational and Design Variables on Windmill Power Coefficient

Form the data obtained it is possible to comment on the effect of collective pitch, control axis angle, tip speed ratio and twist on the variation of windmill power coefficient. This will be done via a series of graphs which will be discussed in the following sections.

### 5.1.1 The Effect of Control Axis Angle and Tip Speed Ratio on Windmill Power Coefficient

Figure ( 5.1 )* shows $C_{PW}$ plotted against the control axis angle ( $\alpha_C$ ) for a typical twist for four different tip speed ratios.

It can be seen from this graph that the maximum $C_{PW}$ is achieved at the least value of tip speed ratio. In other words at lower values of tip speed ratio $C_{PW}$ curves are sharper and higher. It can be shown that when $\mu = 0$ or $\alpha_C = 90°$, this corresponds to a conventional horizontal axis windmill. It will be shown later that operation at such a control axis angle is not possible for the gyromill.

Form fig ( 5.1 ) it is also seen that the possible range of $\alpha_C$ for each $\mu$ is broader at higher values of tip speed ratio, although, the peak value of $C_{PW}$ falls dramatically. In this graph the abscissa represents the autorotation line, where $C_{PW}$ equals zero.

Fig ( 5.2 ) shows the maximum obtainable value of $C_{PW}$ as a function of $\mu$.

It can be seen that the highest value of $C_{PW}$ is achieved at the least tip speed ratio. Also the control axis angle for maximum $C_{PW}$ decreases as tip speed ratio increases.

### 5.1.2 Variation of $C_{PW}$ with Collective Pitch Angle ($\theta_0$)

The data obtained from the program gives valuable information about the influence of collective pitch on $C_{PW}$.

Fig ( 5.3 ) shows the relationship between $C_{PW}$ and $\theta_0$ (collective pitch) for a typical value of twist. It can been seen that the collective pitch range is almost the same for all tip speed ratios. The beginning and the end of this

*In Figures (5.1),(5.2),(5.3) the value of twist was chosen arbitrarily for demonstration purposes only.

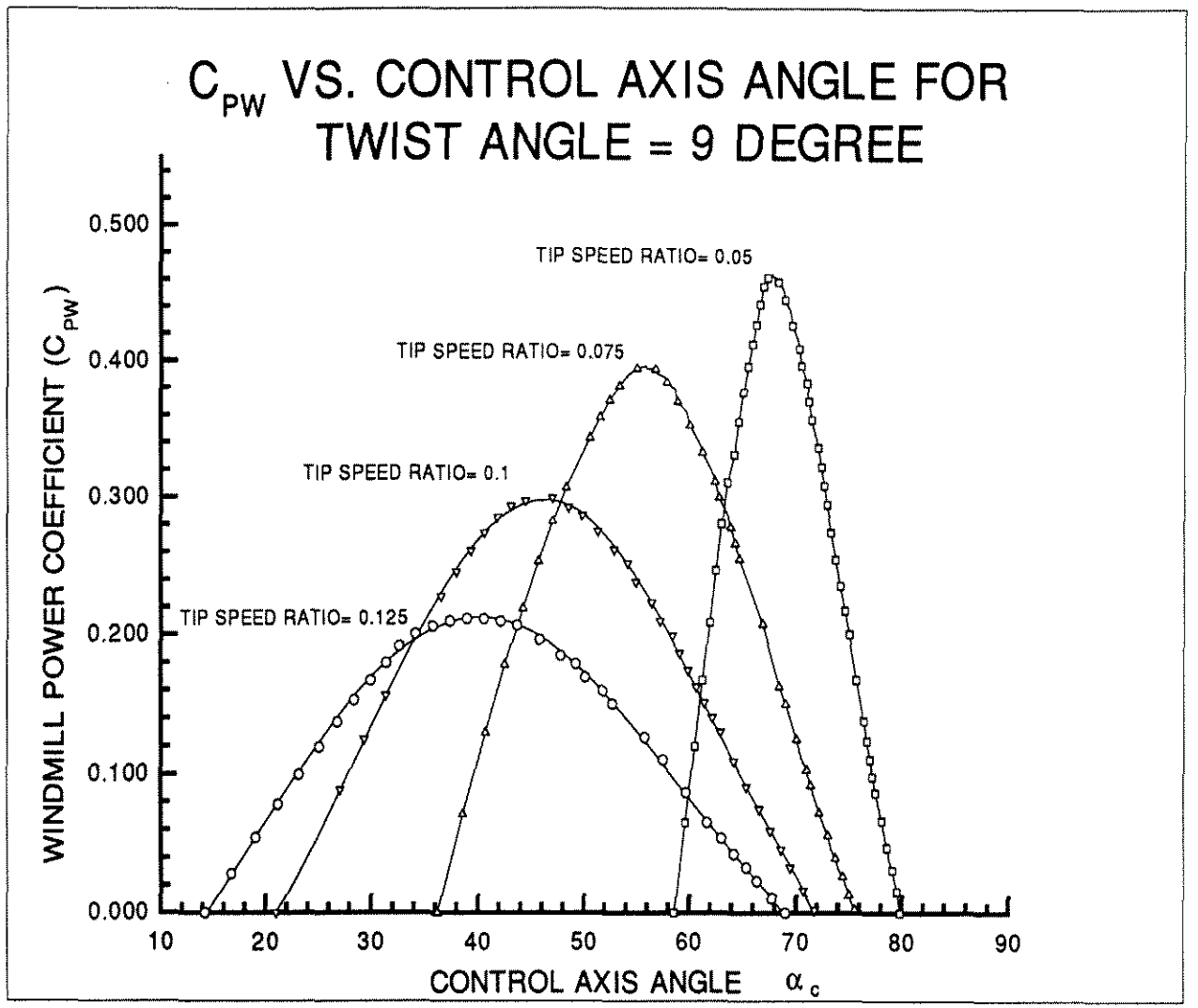
$C_{PW}$ VS. CONTROL AXIS ANGLE FOR
TWIST ANGLE = 9 DEGREE
WINDMILL POWER COEFFICIENT ($C_{PW}$)
0.500
0.400
0.300
0.200
0.100
0.000
TIP SPEED RATIO= 0.05
TIP SPEED RATIO= 0.075
TIP SPEED RATIO= 0.1
TIP SPEED RATIO= 0.125
10
20
30
40
50
60
70
80
90
CONTROL AXIS ANGLE $\alpha_c$

**Fig ( 5.1 )**

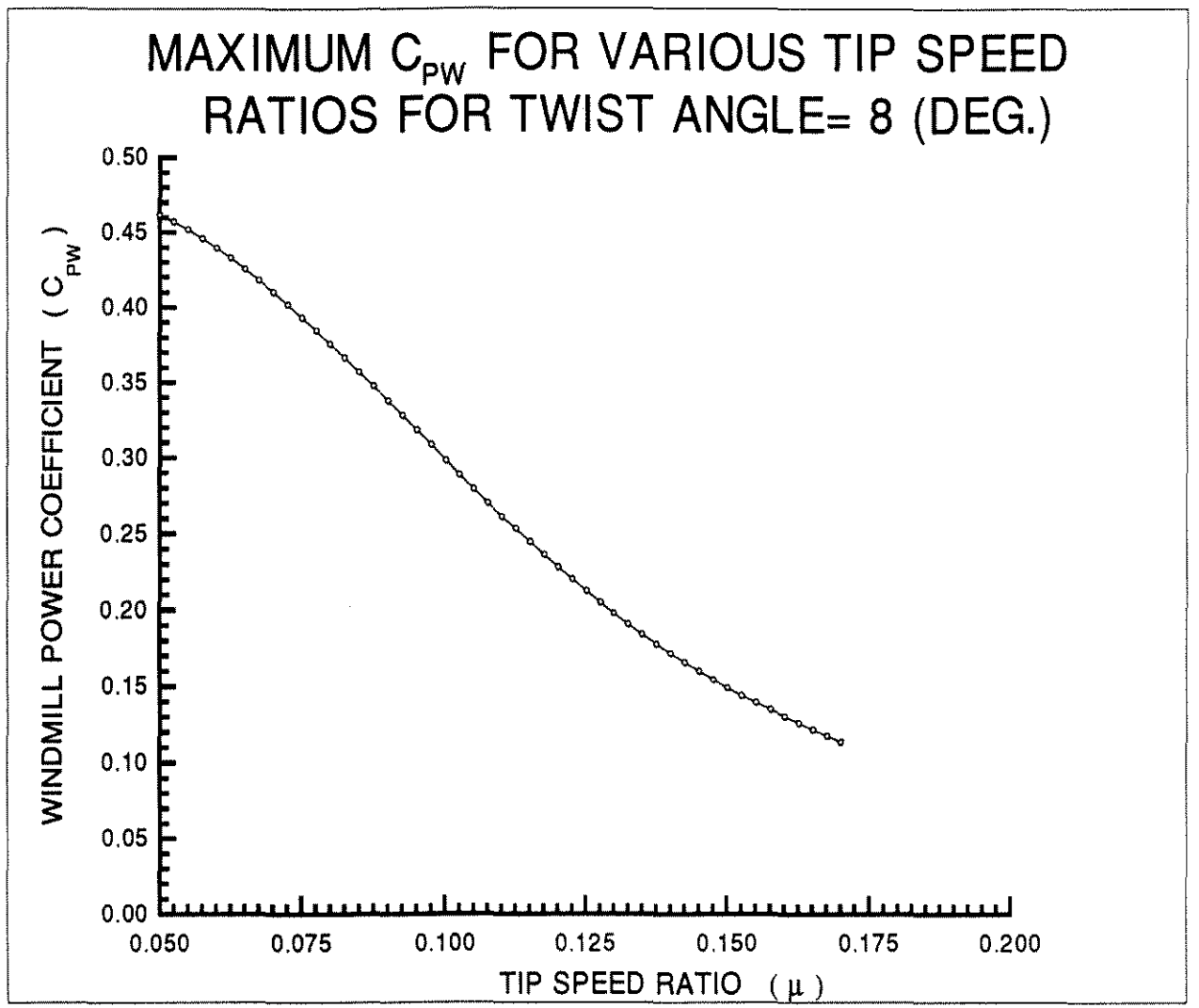
MAXIMUM $C_{PW}$ FOR VARIOUS TIP SPEED RATIOS FOR TWIST ANGLE= 8 (DEG.)
WINDMILL POWER COEFFICIENT ( $C_{PW}$ )
0.50
0.45
0.40
0.35
0.30
0.25
0.20
0.15
0.10
0.05
0.00
0.050
0.075
0.100
0.125
0.150
0.175
0.200
TIP SPEED RATIO ( μ )

Fig ( 5.2)

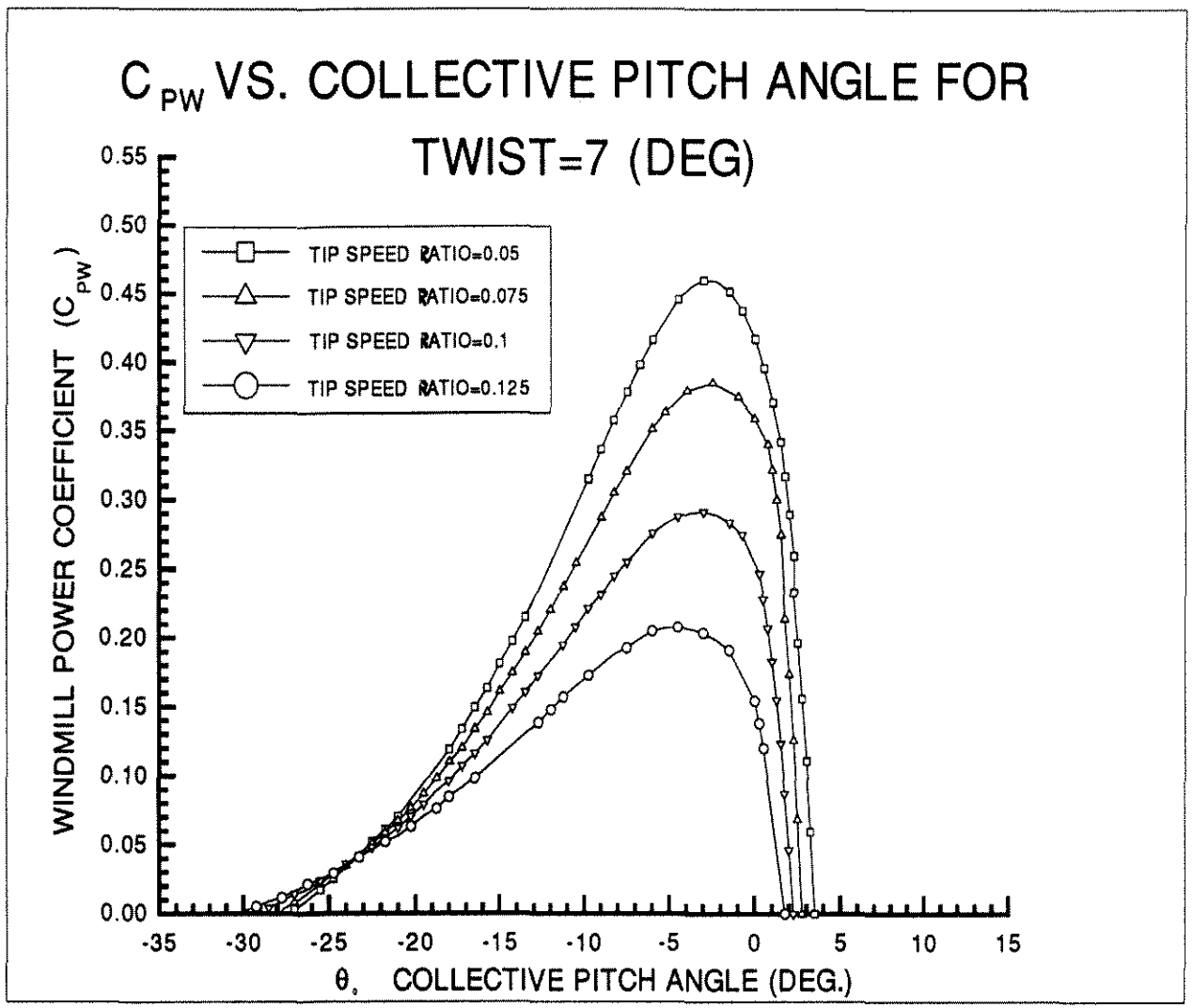
C PW VS. COLLECTIVE PITCH ANGLE FOR
TWIST=7 (DEG)
TIP SPEED RATIO=0.05
TIP SPEED RATIO=0.075
TIP SPEED RATIO=0.1
TIP SPEED RATIO=0.125
WINDMILL POWER COEFFICIENT (C PW)
0.55
0.50
0.45
0.40
0.35
0.30
0.25
0.20
0.15
0.10
0.05
0.00
-35
-30
-25
-20
-15
-10
-5
0
5
10
15
θ0 COLLECTIVE PITCH ANGLE (DEG.)

Fig ( 5.3 )

range shifts slightly to the left ( negative values of pitch ) as the tip speed ratio decreases.

It can also be seen from the same graph that $C_{PW}$ falls sharply as pitch increases near the right side of the curves. This implies that operation in this range is very sensitive to collective pitch changes and only a small change in collective pitch can have a significant effect on $C_{PW}$.

### 5.1.3 Influence of Twist on $C_{PW}$

Positive values of twist are usually used for windmilling operation. Data was obtained for twist angles between 0° and 24° for four typical values of $\mu$. This was done to examine the effect of twist on the power coefficient. The maximum value of $C_{PW}$ was chosen to compare the result in all cases.

Fig ( 5.4 ) shows how maximum $C_{PW}$ changes with twist. It can be seen that for each value of $\mu$ there is a peak point. The twist at this point could be chosen as the optimal. It can be seen that this optimal value is slightly dependant on $\mu$. It should be pointed out that this value is optimum when using the maximum $C_{PW}$ as the criterion.

Table ( 5.1 ) shows the improvement of $C_{PW}$ due to optimal twist compared to zero twist. The chart relates to four typical values of $\mu$.

**Table 5.1**

| $\mu$ | $C_{PW}$ | | Predicted Improvement in $C_{PW}$ % |
|---|---|---|---|
| | Twist = 0° | Best Twist | |
| 0.05 | 0.4467 | 0.4660 | 4.32 |
| 0.075 | 0.3665 | 0.4015 | 9.55 |
| 0.1 | 0.2669 | 0.3108 | 16.45 |
| 0.125 | 0.1863 | 0.2254 | 21 |

Fig ( 5.5 ) shows the optimum twist using $C_{PW}$ as the criterion. It is quite clear that the optimum twist depends upon the tip speed ratio. This optimal twist varies between 12° to 16° depending upon the value of $\mu$. The precision for twist in this graph is 1°. This is because the twist steps which were used in the program were 1°. More precise curves for optimum twist can be obtained by using finer steps. However, the program's run-time is dependant on the step size, and 1° was considered to be a reasonable lower limit.

## 5.2 The Influence of Operational Variables on the Windmill Lift Coefficient ( $C_{LW}$ )

One other important performance parameter is the lift coefficient, $C_{LW}$. Data has been prepared to examine the effects of the different variables on the value of $C_{LW}$. This will be now discussed.

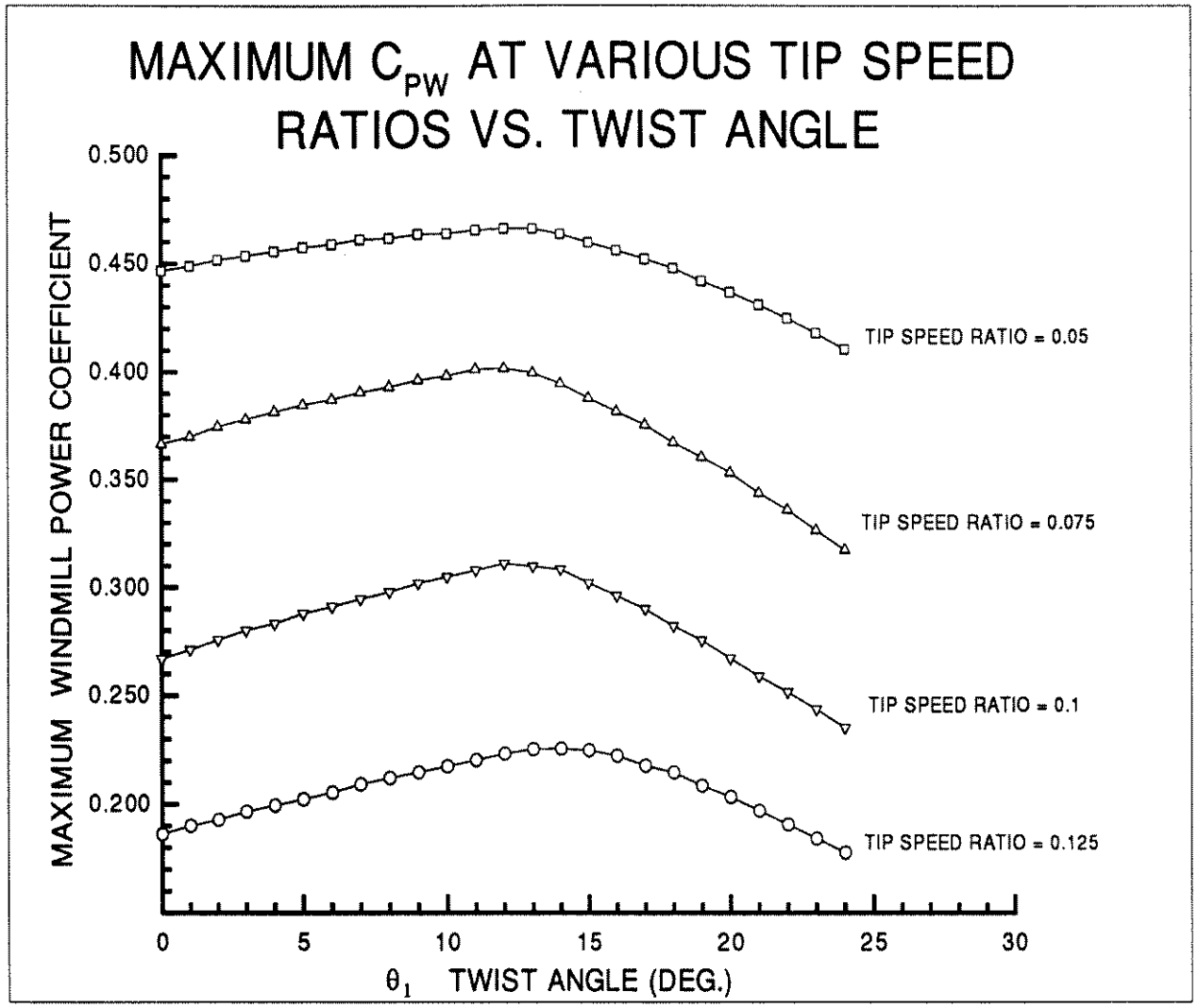
MAXIMUM $C_{PW}$ AT VARIOUS TIP SPEED RATIOS VS. TWIST ANGLE
MAXIMUM WINDMILL POWER COEFFICIENT
0.500
0.450
0.400
0.350
0.300
0.250
0.200
TIP SPEED RATIO = 0.05
TIP SPEED RATIO = 0.075
TIP SPEED RATIO = 0.1
TIP SPEED RATIO = 0.125
0
5
10
15
20
25
30
$\theta_1$ TWIST ANGLE (DEG.)

**Fig ( 5.4 )**

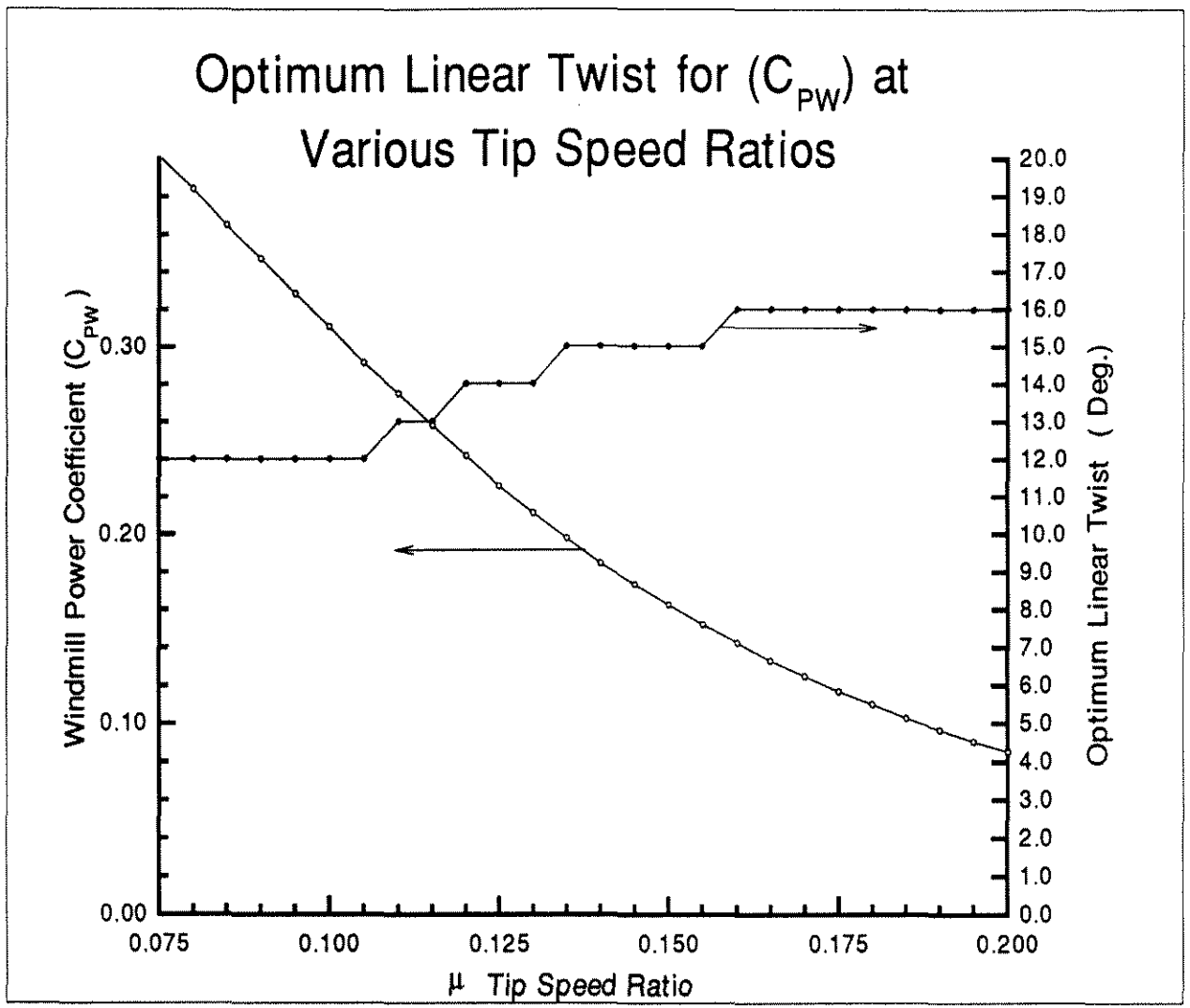
Optimum Linear Twist for ($C_{PW}$) at
Various Tip Speed Ratios
Windmill Power Coefficient ($C_{PW}$)
0.00
0.10
0.20
0.30
0.075
0.100
0.125
0.150
0.175
0.200
μ Tip Speed Ratio
Optimum Linear Twist ( Deg.)
0.0
1.0
2.0
3.0
4.0
5.0
6.0
7.0
8.0
9.0
10.0
11.0
12.0
13.0
14.0
15.0
16.0
17.0
18.0
19.0
20.0

**Fig ( 5.5 )**

### 5.2.1 The Influence of Tip Speed Ratio and Control Axis Angle

Fig ( 5.6 ) shows $C_{LW}$ potted against $\alpha_C$ for a typical value of twist. The following points can be seen in this graph.

- The range of $\alpha_C$ depends on $\mu$. This permissible range of $\alpha_C$ is more extensive for higher values of $\mu$.
- There is a maximum $C_{LW}$ for each value of $\mu$. These points are at the end of each curve and represent the condition at where the blade element angle of attack at $U_T = 0.4$ and $\psi = 270°$, reaches the 13° limit. These points also represent where $C_Q = 0$. ( See also Figs. (5.7) and (5.27))
- At large control axis angles we find the least value of $C_{LW}$.
- There is a particular $\mu$ value, namely $\mu = 0.075$, which produces the maximum possible $C_{LW}$. ( See also Fig. (5.7))

Fig ( 5.7 ) shows the $C_{LW}$ envelope for various values of $\mu$ with a twist of 8°. The thick line connecting the end point of each curve is the autorotation line. This line will separate the generating and motoring regions. The generating mode, as mentioned before, refers to the conditions where there is a useful energy output from the system. The motoring state requires an energy to the system, and hence $C_Q < 0$.

The dependence of the maximum value of $C_{LW}$ on $\mu$ can be seen in fig ( 5.8 ). This figure shows that the maximum value of $C_{LW}$ is achieved at $\mu = 0.075$ .

### 5.2.2 The Influence of Twist

The importance of twist in the determination of $C_{LW}$ can be seen in fig ( 5.9 ). This figure shows the maximum value of $C_{LW}$ for four typical values of $\mu$, each plotted against twist. This graph reveals that for each $\mu$ there is a twist

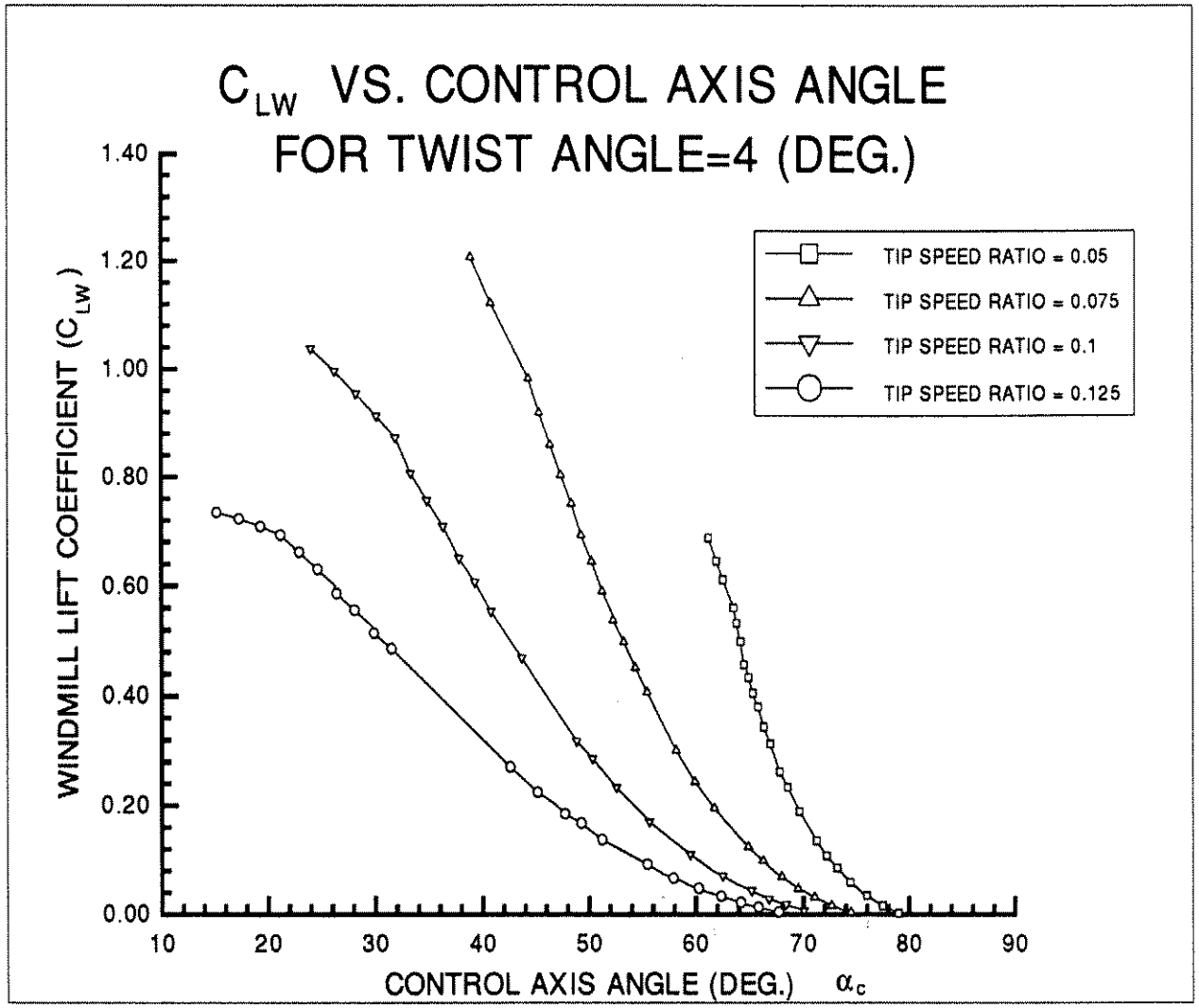
$C_{LW}$ VS. CONTROL AXIS ANGLE
FOR TWIST ANGLE=4 (DEG.)
WINDMILL LIFT COEFFICIENT ($C_{LW}$)
1.40
1.20
1.00
0.80
0.60
0.40
0.20
0.00
10
20
30
40
50
60
70
80
90
CONTROL AXIS ANGLE (DEG.) $\alpha_c$
TIP SPEED RATIO = 0.05
TIP SPEED RATIO = 0.075
TIP SPEED RATIO = 0.1
TIP SPEED RATIO = 0.125

**Fig ( 5.6 )**

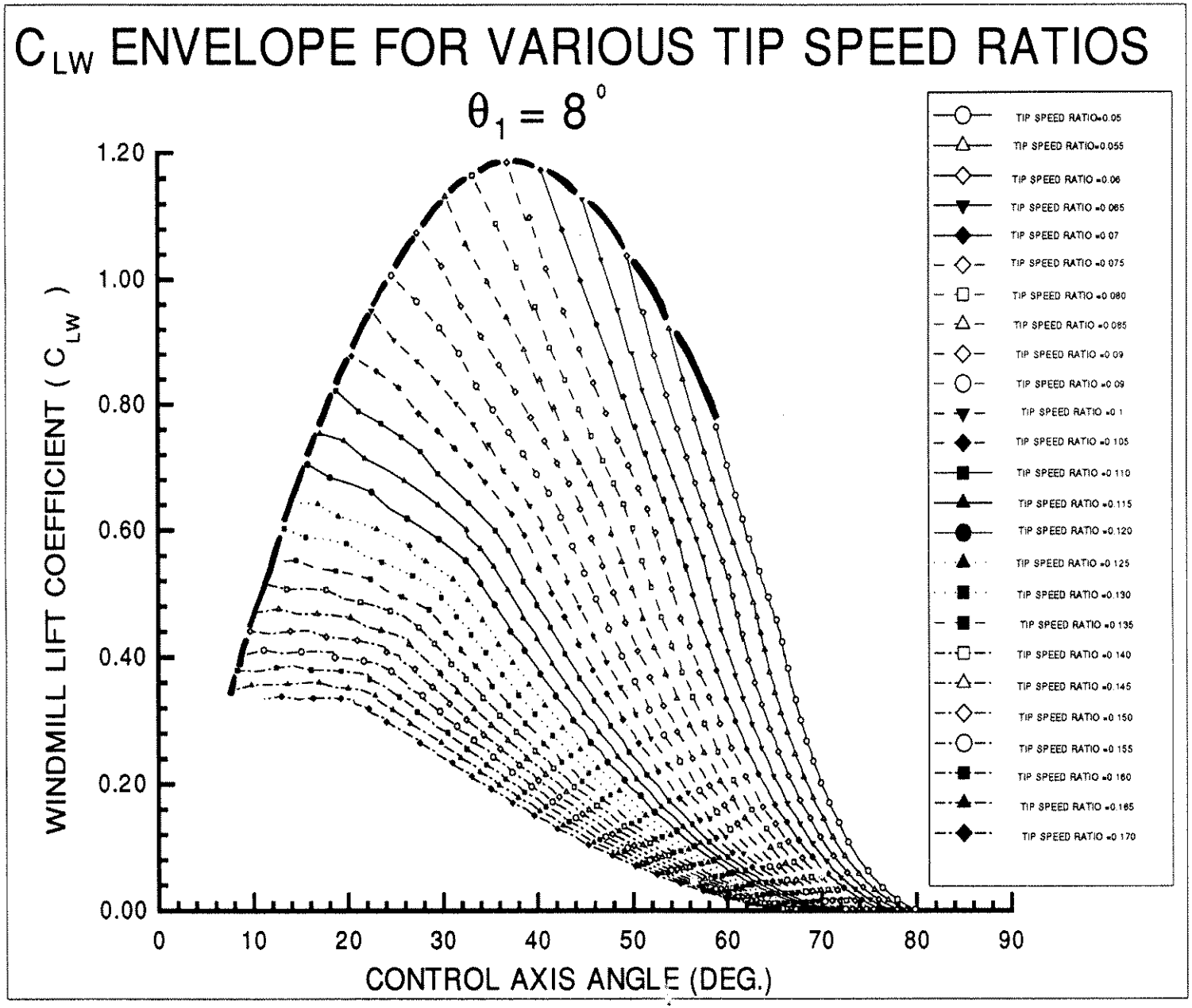
$C_{LW}$ ENVELOPE FOR VARIOUS TIP SPEED RATIOS
$\theta_1 = 8^0$
WINDMILL LIFT COEFFICIENT ( $C_{LW}$ )
1.20
1.00
0.80
0.60
0.40
0.20
0.00
0
10
20
30
40
50
60
70
80
90
CONTROL AXIS ANGLE (DEG.)
TIP SPEED RATIO=0.05
TIP SPEED RATIO=0.055
TIP SPEED RATIO =0.06
TIP SPEED RATIO =0.065
TIP SPEED RATIO =0.07
TIP SPEED RATIO =0.075
TIP SPEED RATIO =0.080
TIP SPEED RATIO =0.085
TIP SPEED RATIO =0.09
TIP SPEED RATIO =0.09
TIP SPEED RATIO =0.1
TIP SPEED RATIO =0.105
TIP SPEED RATIO =0.110
TIP SPEED RATIO =0.115
TIP SPEED RATIO =0.120
TIP SPEED RATIO =0.125
TIP SPEED RATIO =0.130
TIP SPEED RATIO =0.135
TIP SPEED RATIO =0.140
TIP SPEED RATIO =0.145
TIP SPEED RATIO =0.150
TIP SPEED RATIO =0.155
TIP SPEED RATIO =0.160
TIP SPEED RATIO =0.165
TIP SPEED RATIO =0.170

**Fig ( 5.7 )**

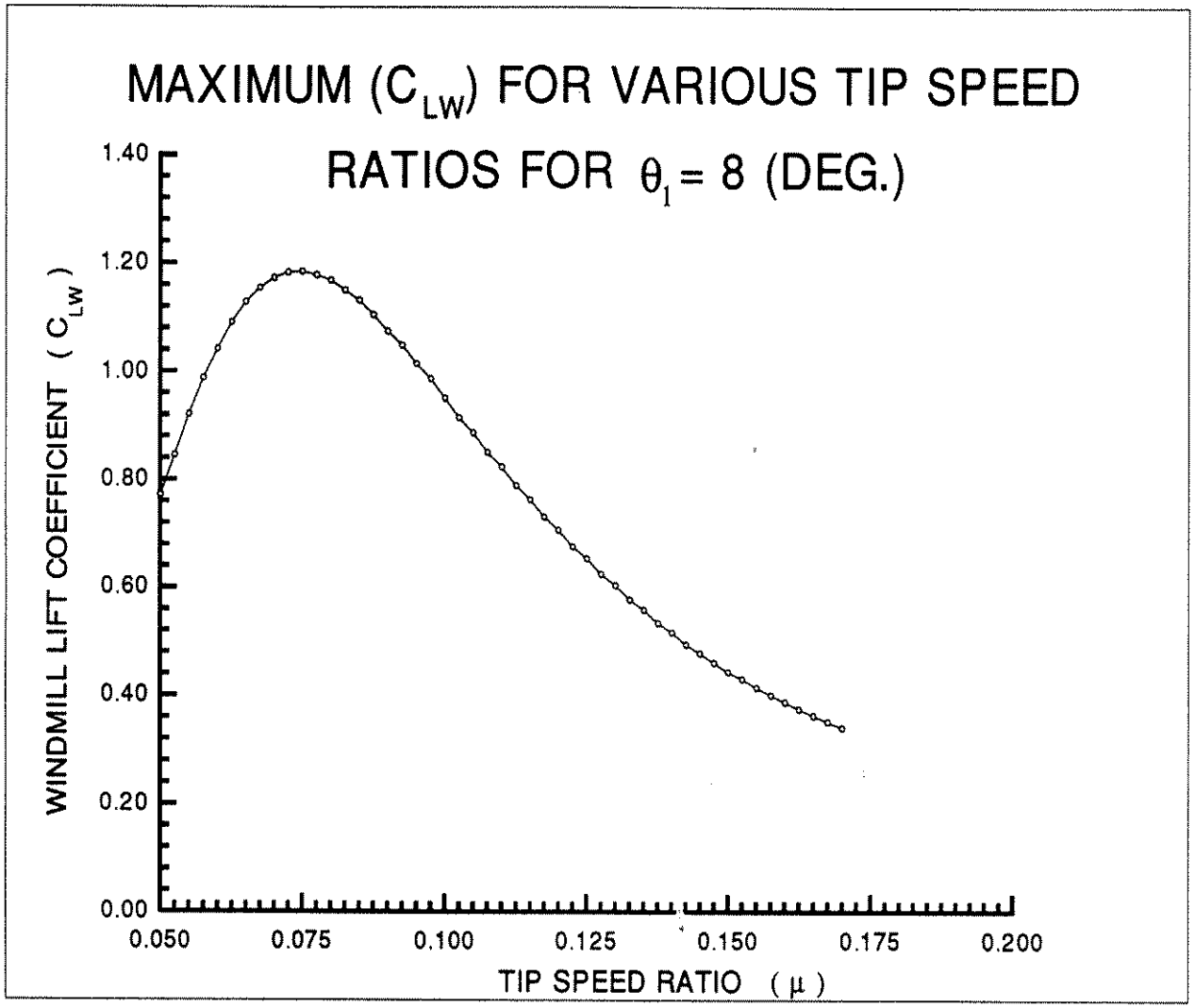
MAXIMUM ($C_{LW}$) FOR VARIOUS TIP SPEED
RATIOS FOR $\theta_1$ = 8 (DEG.)
WINDMILL LIFT COEFFICIENT ( $C_{LW}$ )
1.40
1.20
1.00
0.80
0.60
0.40
0.20
0.00
0.050
0.075
0.100
0.125
0.150
0.175
0.200
TIP SPEED RATIO ( $\mu$ )

**Fig ( 5.8 )**

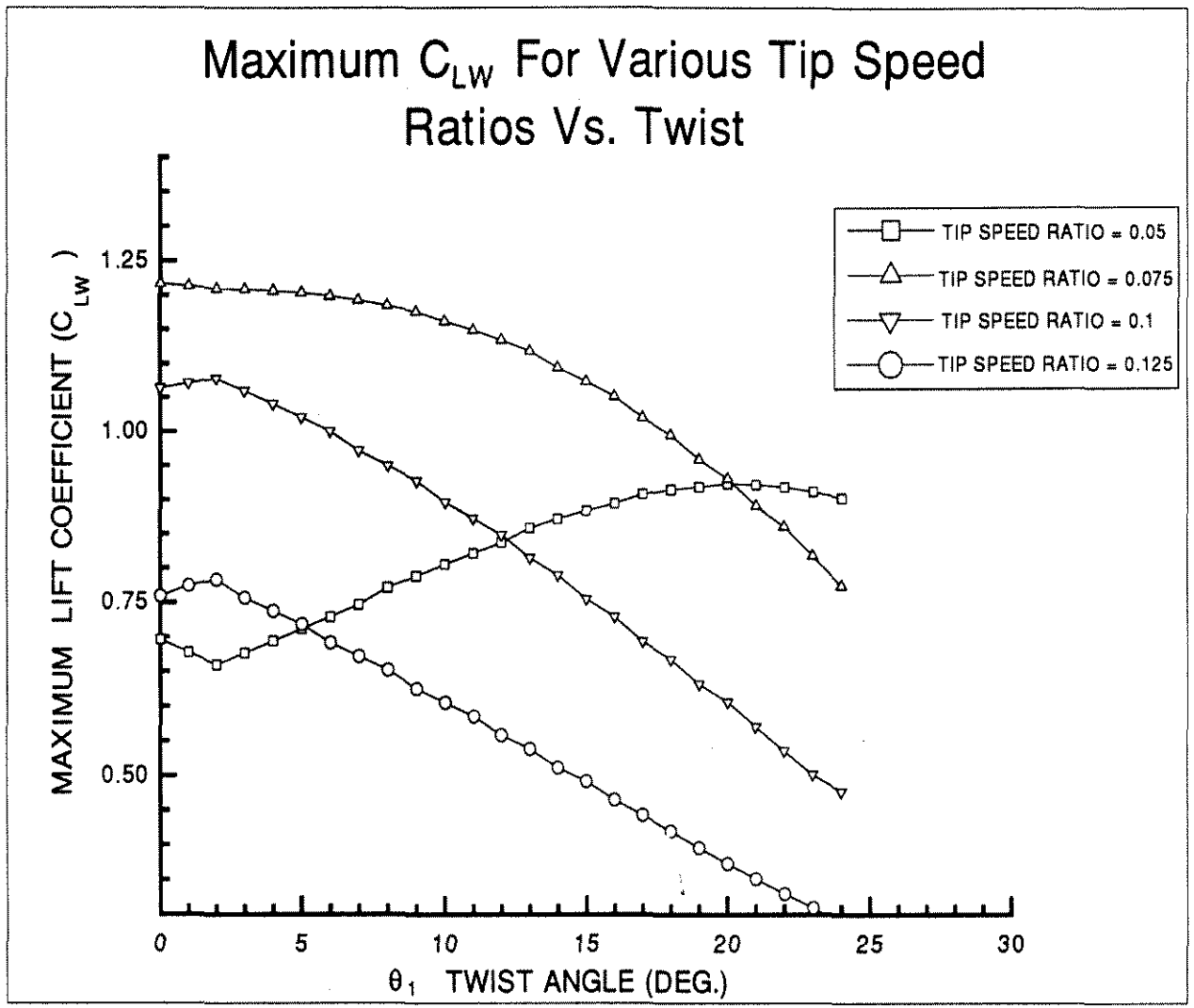


Fig ( 5.9 )

* The dramatic change in shape for $\mu = 0.05$ curve is believed by the author to be due to the change in gradiant $\frac{dC_{LW}}{d\mu}$ at these $\mu$ values. (See Fig 5.8)

at which $C_{LW}$ has its highest value. This best twist depends on $\mu$ and, except for $\mu = 0.05$, its value is around 2°.

Table 5.2 shows the percentage improvement in $C_{LW}$ for the best twist case compared to a twist of 13° as a reference which is used for MK2.

**Table 5.2**

| $\mu$ | $C_{LW}$ | | Predicted Improvement in $C_{LW}$ % |
|---|---|---|---|
| | Twist = 13° | Best Twist | |
| 0.05 | 0.8583 | 0.9224 | 9 |
| 0.075 | 1.1117 | 1.2168 | 19.4 |
| 0.1 | 0.8147 | 1.0784 | 32.4 |
| 0.125 | 0.5383 | 0.7832 | 45.5 |

### 5.2.3 Optimum Twist Using $C_{LW}$ as the Criterion

As we discussed in the previous section the best twist for obtaining the maximum $C_{LW}$ depends upon the tip speed ratio. Fig ( 5.10 ) shows the optimum twist using $C_{LW}$ as the criterion. The results clearly show that the optimum twist lies between 0 to 3 degrees, while a twist angle equal to 2° is dominant in the majority of tip speed ratio range.

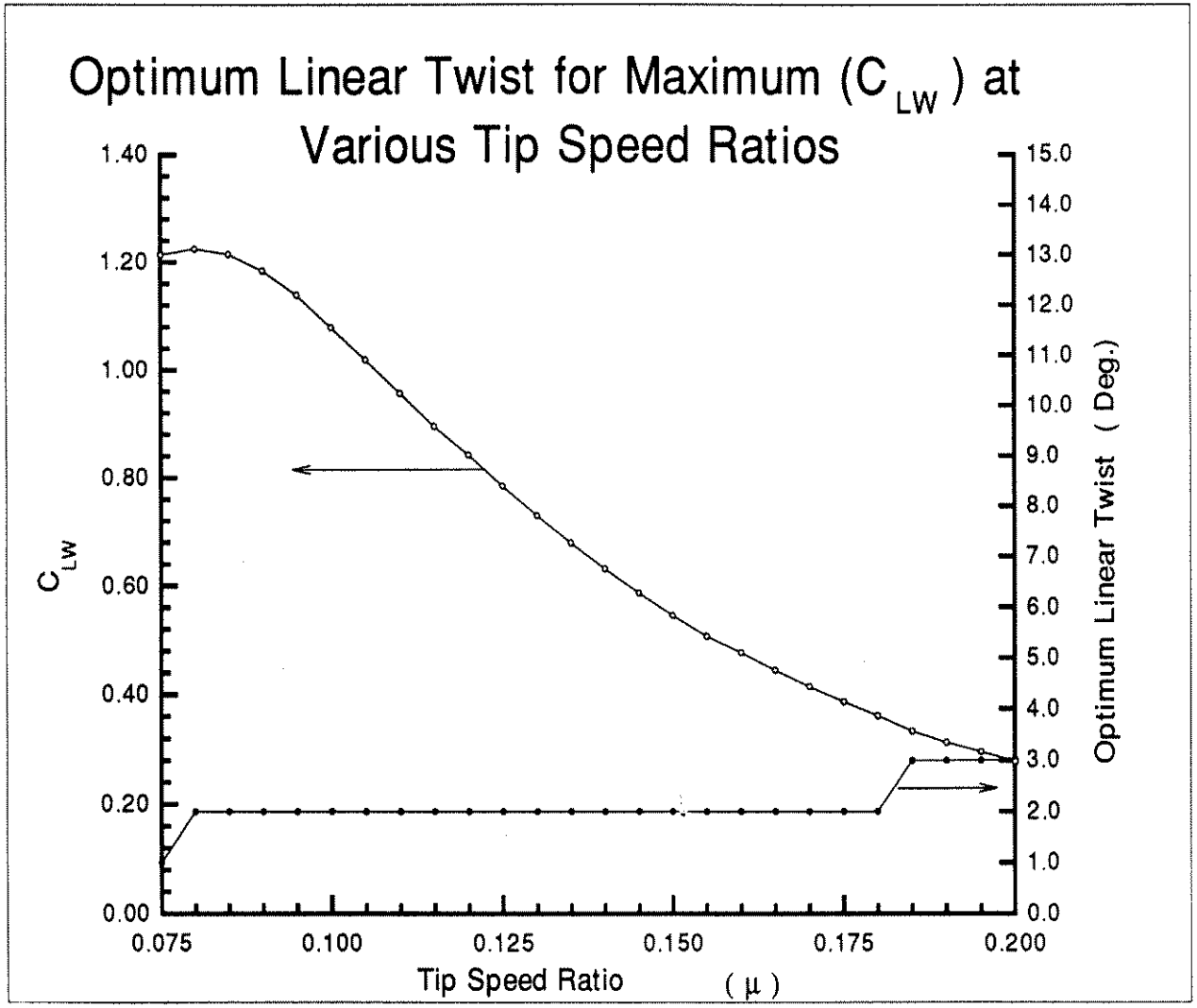
Optimum Linear Twist for Maximum ($C_{LW}$) at
Various Tip Speed Ratios
$C_{LW}$
1.40
1.20
1.00
0.80
0.60
0.40
0.20
0.00
0.075
0.100
0.125
0.150
0.175
0.200
Tip Speed Ratio ( μ )
15.0
14.0
13.0
12.0
11.0
10.0
9.0
8.0
7.0
6.0
5.0
4.0
3.0
2.0
1.0
0.0
Optimum Linear Twist ( Deg.)

**Fig ( 5.10 )**

## 5.3 The Effect of Operational Variables on the Disk loading to Dynamic Pressure Ratio

It was suggested in section 3.2.6 that for a chosen tether angle it is possible to define the disk loading to dynamic pressure ratio as expressed by eq. ( 3.19 ).

To simplify our analysis the left hand side of eq.( 3.19 ) will be defined by $C_{LWOP}$[1], hence

$$C_{LWOP} = C_{LW}(1 - \tan(\alpha_c + a_1)\tan\beta') \tag{5.1}$$

This nondimensional parameter is an important criterion in the current optimisation study. Because high values of $C_{LWOP}$ result in high payloads at low wind speeds, therefore one of our objectives will be to maximise the parameter $C_{LWOP}$.

### 5.3.1 Maximum Operational Control Axis Angle

Fig ( 5.11.a ) shows the $C_{LWOP}$ envelope, for various values of $\mu$, at a typical twist of 8°. The tether angle is constant and equal to 40°. From the figure it can be readily seen that for control axis angles higher than about 48° the value of $C_{LWOP}$ is always either equal to or less than zero. This occurs for all values of $\mu$.

---

[1]Eq. (5.1) is a *function of $C_{LW}$. It represents the ability of the system to produce enough lift for the tethered rotorcraft. This equation is also very important in any optimisation study. To acknowledge these two important factors, the notation $C_{LWOP}$ has been chosen where (OP)stands for optimisation.*

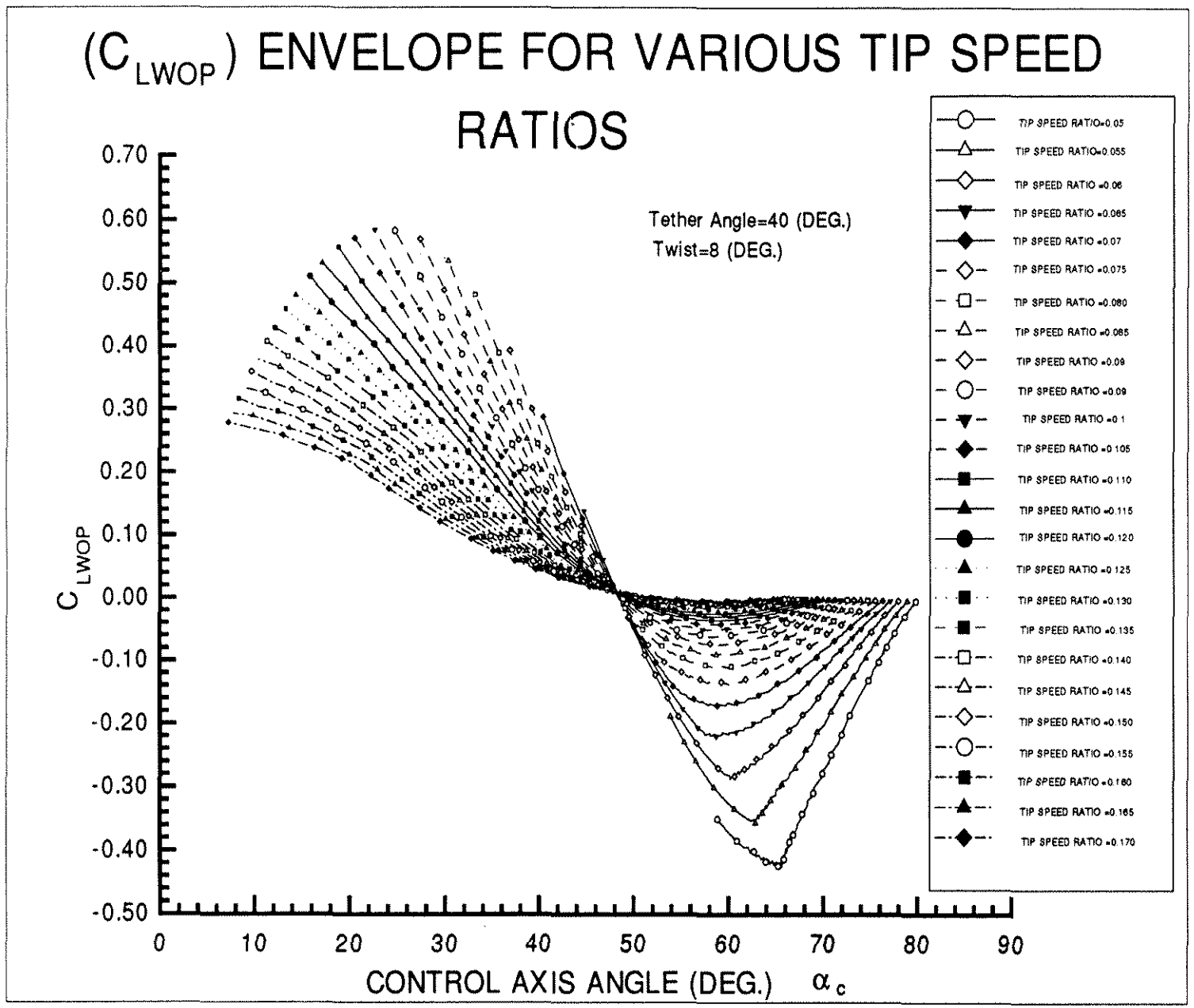
(C LWOP ) ENVELOPE FOR VARIOUS TIP SPEED RATIOS
Tether Angle=40 (DEG.)
Twist=8 (DEG.)
C LWOP
0.70
0.60
0.50
0.40
0.30
0.20
0.10
0.00
-0.10
-0.20
-0.30
-0.40
-0.50
0
10
20
30
40
50
60
70
80
90
CONTROL AXIS ANGLE (DEG.) α c
TIP SPEED RATIO=0.05
TIP SPEED RATIO=0.055
TIP SPEED RATIO =0.06
TIP SPEED RATIO =0.065
TIP SPEED RATIO =0.07
TIP SPEED RATIO =0.075
TIP SPEED RATIO =0.080
TIP SPEED RATIO =0.085
TIP SPEED RATIO =0.09
TIP SPEED RATIO =0.09
TIP SPEED RATIO =0.1
TIP SPEED RATIO =0.105
TIP SPEED RATIO =0.110
TIP SPEED RATIO =0.115
TIP SPEED RATIO =0.120
TIP SPEED RATIO =0.125
TIP SPEED RATIO =0.130
TIP SPEED RATIO =0.135
TIP SPEED RATIO =0.140
TIP SPEED RATIO =0.145
TIP SPEED RATIO =0.150
TIP SPEED RATIO =0.155
TIP SPEED RATIO =0.160
TIP SPEED RATIO =0.165
TIP SPEED RATIO =0.170

**Fig ( 5.11.a )**

This is the situation that was discussed in section 3.2.6 . In these conditions the tip path incidence angle is $(\alpha_C + a_1) > 90 - \beta'$ . Physically this means that it is not possible to operate the gyromill in any autorotation or windmilling modes. It is also evident that it is not possible to operate the system at even lower values of $\alpha_C$ unless eq. ( 3.19 ) is satisfied. Fig (5.11.b) shows the same graph for only positive values of $C_{LWOP}$ .

### 5.3.2 The Influence of Tip Speed Ratio on the Parameter $C_{LWOP}$

The results in fig (5.11.a) indicates that operation in windmilling or autorotation states will not be possible for $\mu$ lower than 0.065. This is because the value of $C_{LWOP}$ is always zero or less than zero at the values of $\mu$ less than 0.065. However, as $\mu$ increases, $C_{LWOP}$ reaches higher values. $C_{LWOP}$ has a peak value at $\mu = 0.0975$ and then falls again as $\mu$ increases. The value of $\mu$ at which $C_{LWOP}$ reaches the peak is slightly dependant on the twist. For example it equals 0.105 for twist of 0°. An average value of $\mu = 0.1$ is suggested as the best tip speed ratio for maximising $C_{LWOP}$ .

Fig ( 5.12 ) show the maximum value of $C_{LWOP}$ at different values of $\mu$. Also shown is the value of $\alpha_C$ at which this occurs.

### 5.3.3 The Influence of Twist on the Parameter $C_{LWOP}$

The maximum value of $C_{LWOP}$ at four typical values of $\mu$ was chosen to compare the results.

Fig ( 5.13 ) shows the effect of twist on $C_{LWOP}$. It can be seen that this effect is quite significant. There is a peak value for $C_{LWOP}$ depending on $\mu$. For $\mu$ values higher than 0.1 the best twist is about constant. Table 5.3 shows the

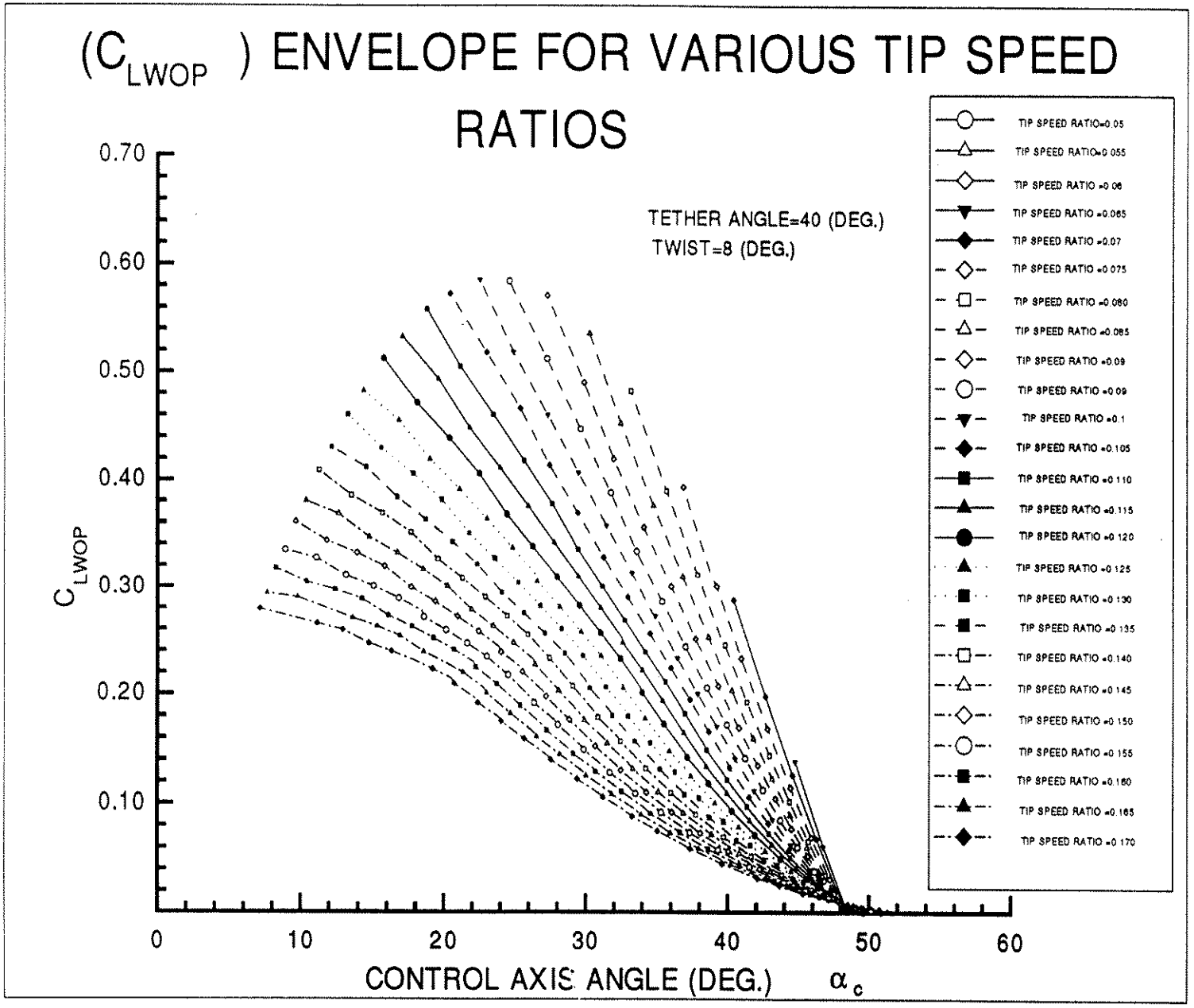
(C_LWOP ) ENVELOPE FOR VARIOUS TIP SPEED RATIOS
TETHER ANGLE=40 (DEG.)
TWIST=8 (DEG.)
C_LWOP
0.70
0.60
0.50
0.40
0.30
0.20
0.10
0
10
20
30
40
50
60
CONTROL AXIS ANGLE (DEG.) α_c
TIP SPEED RATIO=0.05
TIP SPEED RATIO=0.055
TIP SPEED RATIO =0.06
TIP SPEED RATIO =0.065
TIP SPEED RATIO =0.07
TIP SPEED RATIO =0.075
TIP SPEED RATIO =0.080
TIP SPEED RATIO =0.085
TIP SPEED RATIO =0.09
TIP SPEED RATIO =0.09
TIP SPEED RATIO =0.1
TIP SPEED RATIO =0.105
TIP SPEED RATIO =0.110
TIP SPEED RATIO =0.115
TIP SPEED RATIO =0.120
TIP SPEED RATIO =0.125
TIP SPEED RATIO =0.130
TIP SPEED RATIO =0.135
TIP SPEED RATIO =0.140
TIP SPEED RATIO =0.145
TIP SPEED RATIO =0.150
TIP SPEED RATIO =0.155
TIP SPEED RATIO =0.160
TIP SPEED RATIO =0.165
TIP SPEED RATIO =0.170

Fig (5.11.b)

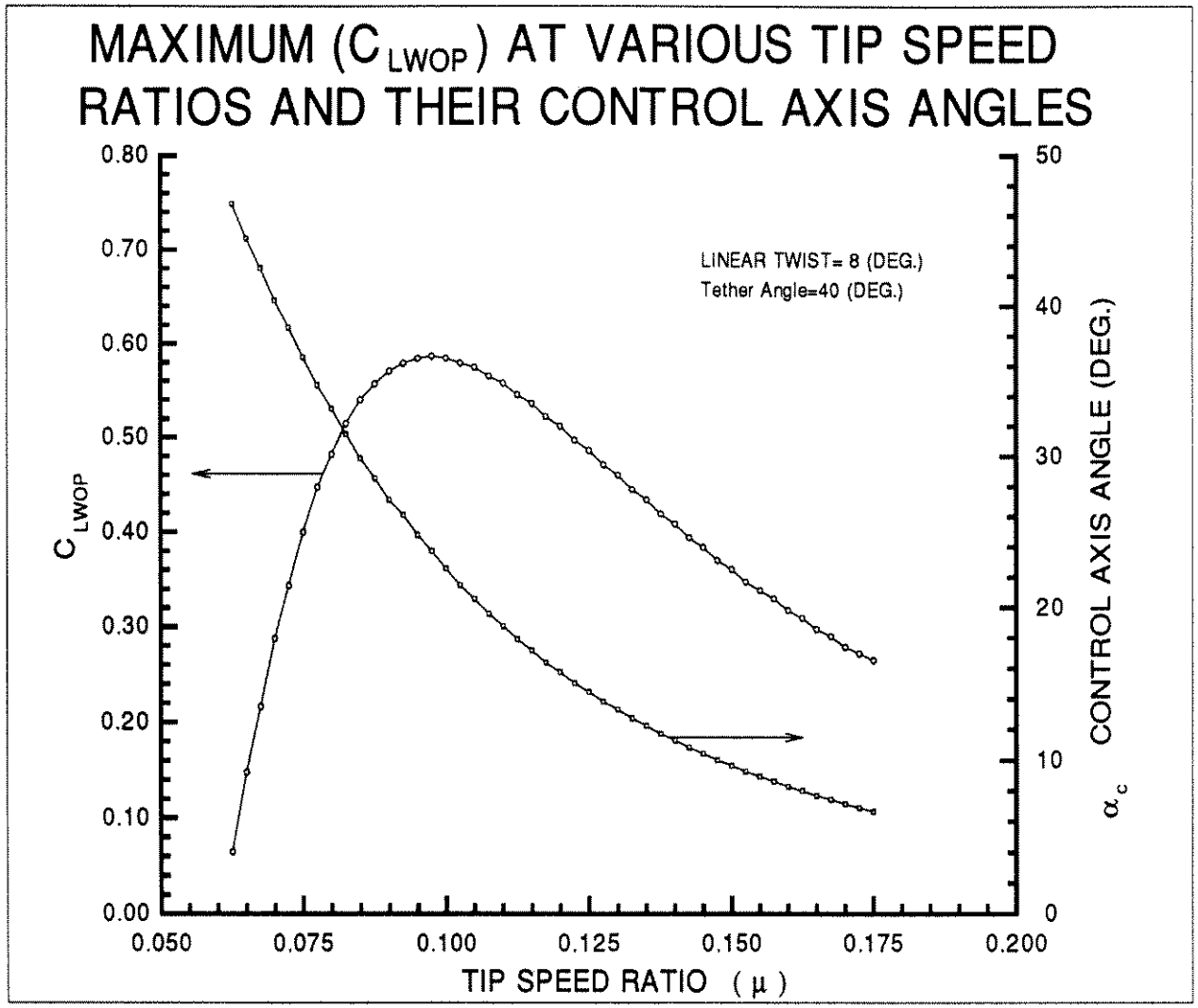
MAXIMUM ($C_{LWOP}$) AT VARIOUS TIP SPEED RATIOS AND THEIR CONTROL AXIS ANGLES
LINEAR TWIST= 8 (DEG.)
Tether Angle=40 (DEG.)
$C_{LWOP}$
0.00
0.10
0.20
0.30
0.40
0.50
0.60
0.70
0.80
0.050
0.075
0.100
0.125
0.150
0.175
0.200
TIP SPEED RATIO ( μ )
$\alpha_c$ CONTROL AXIS ANGLE (DEG.)
0
10
20
30
40
50

Fig ( 5.12 )

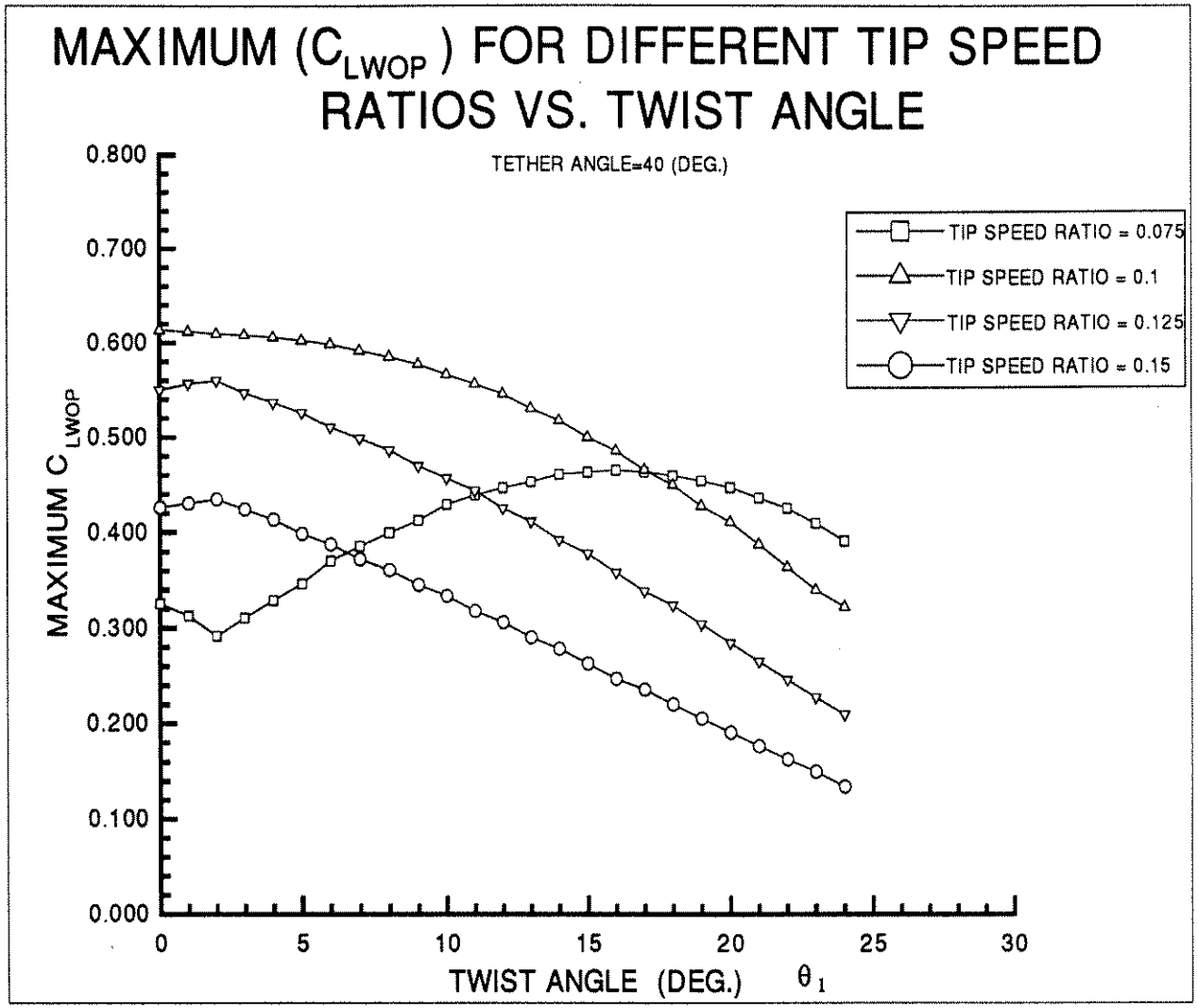
MAXIMUM ($C_{LWOP}$) FOR DIFFERENT TIP SPEED RATIOS VS. TWIST ANGLE
TETHER ANGLE=40 (DEG.)
TIP SPEED RATIO = 0.075
TIP SPEED RATIO = 0.1
TIP SPEED RATIO = 0.125
TIP SPEED RATIO = 0.15
MAXIMUM $C_{LWOP}$
0.800
0.700
0.600
0.500
0.400
0.300
0.200
0.100
0.000
0
5
10
15
20
25
30
TWIST ANGLE (DEG.) $\theta_1$

Fig ( 5.13 )

improvement in $C_{LWOP}$ using the best twist compared to a twist equal to 13°.

**Table 5.3**

| μ | $C_{LWOP}$ | | Predicted Improvement in $C_{LWOP}$ % |
|---|---|---|---|
| | Twist = 13° | Best Twist | |
| 0.075 | 0.4528 | 0.4649 | 2.7 |
| 0.1 | 0.5302 | 0.6135 | 15.7 |
| 0.125 | 0.4108 | 0.5598 | 36.3 |
| 0.15 | 0.2821 | 0.4401 | 56 |

### 5.3.4 Optimum Twist Using $C_{LWOP}$ as Criterion

The dependence of optimum twist on μ can be seen in fig ( 5.14 ). The optimum twist, using $C_{LWOP}$ as the criterion, is between 0° to 3° depending on the μ value. However an optimum twist equal to 2° is dominant in the majority of the range in μ.

### 5.3.5 The Minimum Wind Speed

There is a minimum wind speed below which the tethered wind generator can not remain aloft. This limit can be obtained for both the windmilling and autorotation modes. One of the other significant functions of $C_{LWOP}$ is that it can lead us to the minimum wind velocity requirements of the system.

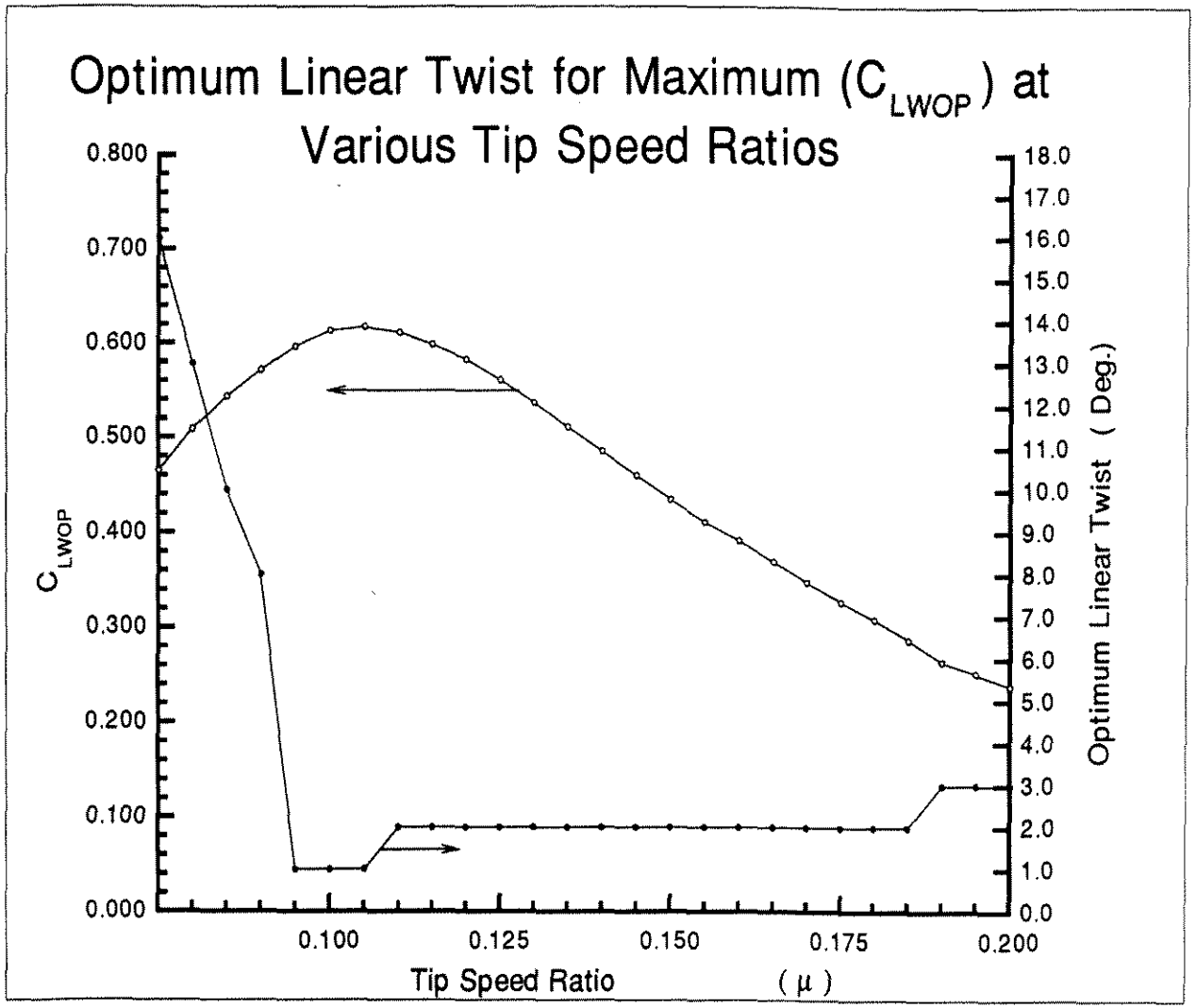
Optimum Linear Twist for Maximum ($C_{LWOP}$) at
Various Tip Speed Ratios
$C_{LWOP}$
0.800
0.700
0.600
0.500
0.400
0.300
0.200
0.100
0.000
0.100
0.125
0.150
0.175
0.200
Tip Speed Ratio ( μ )
18.0
17.0
16.0
15.0
14.0
13.0
12.0
11.0
10.0
9.0
8.0
7.0
6.0
5.0
4.0
3.0
2.0
1.0
0.0
Optimum Linear Twist ( Deg.)

**Fig ( 5.14 )**

As stated before, to ensure enough lift eq.(3.19) should be satisfied. The relationship between the minimum required wind velocity and $C_{LWOP}$ can be obtained by using eqs. (3.19) and (5.1), hence

$$V_{min} = \sqrt{\frac{\frac{mg}{2\pi R^2}}{\frac{1}{2}\rho C_{LWOP}}} \qquad (5.2)$$

Using the data of MK.3 from the table (1.1), (for calculating disk loading) and the results for $C_{LWOP}$ obtained from the program, the minimum wind velocity can be obtained.

Figures (5.15) and (5.16) show the minimum wind speed limit for twist of 2° and 13° respectively. Fig (5.17) shows the autorotation boundary for various values of tip speed ratio for twist of 2°(best twist for $C_{LWOP}$ ) and 13°. It can be seen that there is significant improvement in wind velocity requirements if we use the best twist for $C_{LWOP}$ . Table 5.4 shows the improvement in the autorotation wind velocity requirements for the best twist compared to a 13° twist.

**Table 5.4**

| μ | Autorotation Wind velocity | | Predicted Improvement in $V_{min}$ % |
|---|---|---|---|
| | Twist = 13° | Best Twist | |
| 0.105 | 29.75 | 27.00 | 10 |
| 0.135 | 35.50 | 29.74 | 19.36 |
| 0.165 | 43.66 | 34.87 | 25.2 |
| 0.195 | 53.28 | 42.22 | 26.2 |

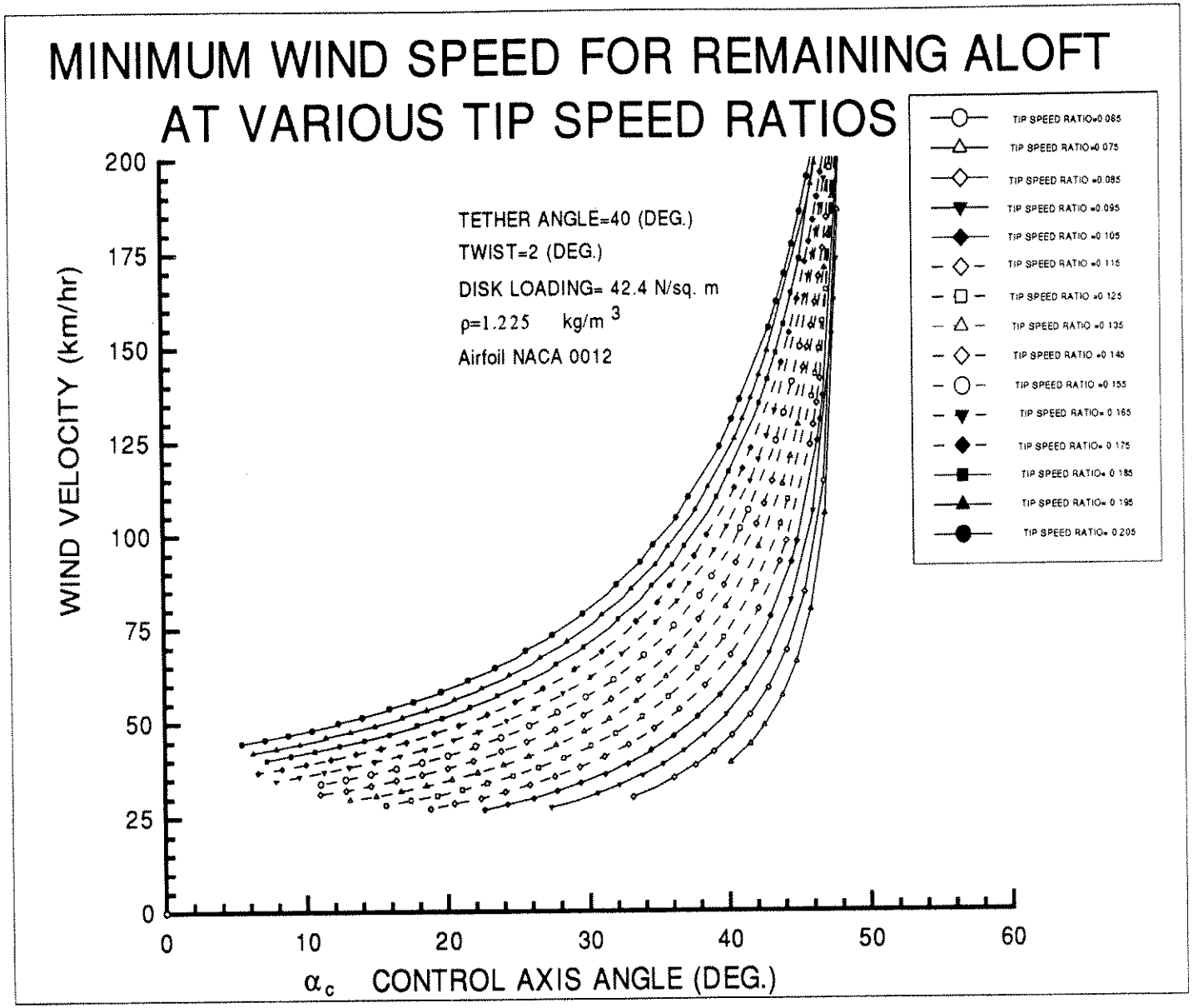
MINIMUM WIND SPEED FOR REMAINING ALOFT
AT VARIOUS TIP SPEED RATIOS
TETHER ANGLE=40 (DEG.)
TWIST=2 (DEG.)
DISK LOADING= 42.4 N/sq. m
ρ=1.225 kg/m 3
Airfoil NACA 0012
WIND VELOCITY (km/hr)
0
25
50
75
100
125
150
175
200
0
10
20
30
40
50
60
αc CONTROL AXIS ANGLE (DEG.)
TIP SPEED RATIO=0.065
TIP SPEED RATIO=0.075
TIP SPEED RATIO =0.085
TIP SPEED RATIO =0.095
TIP SPEED RATIO =0.105
TIP SPEED RATIO =0.115
TIP SPEED RATIO =0.125
TIP SPEED RATIO =0.135
TIP SPEED RATIO =0.145
TIP SPEED RATIO =0.155
TIP SPEED RATIO= 0.165
TIP SPEED RATIO= 0.175
TIP SPEED RATIO= 0.185
TIP SPEED RATIO= 0.195
TIP SPEED RATIO= 0.205

**Fig ( 5.15 )**

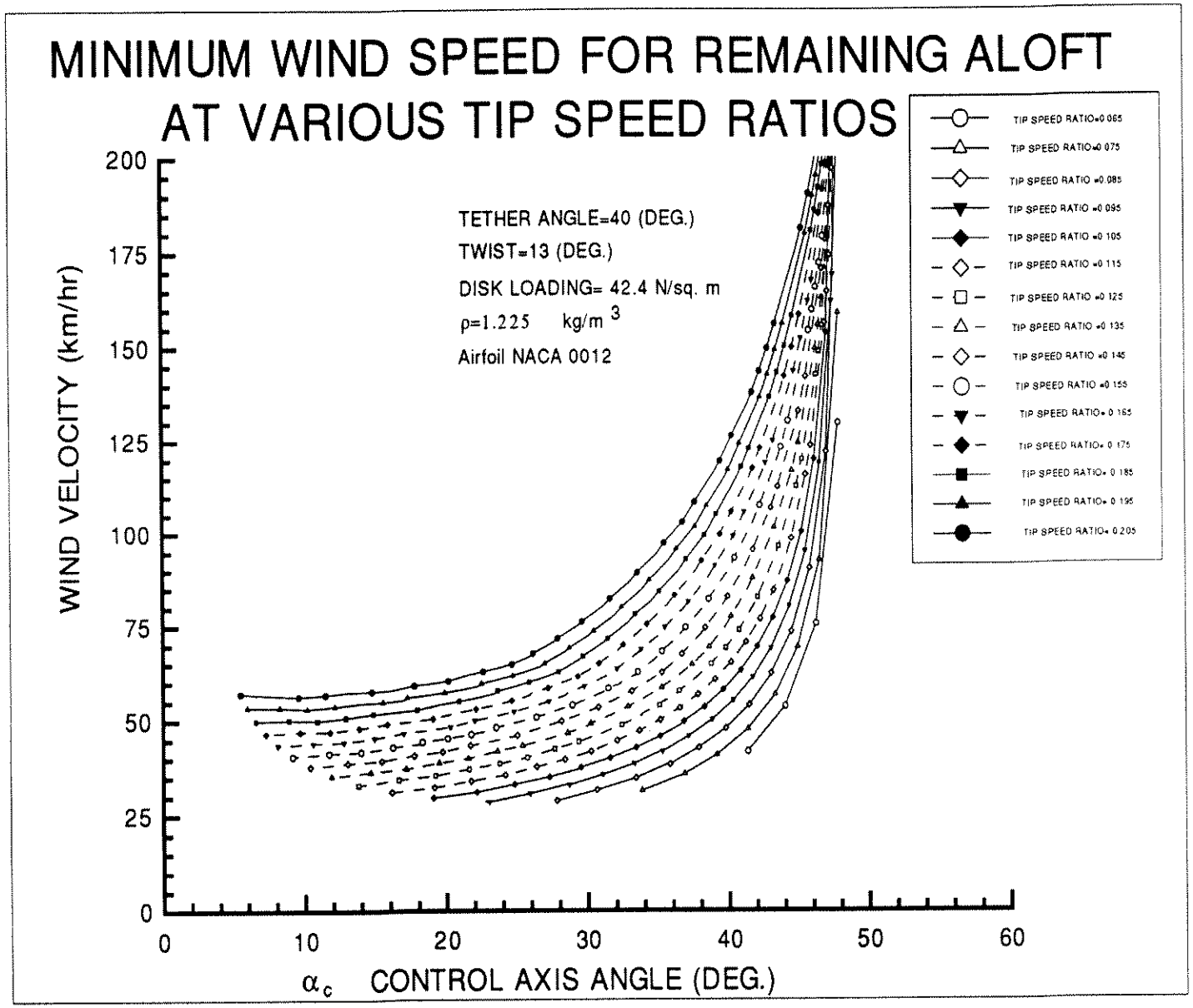
MINIMUM WIND SPEED FOR REMAINING ALOFT
AT VARIOUS TIP SPEED RATIOS
TETHER ANGLE=40 (DEG.)
TWIST=13 (DEG.)
DISK LOADING= 42.4 N/sq. m
ρ=1.225 kg/m 3
Airfoil NACA 0012
WIND VELOCITY (km/hr)
0
25
50
75
100
125
150
175
200
0
10
20
30
40
50
60
αc CONTROL AXIS ANGLE (DEG.)
TIP SPEED RATIO=0.065
TIP SPEED RATIO=0.075
TIP SPEED RATIO =0.085
TIP SPEED RATIO =0.095
TIP SPEED RATIO =0.105
TIP SPEED RATIO =0.115
TIP SPEED RATIO =0.125
TIP SPEED RATIO =0.135
TIP SPEED RATIO =0.145
TIP SPEED RATIO =0.155
TIP SPEED RATIO= 0.165
TIP SPEED RATIO= 0.175
TIP SPEED RATIO= 0.185
TIP SPEED RATIO= 0.195
TIP SPEED RATIO= 0.205

**Fig ( 5.16 )**

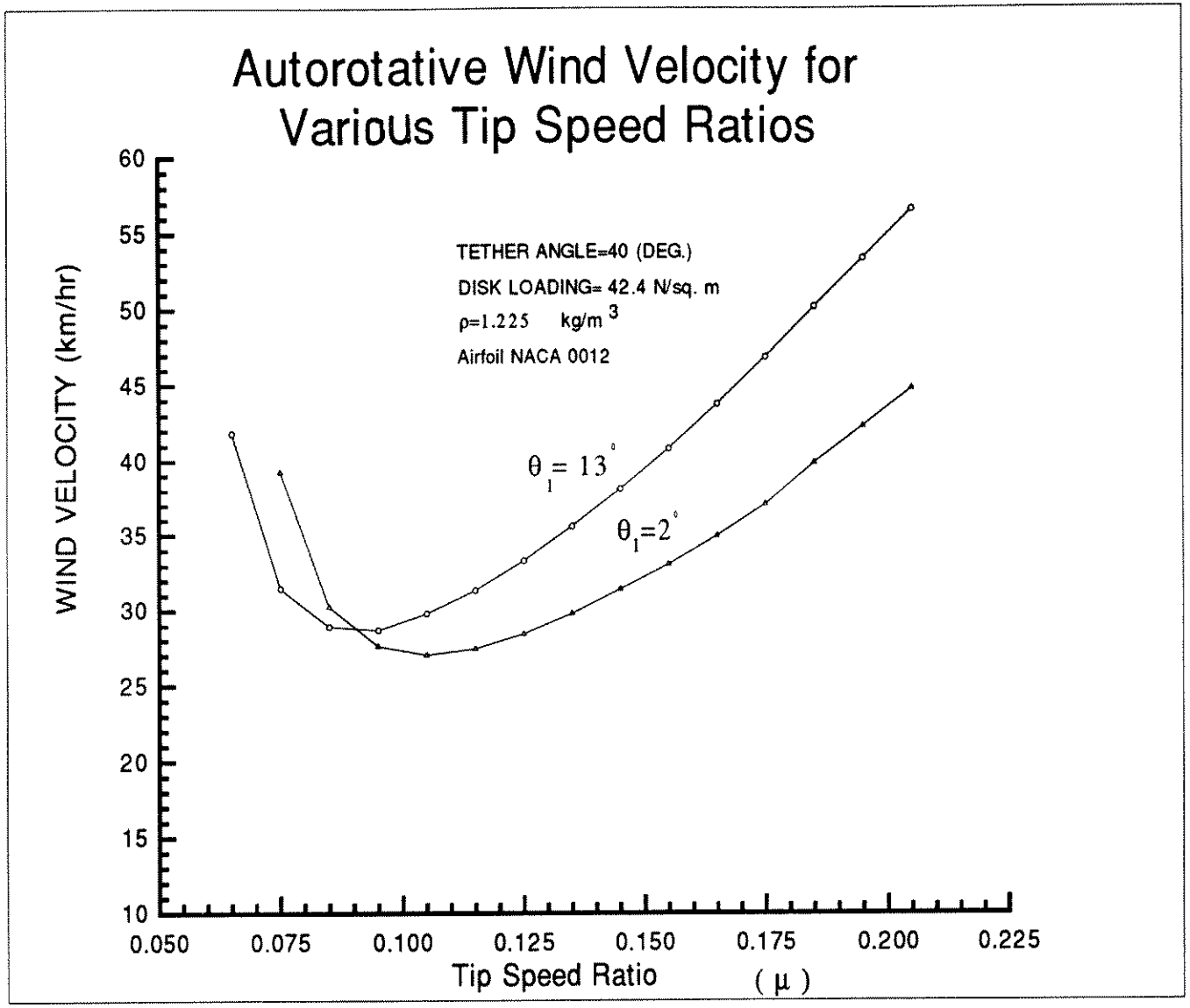
Autorotative Wind Velocity for
Various Tip Speed Ratios
TETHER ANGLE=40 (DEG.)
DISK LOADING= 42.4 N/sq. m
ρ=1.225 kg/m 3
Airfoil NACA 0012
θ1 = 13°
θ1=2°
WIND VELOCITY (km/hr)
60
55
50
45
40
35
30
25
20
15
10
0.050
0.075
0.100
0.125
0.150
0.175
0.200
0.225
Tip Speed Ratio ( μ )

Fig ( 5.17 )

## 5.4 The Influence of Twist on the Windmill Torque Coefficient, $C_{QW}$

Using the same procedure as that described above, it is possible to evaluate the effect of twist on $C_{QW}$. Fig 5.18 shows the influence of twist on the windmill torque coefficient for four typical values of tip speed ratio. Table 5.5 shows the improvement in $C_{QW}$ when a comparison is made between an optimal twisted blade with an untwisted blade.

**Table 5.5**

| μ | $C_{QW}$ | | Predicted Improvement in $C_{QW}$ % |
|---|---|---|---|
| | Twist = 0° | Best Twist | |
| 0.075 | 3.0219 | 3.0535 | 1.05 |
| 0.1 | 1.9776 | 2.1603 | 9.24 |
| 0.125 | 1.2033 | 1.3809 | 14.76 |
| 0.15 | 0.7343 | 0.8630 | 17.27 |

### 5.4.1 Optimum Twist Using $C_{QW}$ as the Criterion

If we use only $C_{QW}$ as the criterion, the optimum twist will maximise $C_{QW}$. Fig 5.19 shows the optimum twist value. Since optimum twist depends on μ, it is plotted against μ. Although the optimum twist varies between 9° and 15° depending on μ, a twist of between 13° and 15° is dominant in the graph.

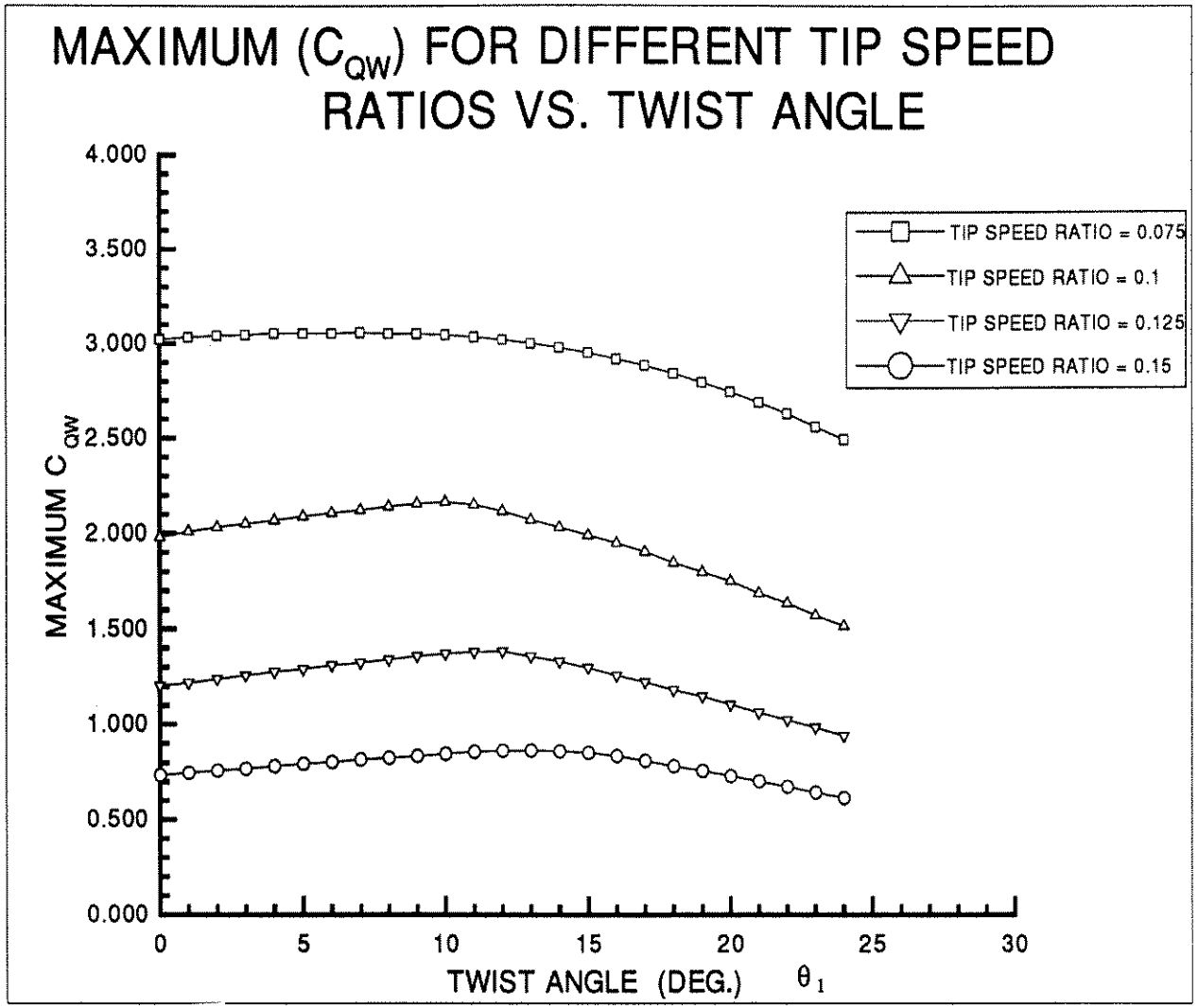
MAXIMUM ($C_{QW}$) FOR DIFFERENT TIP SPEED RATIOS VS. TWIST ANGLE
MAXIMUM $C_{QW}$
4.000
3.500
3.000
2.500
2.000
1.500
1.000
0.500
0.000
0
5
10
15
20
25
30
TWIST ANGLE (DEG.) $\theta_1$
TIP SPEED RATIO = 0.075
TIP SPEED RATIO = 0.1
TIP SPEED RATIO = 0.125
TIP SPEED RATIO = 0.15

Fig ( 5.18 )

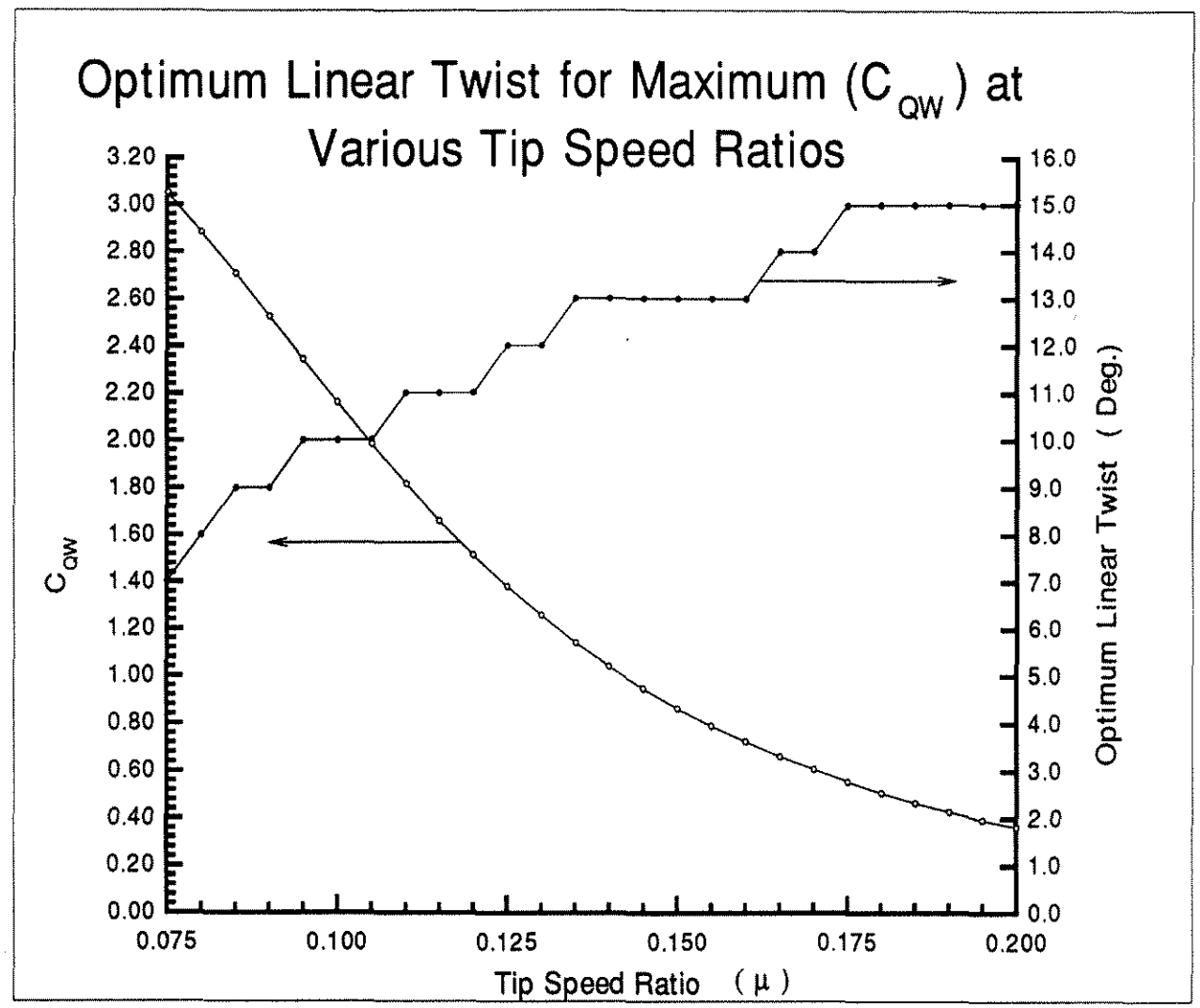
Optimum Linear Twist for Maximum ($C_{QW}$) at
Various Tip Speed Ratios
$C_{QW}$
3.20
3.00
2.80
2.60
2.40
2.20
2.00
1.80
1.60
1.40
1.20
1.00
0.80
0.60
0.40
0.20
0.00
16.0
15.0
14.0
13.0
12.0
11.0
10.0
9.0
8.0
7.0
6.0
5.0
4.0
3.0
2.0
1.0
0.0
Optimum Linear Twist ( Deg.)
0.075
0.100
0.125
0.150
0.175
0.200
Tip Speed Ratio ( μ )

**Fig ( 5.19 )**

## 5.5 Alternative Criteria in the Choice of Optimum Twist

None of the performance parameters discussed in the previous sections of this chapter can be used alone as an ultimate criterion.

For example if we use $C_{PW}$ as the criterion for the selection of optimum twist ( and hence choose a twist of 13° as the optimum twist), this will produce nearly the lowest value of $C_{LW}$ and $C_{LWOP}$. The special nature of the tethered wind generator requires us to consider both power and lift.

This leads to the fact that the ultimate criterion is, say, a simple product of the parameters $C_{LW}$ and $C_{PW}$. In this regard three different criteria could be considered namely,

1. $C_{opt1} = C_{PW} \times C_{LW}$
2. $C_{opt2} = C_{PW} \times C_{LWOP}$
3. $C_{opt3} = C_{QW} \times C_{LWOP}$

In the following sections the effect of twist on these criteria will be evaluated and the optimum twist will be then determined.

### 5.5.1 The Optimum Twist Using $C_{opt1}$ as the Criterion

This criterion is the simple production of $C_{PW}$ and $C_{LW}$. Use of this criterion will result in the optimum twist which considers both $C_{PW}$ and $C_{LW}$. This will improve the output power as well as ensure that enough lift will be developed by the rotor.

Fig ( 5.20 ) shows the effect of twist on $C_{opt1}$. Table 5.6 shows the improvement made by the use of optimum twist. Four different values of $\mu$ are considered.

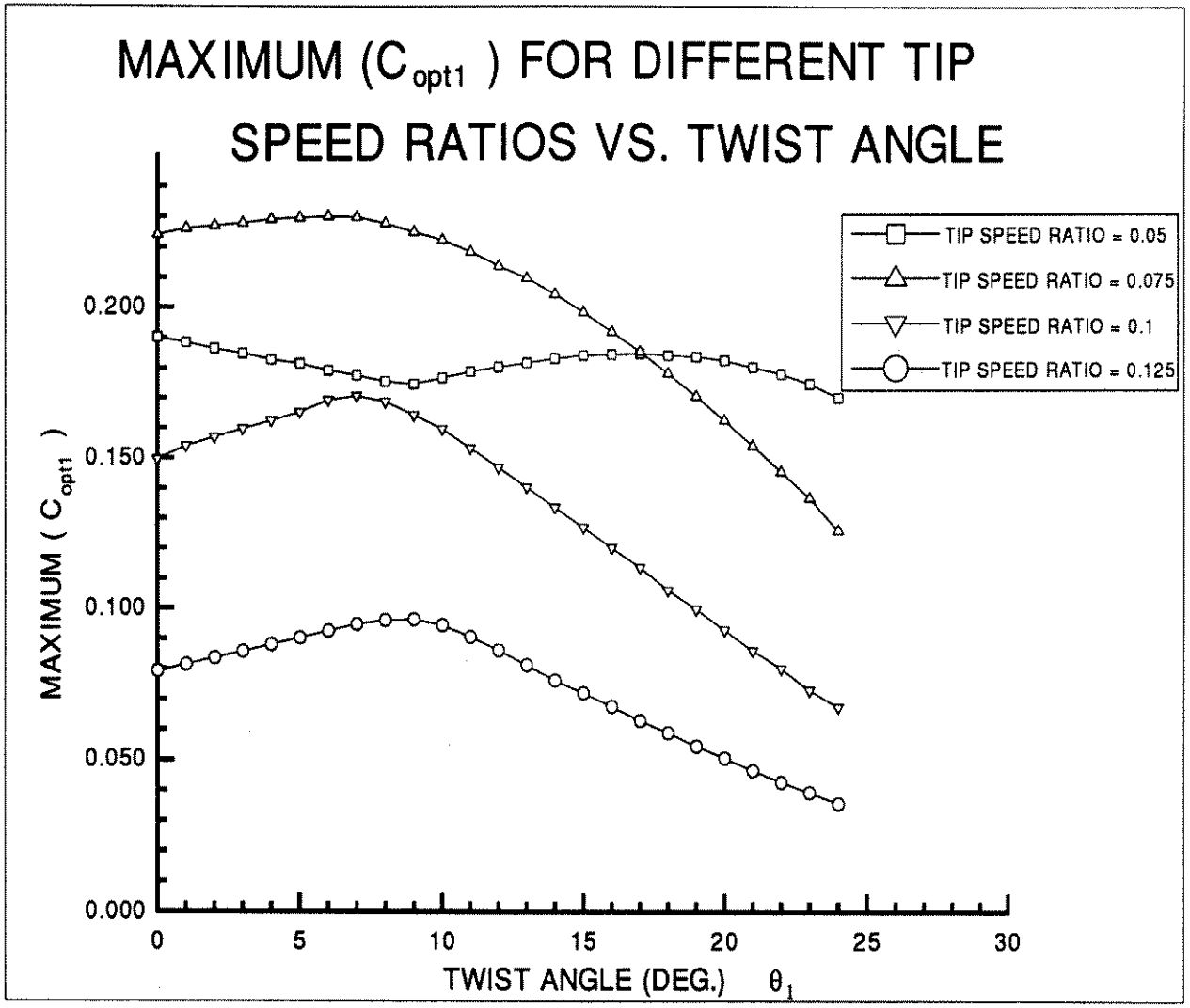
MAXIMUM ($C_{opt1}$ ) FOR DIFFERENT TIP SPEED RATIOS VS. TWIST ANGLE
TIP SPEED RATIO = 0.05
TIP SPEED RATIO = 0.075
TIP SPEED RATIO = 0.1
TIP SPEED RATIO = 0.125
MAXIMUM ( $C_{opt1}$ )
0.000
0.050
0.100
0.150
0.200
0
5
10
15
20
25
30
TWIST ANGLE (DEG.) $\theta_1$

Fig ( 5.20 )

Table 5.6

| μ | $C_{opt1}$ | | Predicted Improvement in $C_{opt1}$ % |
|---|---|---|---|
| | Twist = 0° | Best Twist | |
| 0.05 | 0.1903 | 0.1903 | 0.0 |
| 0.075 | 0.2441 | 0.2299 | 2.4 |
| 0.1 | 0.1496 | 0.1704 | 13.9 |
| 0.125 | 0.0792 | 0.0961 | 21.3 |

Fig ( 5.21 ) shows the optimum twist for $C_{opt\ 1}$ at various value of μ. The dependence of optimum twist on μ is quite clear.

Depending on the μ, value of the optimum twist is between 6° to 12°, while its average value is about 9° or 10°.

## 5.5.2 The Optimum Twist Using $C_{opt2}$ as the Criterion

$C_{opt2}$ is the product of $C_{PW}$ and $C_{LWOP}$ . Both parameters were fully defined in sections 3.2.3 , 3.2.6 ,5.1 and 5.3 . Using this criterion gives a balanced optimum twist which would improve both power and lift capabilities.

Fig. (5.22) demonstrates the effect of the twist on $C_{opt2}$. This shows how it is important to determine the optimum twist. The improvement obtained by using a optimum twist, compared to an untwisted blade, is given in Table 5.7.

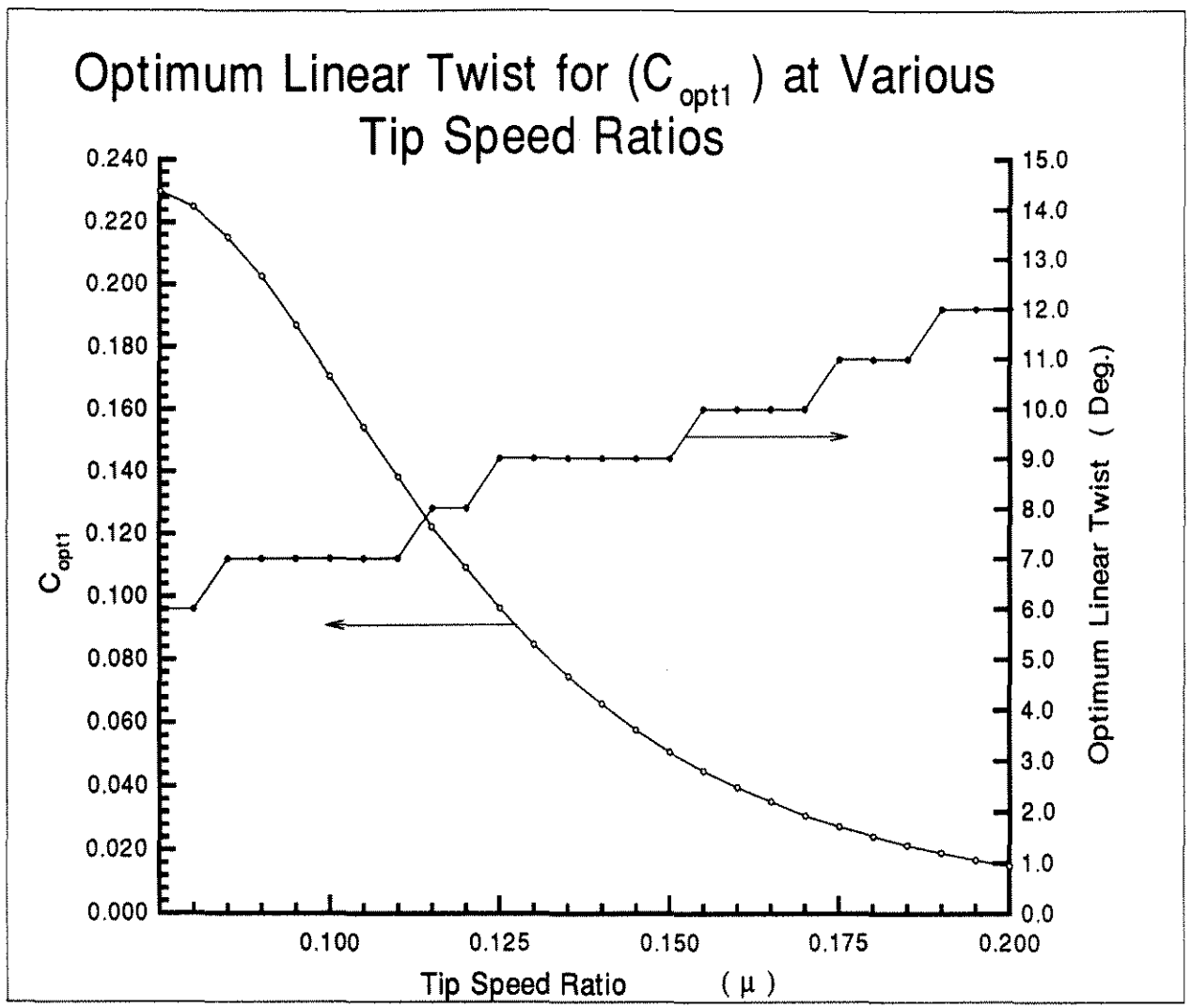
Optimum Linear Twist for ($C_{opt1}$ ) at Various
Tip Speed Ratios
0.240
0.220
0.200
0.180
0.160
0.140
0.120
0.100
0.080
0.060
0.040
0.020
0.000
$C_{opt1}$
15.0
14.0
13.0
12.0
11.0
10.0
9.0
8.0
7.0
6.0
5.0
4.0
3.0
2.0
1.0
0.0
Optimum Linear Twist ( Deg.)
0.100
0.125
0.150
0.175
0.200
Tip Speed Ratio ( μ )

**Fig ( 5.21 )**

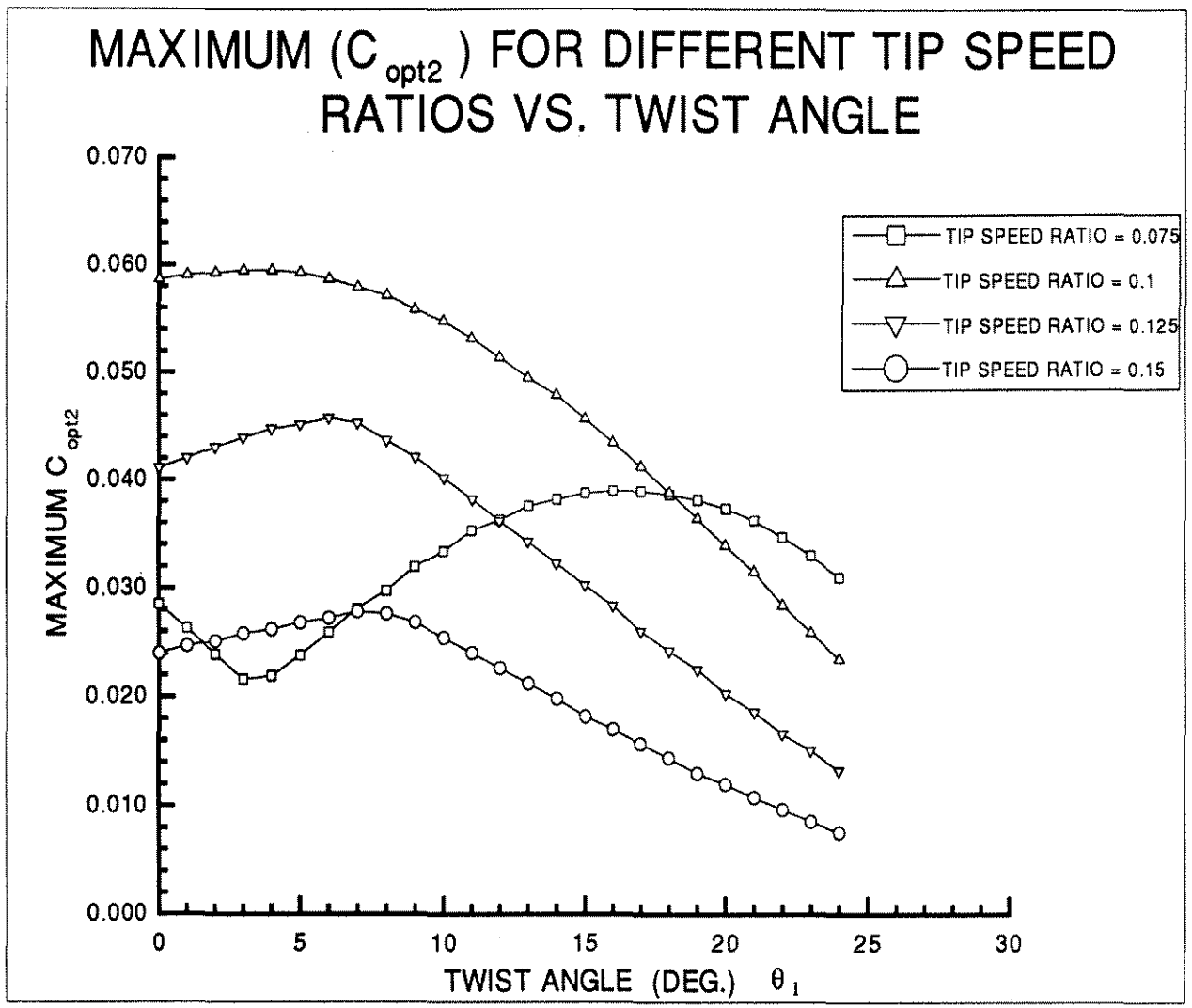
MAXIMUM ($C_{opt2}$) FOR DIFFERENT TIP SPEED RATIOS VS. TWIST ANGLE
MAXIMUM $C_{opt2}$
0.070
0.060
0.050
0.040
0.030
0.020
0.010
0.000
0
5
10
15
20
25
30
TWIST ANGLE (DEG.) $\theta_1$
TIP SPEED RATIO = 0.075
TIP SPEED RATIO = 0.1
TIP SPEED RATIO = 0.125
TIP SPEED RATIO = 0.15

**Fig ( 5.22 )**

Table 5.7

| μ | $C_{opt2}$ | | Predicted Improvement in $C_{opt2}$ % |
|---|---|---|---|
| | Twist = 13° | Optimum Twist | |
| 0.075 | 0.0285 | 0.0389 | 36 |
| 0.1 | 0.0587 | 0.0595 | 1.3 |
| 0.125 | 0.0411 | 0.0457 | 11.2 |
| 0.15 | 0.0240 | 0.0278 | 15.8 |

Since the optimum twist ultimately depends on μ, it is more appropriate to show it as a function of μ . Fig (5.23) shows the optimum twist over various values of μ. It can be seen that the optimum twist lies between 4° to 10°. An average value of about 7° is apparent.

### 5.5.3 The Optimum Twist Using $C_{opt3}$ as the Criterion

Another criterion can be defined using an optimum twist which would enhance both rotor torque and its capabilities for lift. $C_{opt3}$ is the product of $C_{QW}$ and $C_{LWOP}$ . The significant role of twist in this criterion can be seen by plotting the twist against $C_{opt3}$ .

Fig (5.24) shows this criterion for four typical values of μ over a large range of twist. It should be pointed out that the maximum value of $C_{opt3}$, at a given twist, has been chosen for comparison purposes.

Table 5.8 shows the predicted improvement in this parameter for a blade with optimum twist compared to an untwisted blade.

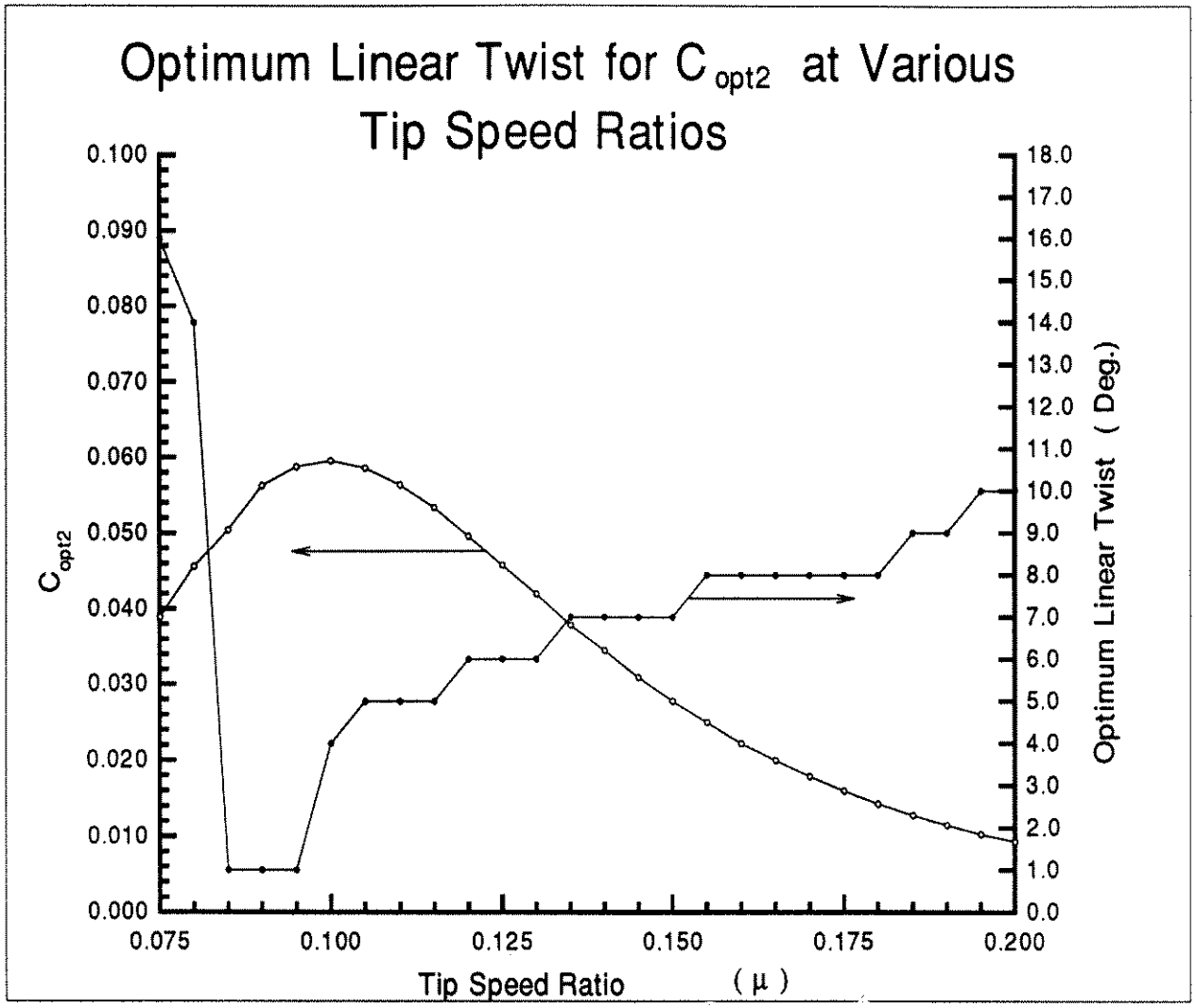
Optimum Linear Twist for $C_{opt2}$ at Various Tip Speed Ratios
$C_{opt2}$
0.100
0.090
0.080
0.070
0.060
0.050
0.040
0.030
0.020
0.010
0.000
0.075
0.100
0.125
0.150
0.175
0.200
Tip Speed Ratio ( μ )
Optimum Linear Twist ( Deg.)
18.0
17.0
16.0
15.0
14.0
13.0
12.0
11.0
10.0
9.0
8.0
7.0
6.0
5.0
4.0
3.0
2.0
1.0
0.0

**Fig ( 5.23 )**

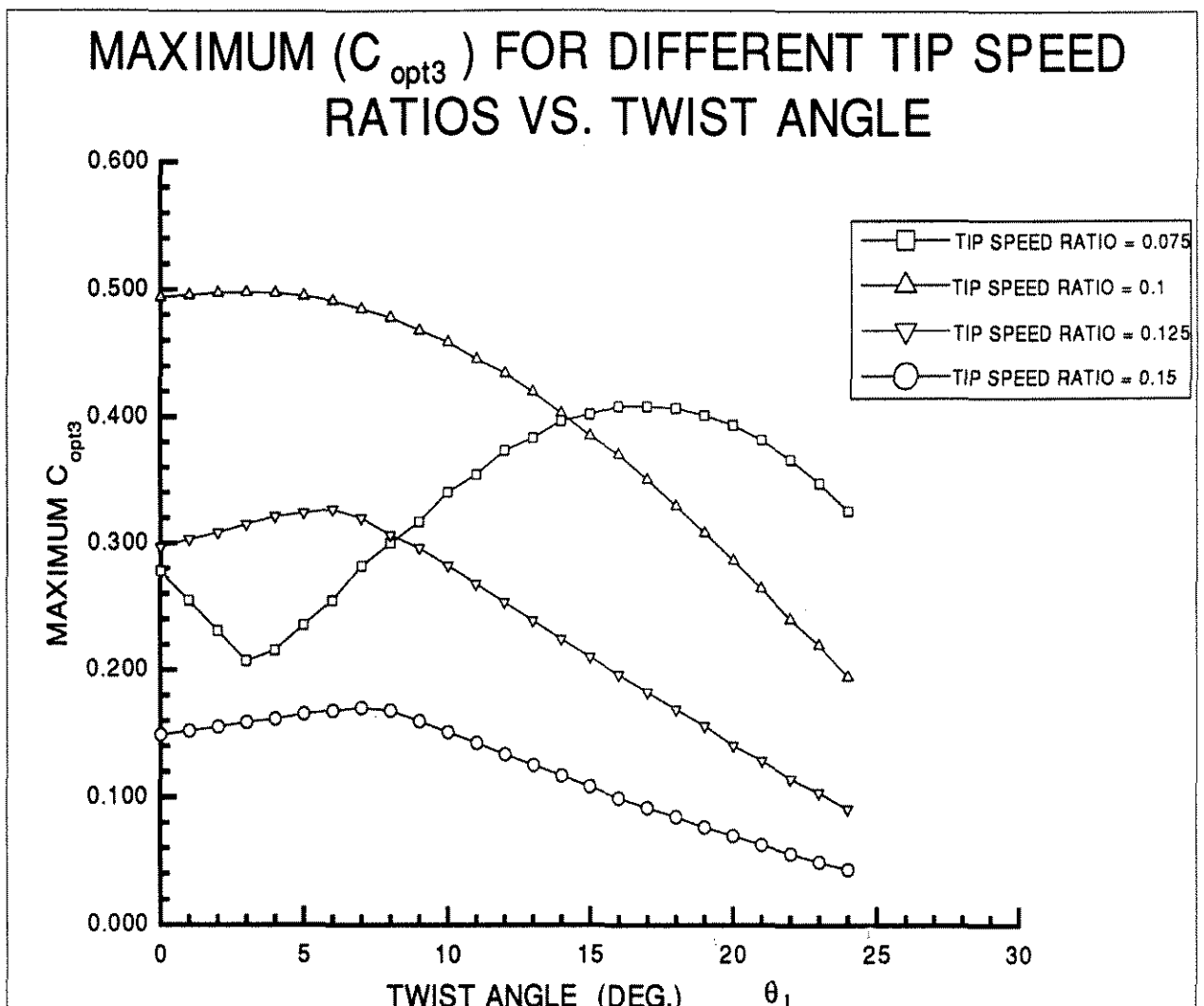
MAXIMUM ($C_{opt3}$) FOR DIFFERENT TIP SPEED RATIOS VS. TWIST ANGLE
MAXIMUM $C_{opt3}$
0.600
0.500
0.400
0.300
0.200
0.100
0.000
0
5
10
15
20
25
30
TWIST ANGLE (DEG.) $\theta_1$
TIP SPEED RATIO = 0.075
TIP SPEED RATIO = 0.1
TIP SPEED RATIO = 0.125
TIP SPEED RATIO = 0.15

Fig ( 5.24 )

**Table 5.8**

| μ | $C_{opt3}$ | | Predicted Improvement in $C_{opt3}$ % |
|---|---|---|---|
| | Twist = 0° | Optimum Twist | |
| 0.075 | 0.0285 | 0.0389 | 36 |
| 0.1 | 0.0587 | 0.0595 | 1.3 |
| 0.125 | 0.0411 | 0.0457 | 11.2 |
| 0.15 | 0.0240 | 0.0278 | 15.8 |

As we discussed before the, final decision in determining optimum twist would depend on the value of μ. This dependence is illustrated in fig. (5.25) for various values of μ. This figure shows an optimum twist between 1° to 9°. The higher values may be used for extremely low values of μ . An average value of 7° is dominant.

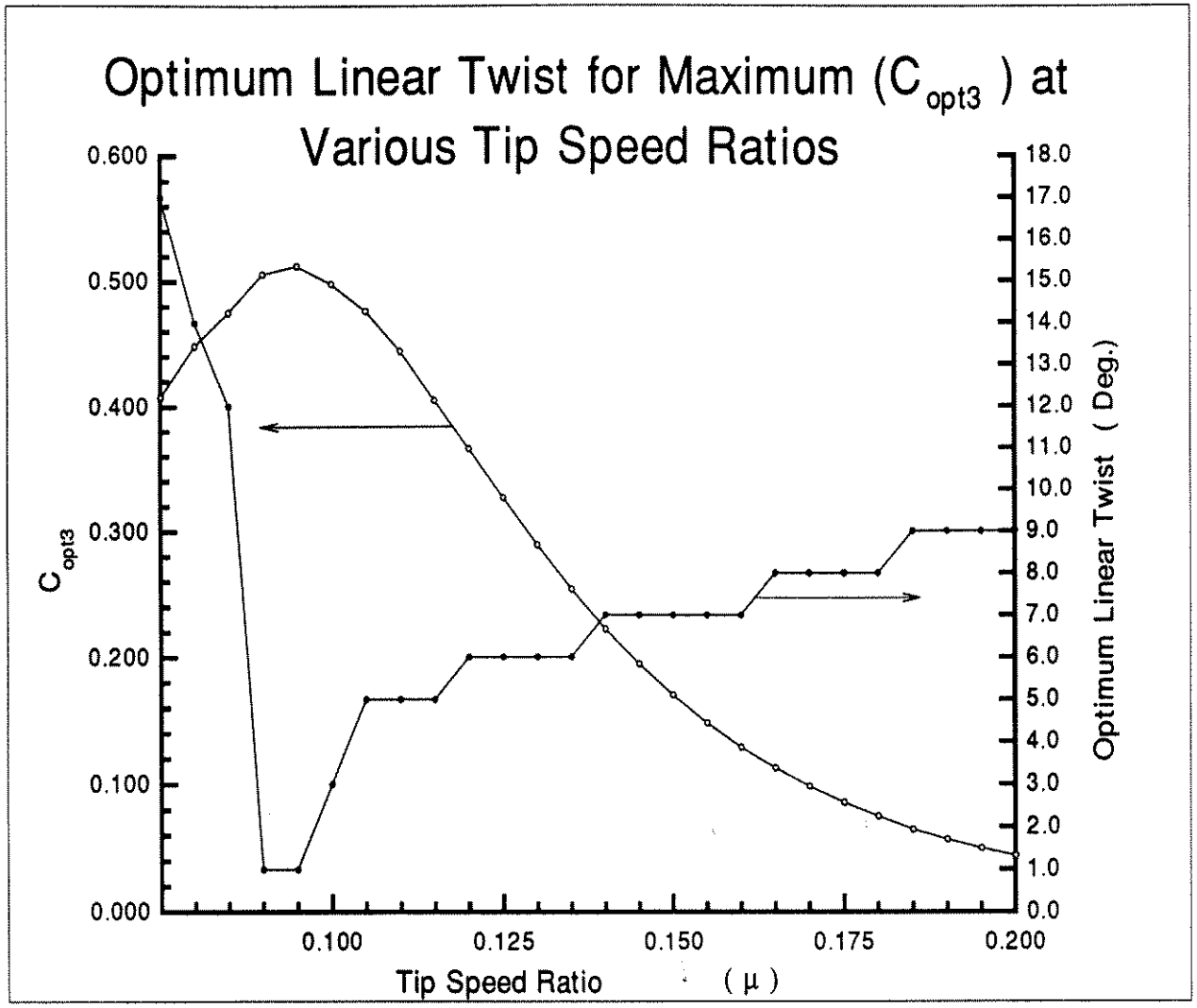
Optimum Linear Twist for Maximum ($C_{opt3}$) at
Various Tip Speed Ratios
$C_{opt3}$
0.600
0.500
0.400
0.300
0.200
0.100
0.000
0.100
0.125
0.150
0.175
0.200
Tip Speed Ratio ( μ )
18.0
17.0
16.0
15.0
14.0
13.0
12.0
11.0
10.0
9.0
8.0
7.0
6.0
5.0
4.0
3.0
2.0
1.0
0.0
Optimum Linear Twist ( Deg.)

**Fig ( 5.25 )**

## 5.6 Choice of the Ultimate Criterion

Any ultimate criterion should be chosen from the three criterion given in section 5.5, namely $C_{opt1}$, $C_{opt2}$ and $C_{opt3}$.

$C_{LW}$ not necessarily maximises the lifting capability of the system, because this coefficient is not dependant on the craft's weight and the tether tension forces. As we discussed before the capability of the system to remain aloft is evaluated by using $C_{LWOP}$. Thus we can conclude that in any optimisation criterion $C_{LWOP}$ should be included rather than $C_{LW}$. Considering the above, $C_{opt1}$ can not be considered as the ultimate criterion for the current optimisation.

Both $C_{opt2}$, $C_{opt3}$ can be used as the criterion depending on the design requirements. We should realise that unlike helicopter terminology, in windmill terminology power and torque coefficients are not equal. Thus, in order to obtain a good power output and reasonable lift, $C_{opt2}$ should be used as the criterion.

Sometimes we might need to maximise the torque of certain design requirements. In such cases $C_{opt3}$ should be used as the criterion.

The optimal results obtained for $C_{opt2}$ and $C_{opt3}$ are only slightly different and there is only 1° difference between optimum twist.

## 5.6 Proposal for Future Research

Determination of the optimum operation of the tethered windmill could be the subject of future research. In this regard two proposal could be investigated:

### 5.6.1 Operation in a Steady Wind

At any site at which the gyromill is installed there will be a tip speed ratio at which we can satisfy both lift and power requirements under steady wind conditions. To find this value apply the following procedure:

- Refer to the minimum wind velocity envelope ,fig( 5.26), for a given wind velocity. Find the range of tip speed ratio at which the windmilling operation is possible.
- From the same graph find the relevant, $\alpha_C$ for each possible value of $\mu$.
- Refer to the $C_{PW}$ envelope in fig( 5.27 ) and find $C_{PW}$ for each pair of $\mu$ and $\alpha_C$ values obtained in previous steps.
- Compare the values of $C_{PW}$ and choose the value of $\mu$ at which $C_{PW}$ is maximum.
- Choose this point as the best operation condition.

### 5.6.2 Operation at Variable Values of $\mu$

When the wind speed is not stable $\mu$ will change. So that we need to find the best value for $\mu$ and hence $\alpha_C$ each time that the wind velocity changes. The procedure for finding the best value of $\mu$ and $\alpha_C$ is the same as that mentioned in section 5.6.1.

A computer program can be written to do the above mentioned procedure and results can be supplied to a control device to optimise the parameters such as $\alpha_C$ ,$\Omega$ ,$\theta_0$ etc. of the gyromill.

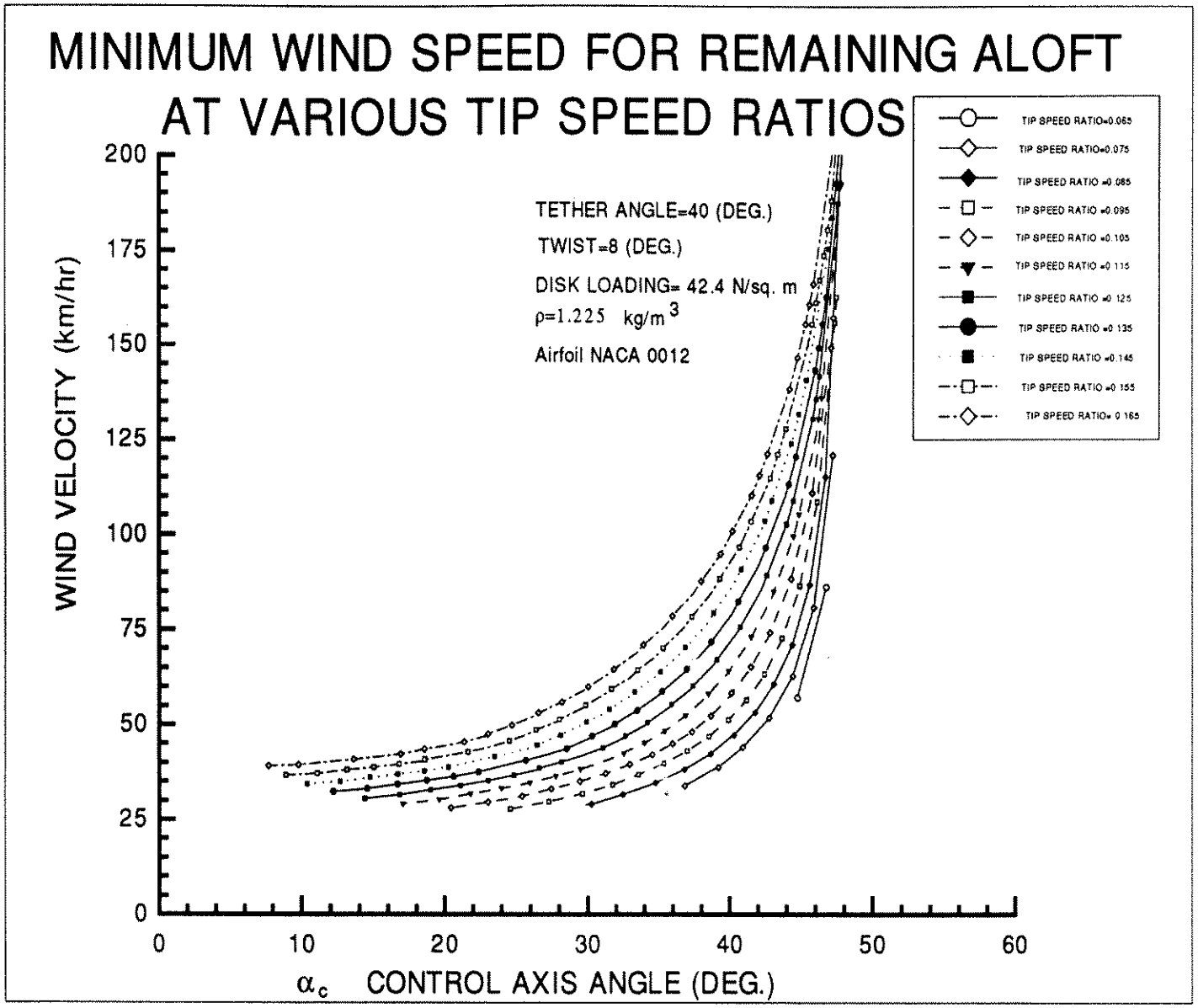
MINIMUM WIND SPEED FOR REMAINING ALOFT
AT VARIOUS TIP SPEED RATIOS
TETHER ANGLE=40 (DEG.)
TWIST=8 (DEG.)
DISK LOADING= 42.4 N/sq. m
ρ=1.225 kg/m 3
Airfoil NACA 0012
TIP SPEED RATIO=0.065
TIP SPEED RATIO=0.075
TIP SPEED RATIO =0.085
TIP SPEED RATIO =0.095
TIP SPEED RATIO =0.105
TIP SPEED RATIO =0.115
TIP SPEED RATIO =0.125
TIP SPEED RATIO =0.135
TIP SPEED RATIO =0.145
TIP SPEED RATIO =0.155
TIP SPEED RATIO= 0.165
WIND VELOCITY (km/hr)
0
25
50
75
100
125
150
175
200
0
10
20
30
40
50
60
$\alpha_c$ CONTROL AXIS ANGLE (DEG.)

Fig ( 5.26 )

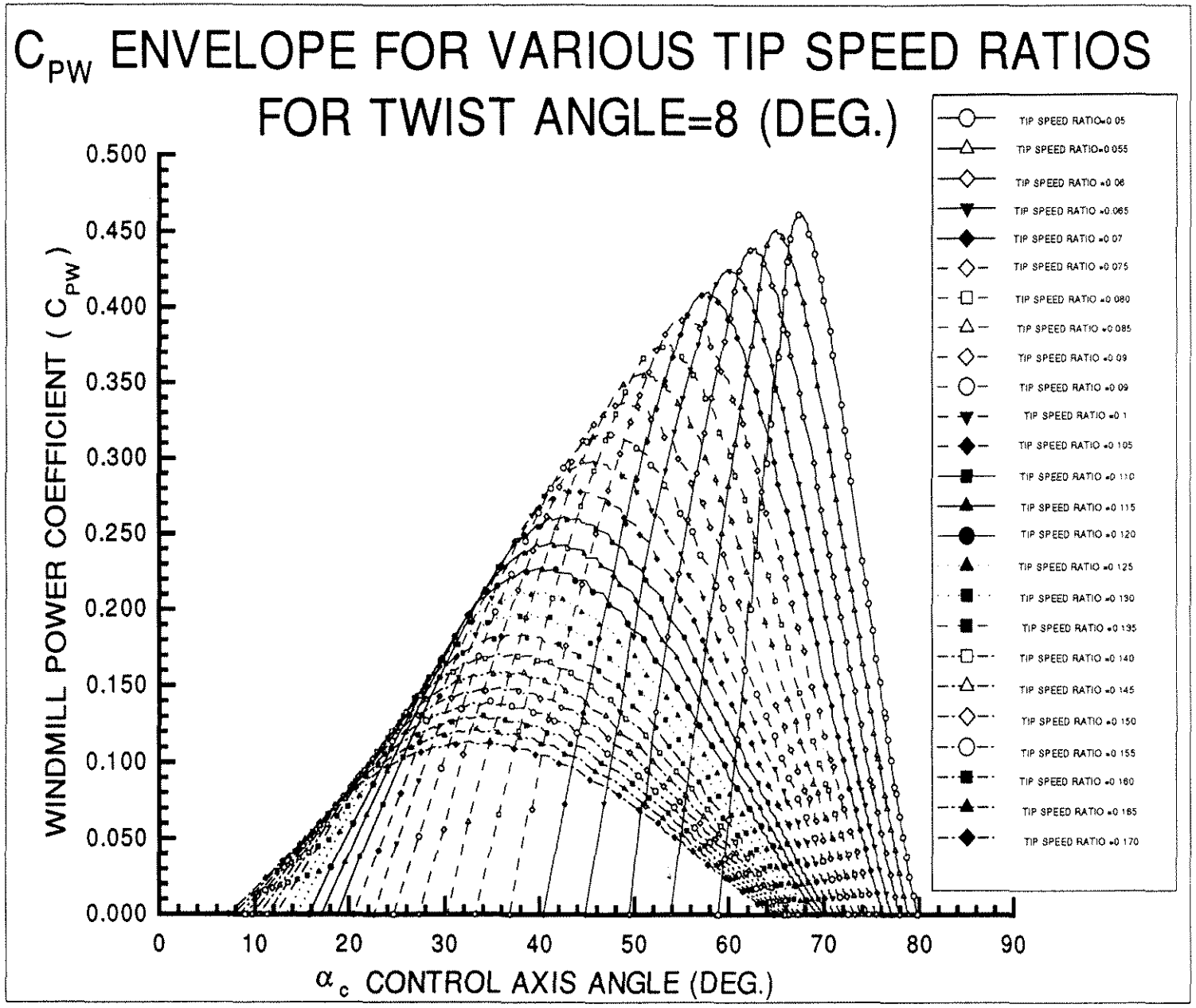
$C_{PW}$ ENVELOPE FOR VARIOUS TIP SPEED RATIOS
FOR TWIST ANGLE=8 (DEG.)
WINDMILL POWER COEFFICIENT ( $C_{PW}$ )
0.500
0.450
0.400
0.350
0.300
0.250
0.200
0.150
0.100
0.050
0.000
0
10
20
30
40
50
60
70
80
90
$\alpha_c$ CONTROL AXIS ANGLE (DEG.)
TIP SPEED RATIO=0.05
TIP SPEED RATIO=0.055
TIP SPEED RATIO =0.06
TIP SPEED RATIO =0.065
TIP SPEED RATIO =0.07
TIP SPEED RATIO =0.075
TIP SPEED RATIO =0.080
TIP SPEED RATIO =0.085
TIP SPEED RATIO =0.09
TIP SPEED RATIO =0.09
TIP SPEED RATIO =0.1
TIP SPEED RATIO =0.105
TIP SPEED RATIO =0.110
TIP SPEED RATIO =0.115
TIP SPEED RATIO =0.120
TIP SPEED RATIO =0.125
TIP SPEED RATIO =0.130
TIP SPEED RATIO =0.135
TIP SPEED RATIO =0.140
TIP SPEED RATIO =0.145
TIP SPEED RATIO =0.150
TIP SPEED RATIO =0.155
TIP SPEED RATIO =0.160
TIP SPEED RATIO =0.165
TIP SPEED RATIO =0.170

**Fig ( 5.27 )**

# CHAPTER SIX

## Conclusions

### 6.1 Introduction

The main objective of this research has been to find the optimum twist for the windmill and autorotative states of a tethered rotorcraft.

In this study an appropriate theory has been employed as well as a computer code. The numerical results allowed the determination of the optimum twist for several different criteria.

Each criterion was closely examined in order to suggest an ultimate criterion. Although the first goal of the study was to determine the optimum twist it led us to some other useful conclusions in this tether rotorcraft theory.

## 6.2 Conclusions in detail

The followings are the major conclusions to this study.

- the highest values of power coefficient can be obtained at the least values of $\mu$.
- Higher values of tip speed ratio provide broader ranges for $\alpha_c$.
- The optimum twist using $C_{PW}$ as the criterion has an average value of 13°.
- There is a value of $\mu$ at which we can reach the highest value for $C_{LW}$. The best tip speed ratio in this regard is about $\mu = 0.075$.
- The operation of the system at large control axis angles, $\alpha_c$, can result in a loss of $C_{LW}$.
- The optimum twist using $C_{LW}$ as the criterion is about 2°.
- A new term namely, $C_{LWOP}$, can be defined. This term represents the autorotation and/or lift capability of the tethered rotorcraft. If it is assumed that the tether angle is constant in any trimmed condition, then to produce enough lift in this condition, the tip path incidence angle, $(\alpha_c + a_1)$, must be lower than ( $90° - \beta'$ ) . For $\beta'$ of 40° the control axis angle must be lower than about 48°.
- The operation of the tethered rotorcraft is not practical for $\mu$ values less than about 0.065.
- There is a $\mu$ value at which the system produces the most effective lift. In this condition it can remain aloft at the least possible wind velocity. This occurs where the parameter $C_{LWOP}$ is maximum. This value of $\mu$ is only slightly dependant on twist. In this state the values of $\mu$ are 0.105 and 0.095 for twist equal to 2° and 13° respectively.

- The minimum wind velocity for autorotation of MK3 is about 27 km/hr at a $\mu$ value of 0.105. Hence, $\alpha_c$ equals 22° for a twist of 2°. These figures are almost identical for an untwisted blade.
- Optimum twist for best autorotation capability is obtained at 2°. This twist maximise $C_{LWOP}$ .
- Considering $C_{QW}$ as the criterion,the average value of optimum twist is 14°.
- The ultimate optimum twist should consider the functions ($C_{PW} \times C_{LWOP}$ ) or ($C_{QW} \times C_{LWOP}$). In this case we would enhance both autorotation capability and the energy output. In this regard two alternatives can be considered.
- For balanced operation between a good windmill power coefficient and the autorotation capability the average optimum twist is about 8°.
- To obtain both the best windmill torque coefficient and the autorotation capability the average optimum twist is about 7°.
- For all criteria the optimum twist ultimately depends upon the tip speed ratio. In this regard the graphs provided in this thesis will be helpful in choosing the best.
- All results in this thesis refer to the input data mentioned in section 4.4. For other rotor assemblies the same procedure applies. The program given in the Appendix can be employed to obtain the suitable results.

# References


1- **Roberts, B.W. and Blackler, J.**

" Various systems for generation of electricity using upper atmospheric winds."

Proceedings of the SERI 2nd wind energy innovation systems conference, Vol. 1, (pp. 67-90),SERI, Golden, Co.,Dec. 1980.

2. **Gessow, A. and Myers, G.C.**

"Aerodynamics of the helicopter."

Frederick Ungar Publishing Co., New York, 1978.

3. **Bailey F.J.**

" A simplified theoretical method of determining the characteristics of a lifting rotor in forward flight."

A.R.C. Report No. 716, 1941.

4. **Gessow A. and Crim, A.D.**

"An extension of lifting rotor theory to cover operation at large angles of attack and high inflow conditions."

NACA, Technical note 2665, April 1952.

5. **Wheatley, J.B.**

" An aerodynamic analysis of the autogyro rotor with a comparison between calculated and experimental results."

A.R.C. Report No. 487, 1934.

6. **Ho. R.**

" Lateral control and stability of flying wind generator."

Master of Engineering Science thesis, Department of Mechanical Engineering , University of Sydney 1993.

7. **Kovarik,T. ,Pipher, C. and Hurst, J.**

"Wind Energy."

Prism Press, United Kingdom, 1979.

8. **Putman and Palmer Gosslett**

" Power from the wind."

Van Nostrand Reinhol, New York, 1974.

9. **Fletcher, C.A.J. and Roberts B.W.**

" Electricity generation from jet stream winds."

J. Energy, Vol.3 No. 4,July-August 1979,(pp. 241-249).

10. **Fletcher, Clive A. J.**

" On the rotary wing concept for jet stream electricity generation."

J. Energy, Vol. 7, No. 1, Jan- Feb 1983,(pp. 90-92)

11. **Wortman A.**

" Optimum performance propeller wind turbine Blades."

Technical Note, J. Energy No. 1, 1983, (pp. 86-87).

12. **Juul N. H.**

"Optimum design points geometry and performance of propeller type wind turbines."

13. **Vick B.D., Wrigglesworth W., Scott L.B. and Ragsdell K.M.**
"Optimal design of wind turbines using BIAS a method of multipliers code."
Proceeding for ASME design automation conference in 1988,
Published by ASME, New York,USA,1988 (pp 201-210).

14. **Atkinson J.D. , Fletcher C.A.J. , Milthrope and Roberts B.W.**
" The use of australian upper wind data in the design of an electrical generating platform."
Charles Kolling Res. Lab. , T.N. D-17, June 1979, University of Sydney.

15. **O'Doherty, R.J. and Roberts, B.W.**
" The application of U.S. upper wind data in one design of tethered wind energy system."
Solar Energy Research Institute, SERI/TR-211-1400, February, 1982.

16. **" Britannica Encyclopedia."**
Vol. 6, 1991, Britannica Encyclopedia Inc. ,(p.534).

17. **Bailey , F.J. Jr.**
" A study of the torque equilibrium of an autogyro rotor."
A.R.C. Report No. 623, 1938.

18. **Bramwell, A.R.S.**
" Helicopter Dynamics."
Edward Arnold, 1976.

# Appendix A

**The program in this appendix determines the optimum twist for various values of tip speed ratio for different criteria.**

```
      PROGRAM GC

C     THIS PROGRAM CALCULATES THE ROTOR CHARACTERISTICS
C     USING GESSOW AND CRIM'S HIGH INFLOW THEORY.

      REAL M,L1,L2,K1,K2,K3,K4,K5,K6,K7,K8,K9,K10,K11,BETA,BETAD,
     *     K12,K13,K14,K15,K16,K17,K18,L,LH,ACD(1000),COPT1(1000)
     *,CPW(1000),CLW(1000),DMAX1(100),DMAX2(100),DMAX3(100)
     *,DMAX4(100),CLWOP(1000),ALCA1D(1000),COPT2(1000)
     *,CQW(1000),COPT3(1000),CPWX(100),CLWX(100),CQWX(100),CLWOPX(100)
     *,COPT1X(100),COPT2X(100),COPT3X(100),DT1X1(100),DT1X2(100)
     *,DT1X3(100),DT1X4(100),DT1X5(100),DT1X6(100),DT1X7(100)
     *,CPWX1(100),CLWX1(100),CQWX1(100),CLWOPX1(100),COPT1X1(100)
     *,COPT2X1(100),COPT3X1(100),MM(100),D1T1(25),D2T1(25),D3T1(25),
     *D4T1(25),D5T1(25),D6T1(25),D7T1(25)

      INTEGER KLID,K,N,NT0,NT1,NCQS,NM
      CHARACTER F*30

C     THIS PROGRAM CALCULATES MAXIMUM VALUES FOR DIFFERENT WINDMILL
C     PARAMETERS AT VARIOUS TIP SPEED RATIOS FOR A DEFINED RANGE OF
C     TWIST. AFTER COMPARING THE RESULTS THE OPTIMUM TWIST FOR VARIOUS
C     TIP SPEED RATIOS IS DETERMINED FOR DIFFERENT CRITERIA.THE RESULTS
C     FILE NAME IS ( NAME OF THE OPTIMISATION CRITERIA +T1.DAT)(eg.
C     CPWT1.DAT).

C     AL IS THE STALL LIMIT
      AL=13

C     DEFINE THE RANGE OF TIP SPEED RATIO
      DO 3000 NM=0,4
      NMT=NM+1
      M=NM*0.005+0.075

C     DEFINE THE RANGE OF LINEAR TWIST
      DO 4000 NT1=0,20
      D1T1(NT1)=NT1
      D2T1(NT1)=NT1
      D3T1(NT1)=NT1
      D4T1(NT1)=NT1
      D5T1(NT1)=NT1
      D6T1(NT1)=NT1
      D7T1(NT1)=NT1
      T1D=NT1
      I=0

C     DEFINE THE RANGE OF CQ/σ
      DO 1000 NCQS=0,35
      CQS=NCQS*0.000625
      DO 1000 NT0=-400,100
      T0D=NT0*0.1
      KLID=0
      CV=57.29578
      T0=T0D/CV
```

```
      T1=T1D/CV

C     INPUT THE CHARACTERISTICS OF THE ROTOR AND THE TETHERED SYSTEM
      DATA A,B,GA,S,BETAD/5.73,0.97,10.,0.05,40./
      BETA=BETAD/CV
      A0=0.0
      A1=0.0
      B1=0.0
      A2=0.0
      B2=0.0
      A0H=0.0
      LH=0.0
      K=0
      N=0
      CL=1.2
      CD=1.1
      D0=0.0087
      D1=-0.0216
      D2=0.40

C     EVALUATION OF LAMBDA FOR VARIOUS CQ/S VALUES
C     AA = COFFICIENT OF L**2.
C     BB = COFFICIENT OF L**1.
C     CC = COFFICIENT OF L**0.

      F1=T1**3*B**5/30.-T1*B**3/3.
      F2=B**2/2.-T1**2*B**4/8.
      K1=D0+D1*SIN(T0)+D2*(SIN(T0)**2)
      K7=D1*COS(T0)+D2*SIN(2.*T0)
      K8=T1*(2.*D2*COS(2.*T0)-D1*SIN(T0))
      K9=T1**2*(D1/2.*COS(T0)+D2*2.*SIN(2.*T0))

      K10=T1**3*(D1/6.*SIN(T0)-4.*D2/3.*COS(2.*T0))
      K11=T1**4*(D1/24.*COS(T0)+2.*D2/3.*SIN(2.*T0))
      K2=K7*T1
      K3=K8*T1/2.
      K4=K9*T1/3.
      K5=K10*T1/4.
      K6=K11*T1/5.
      K12=T1**5.*(4.*D2/15.*COS(2.*T0)-D1*SIN(T0)/120.)
      K13=D2*COS(T0)**2
      K14=D2*SIN(2.*T0)*T1
      K15=D2*COS(2.*T0)*T1**2
      K16=2./3.*D2*SIN(2.*T0)*T1**3
      K17=D2/3.*COS(2.*T0)*T1**4
      K18=2.*D2/15.*SIN(2.*T0)*T1**5
      G1=K13/2.-K14/3.-K15/4.+K16/5.+K17/6.-K18/7.
   54 K=K+1
      C2=M*A1*B2/2.-M*A0*B1-M/2.*B1*A2
      C3=A1**2/2.+B1**2/2.+2.*A2**2+2.*B2**2
      F3=M*M/2.*A0*A0+.375*M*M*A1*A1+.125*M*M*B1*B1-M*M/2.*A0*A2

      AA=-G1+K13/8.*M**2+A*(F1*SIN(T0)+COS(T0)*(F2-M**2/8.)
     *  -CL/8./A*(M*(1.-M/2.))**2)
      BB=-(G1*M*A1-3.*K13/16.*M**3*A1+K7/3.+K8/4.-K9/5.
     *  +K10/6.+K11/7.+K12/8.)-M**3*((K7-A*SIN(T0))/28.27
```

```
     *   -(A1*0.1875*(A*COS(T0)))-CD/28.27*(1.-M/2.))
     *   +SIN(T0)*A*(F1*M*A1+B**3/3.-B**5*T1**2/10.)
     *   +COS(T0)*A*(B**4*T1/4.-B**6*T1**3/36.+F2*M*A1)
     *   -K8*M**4/64.
      CC=A*SIN(T0)*(F1*F3+B2*(M*B)**2/8.-C2/4.*T1*B**4
     *   -C3/5.*T1*B**5)+A*COS(T0)*(F2*F3+M**2*B2*B**3*T1/12.
     *   +C2*B**3/3.+C3*(B**4/4.-T1**2*B**6/12.))-2.*CQS
     *   -(F3*G1-M**4*(K13/32.*A0**2+K1/64.+CD/128.)
     *   +K1/4.+K2/5.+K3/6.-K4/7.+K5/8.+K6/9.
     *   +M**2*(K1/4.+K2/6.+K3/8.-K4/10.+K5/12.+K6/14.)
     *   +M**2*B2*(K7/8.+K8/12.-K9/16.+K10/20.+K11/24.+K12/28.)
     *   +C2*(K13/3.-K14/4.-K15/5.+K16/6.+K17/7.-K18/8.)
     *   +C3*(K13/4.-K14/5.-K15/6. +K16/7.+K17/8.-K18/9.))

C     SOLVING FOR LAMBDA VALUES

C      THIS PART WAS MODIFIED TO GET ONLY POSITIVE VALUES OF LAMBDA AND
IN
C     THE CASE THAT BOTH VALUES ARE POSITIVE GET THE RESULTS FOR BOTH
C      VALUES
C     OF LAMBDA. (A. JABBARZADEH 18.3.93)

      IF((BB**2-4.*AA*CC).LT.0.0)GOTO 1000
      L1=SQRT(BB**2-4.*AA*CC)
      L2=(L1+BB)/((-2.)*AA)
      L1=(L1-BB)/(2.*AA)
      IF((L1.LT.0.0).AND.(L2.LT.0.0))GOTO 1000
      L=L1
      IF (L.LT.0.0) L=L2
      ERR= ABS(L-LH)
      IF ((ERR).LT.0.000001)GO TO 70
      LH=L
      IF(K-20)24,24,65

C     COMPARE THE RESULTS TO BE IN THE RANGE OF NONSTALL LIMIT.(αr.4,1<13)
   70 AR4=(2.5*L+T0+(0.4+M)*T1+(1.+2.5*M)*A1)*CV
      AR1=(L+T0+(1.+M)*T1+(1.+M)*A1)*CV
      IF(((AR4.LT.AL).AND.(AR1.LT.AL)).AND.((ABS(AR4-AL).LT.0.25).OR.
     *(ABS(AR1-AL).LT.0.25)))THEN
      IF(KLID.EQ.1)GOTO 24
      IF(KLID.EQ.0)GOTO 64
      ENDIF
      GOTO 1000

C     ITERATING FOR VALUES OF A0,A1,B1,A2,B2
C     Corrections to ao to b2 inserted 4/11/91

   24 N=N+1
      A0=GA/2.*(COS(T0)*(B**3*L/3.+M*M/8.*B2*B*B
     *   +0.0398*L*M**3+0.033*A1*M**4+T1*(B**5/5.+M*M/6.*B**3)
     *   -T1*T1/2.*B**5/5.*L-T1**3/42.*B**7)
     *   +SIN(T0)*(B**4/4.+(B*M)**2/4.-M**4/64.
     *   -T1*(L*B**4/4.+L*M**4/64.)
     *   -T1*T1/4.*(B**6/3.+B**4*M*M/4.)+T1**3/36.*B**6*L
     *   +T1**4/192.*B**8.)+CL*M**4./A/128.
     *   +L*L*M*M/A/8.*CD*(1.-M/2.)**2
```

```
     *   +0.0398/A*M**3*L*CL*(1.-M/2.)+0.0199/A*L*
     *   (1.-M/2.)*M**3*CD)
      B1=(COS(T0)*(M*B**5/10.*A0*T1*T1-M*B**3*A2/6.
     *   -0.05*A2*M**4-M*B**3*A0/3.)
     *   -SIN(T0)*T1*(M*B**4*A2/8.-M*B**4/4.*A0))
     *   /(SIN(T0)*(T1*B**5/5.+T1*M*M*B**3/12.
     *   -T1**3*B**7/42.)-COS(T0)*(B**4/4.
     *   +M*M*B*B/8.-T1**2/12.*B**6))
      A1=(SIN(T0)*(M*B**3*2./3.+0.0265*M**4
     *   -T1*(M*L*B**3/3.-M*B2*B**4/8.-0.0265*L*M**4)
     *   -T1*T1/5.*M*B**5)+COS(T0)*(M*L*B*B/2.
     *   -M*B**3*B2/6.-L*M**3/16.+T1*M*B**4/2.
     *   -T1*T1/8.*M*L*B**4-T1**3/18.*M*B**6)
     *   -0.01325*M**4*CL/A-0.2123*L*L*(M*(1.-M/2.))
     *   **2*CD/A-L*M**3/16.*(1.-M/2.)*CL/A-L*(1.-M/2.)
     *   /32.*M**3*CD/A)/(SIN(T0)*(M*M*T1*B**3/12.-T1*B**5/5.
     *   +T1**3*(B**7/42.-M*M*B**5/120.))
     *   +COS(T0)*(B**4/4.-(M*B)**2/8.+M**4/32.+T1*T1/2.
     *   *(M*M*B**4/16.-B**6/6.)+T1**4*B**8/192.))
      B2=GA/6.*(COS(T0)*(M*B**3*B1/3.-M*M*A0*B*B/4.
     *   -A2*B**4/2.+A2/16.*M**4+T1*T1/2.*(M*B**5/5.
     *   *B1-A2*B**6/3.))-SIN(T0)*(T1*(M*B1*B**4/4.
     *   -M*M*A0*B**3/6.-0.4*A2*B**5)))
      A2=GA/6.*(SIN(T0)*(M**4/64.-(M*B/2.)**2
     *   -T1*(M*A1*B**4/4.+2.*B2*B**5/5.)
     *   +T1*T1/16.*M*M*B**4)+COS(T0)*(M*B**3/3.*A1
     *   +B**4*B2/2.+0.0265*L*M**3+0.015*A1*M**4
     *   -T1*M*M/6.*B**3-T1*T1/2.*(M*B**5/5.*A1
     *   +B**6/3.*B2))-M**4*CL/128./A
     *   -CD/8./A*(L*M*(1.-M/2.))**2+0.0265/A*M**3*L*CL
     *   *(1.-M/2.)+0.01327/A*L*(1.-M/2.)*M**3*CD)
      IF(KLID.EQ.1)GOTO 64
      IF(ABS(A0-A0H).LT.0.000001) GOTO 54
      A0H=A0
      GOTO 24

C     CALCULATION OF THRUST COEFFICIENT,CONTROL AXIS
C     ANGLE AND WINDMILL PARAMETERS.

   64 TCTSA=SIN(T0)*(B**3/3.+M*M*B/2.-.07073*M**3
     *      -T1*(L*B**3/3.+0.03537*L*M**3)
     *      -T1*T1*(B**5/10.+M*M*B**3/12.)
     *      +T1**3*L*B**5/30.+T1**4*B**7/168.)
     *      +COS(T0)*(L*B*B/2.+M*M*B2*B/4.
     *      +M*M*L/8.+M**3*A1/16.+T1*(B**4/4.
     *      +M*M*B*B/4.-M**4/64.)+T1*T1*(M**4*L/128.
     *      -L*B**4/8.)-T1**3*(B**6/36.+M*M*B**4/48.))
     *      +CL/A*(M*M/8.*L*(1.-M/2.)+M**3/28.27)
     *      +CD/A*(M*L*L/3.142*(1.-M/2.)
     *      +M*M*L/16.)*(1.-M/2.)
      I=I+1
      CT=TCTSA/2.*S*A
      AC=ATAN(L/M+CT/2./M/(SQRT(M*M+L*L)))
      ACD(I)=AC*CV
      CQ=CQS*S
```

```
C     CALCULATION OF WINDMILL PARAMETRS
      TSR=COS(AC)/M
      CPW(I)=2.*CQ*TSR**3
      CTW=2.*CT*TSR**2
      CLW(I)=CTW*COS(A1+AC)
      COPT1(I)=CLW(I)*CPW(I)
      CLWOP(I)=CLW(I)*(1-(TAN(AC+A1))*TAN(BETA))
      ALCA1D(I)=ACD(I)+A1D
      COPT2(I)=CLWOP(I)*CPW(I)
      CQW(I)=CPW(I)*TSR
      COPT3(I)=CQW(I)*CLWOP(I)
      WRITE(*,*)M,T1D,T0D,NCQS,I
      IF(KLID.EQ.1)GOTO 1000
      IF((L1.GT.0.0).AND.(L2.GT.0.0))THEN
      KLID=1
      L=L2
      GOTO 70
      ENDIF
      GO TO 1000
 65   WRITE(6,701)T1D,T0D,ERR,K,L
 701  FORMAT(F6.2,'  ',F6.2,'   NO CONVERGENCE  ERR=',F13.9,'   K=',I5
     *,'   L=',F7.4)
      GO TO 1000
 66   WRITE(6,702)T1D,T0D
 702  FORMAT(F6.2,'  ',F6.2,'   NO REAL SOLUTION FOR LAMBDA   AA**2-4AA*C
     *C<0  K=',I4)
      GOTO 1000
 67   WRITE(6,703)T1D,T0D
 703  FORMAT(F6.2,'  ',F6.2,'   BOTH VALUES OF LAMBDA ARE NEGATIVE')
1000  CONTINUE

      CALL SORT(CLWOP,I)
      CALL MAX(CLWOP,NT1,CLWOPX)
      CALL SORT(CPW,I)
      CALL MAX(CPW,NT1,CPWX)
      CALL SORT(CQW,I)
      CALL MAX(CQW,NT1,CQWX)
      CALL SORT(COPT1,I)
      CALL MAX(COPT1,NT1,COPT1X)
      CALL SORT(COPT2,I)
      CALL MAX(COPT2,NT1,COPT2X)
      CALL SORT(COPT3,I)
      CALL MAX(COPT3,NT1,COPT3X)
      CALL SORT(CLW,I)
      CALL MAX(CLW,NT1,CLWX)

4000  CONTINUE
      CALL SORT2(CPWX,D1T1,NT1)
      CALL MAX2(CPWX,D1T1,NM,CPWX1,DT1X1)
      CALL SORT2(CLWX,D2T1,NT1)
      CALL MAX2(CLWX,D2T1,NM,CLWX1,DT1X2)
      CALL SORT2(CQWX,D3T1,NT1)
      CALL MAX2(CQWX,D3T1,NM,CQWX1,DT1X3)
      CALL SORT2(CLWOPX,D4T1,NT1)
      CALL MAX2(CLWOPX,D4T1,NM,CLWOPX1,DT1X4)
      CALL SORT2(COPT1X,D5T1,NT1)
```

```
      CALL MAX2(COPT1X,D5T1,NM,COPT1X1,DT1X5)
      CALL SORT2(COPT2X,D6T1,NT1)
      CALL MAX2(COPT2X,D6T1,NM,COPT2X1,DT1X6)
      CALL SORT2(COPT3X,D7T1,NT1)
      CALL MAX2(COPT3X,D7T1,NM,COPT3X1,DT1X7)
      MM(NM)=M
 3000 CONTINUE

C     WRITING THE RESULTS IN A PROPER FORMAT TO BE USED IN "TECPLOT"
C     FOR PRODUCING APPROPRIATE GRAPHS.

      OPEN(UNIT=6,FILE='C:\F77L\CPWT1.DAT')
      NMT=NM+1
      WRITE(6,730)NM
  730 FORMAT('title=""'/'variables=Θ1,CPW,M'/'Zone t="zone 1",i=',I3,
     *',f=point')
      WRITE(6,734)(DT1X1(I),CPWX1(I),MM(I),I=0,NM)
  734 FORMAT(F5.2,'    ',F7.4,'    'F7.4)
      CLOSE(UNIT=6)
      OPEN(UNIT=6,FILE='C:\F77L\CLWT1.DAT')
      NMT=NM+1
      WRITE(6,731)NM
  731 FORMAT('title=""'/'variables=Θ1,CLW,M'/'Zone t="zone 1",i=',I3,
     *',f=point')
      WRITE(6,735)(DT1X2(I),CLWX1(I),MM(I),I=0,NM)
  735 FORMAT(F5.2,'    ',F7.4,'    'F7.4)
      CLOSE(UNIT=6)
      OPEN(UNIT=6,FILE='C:\F77L\CQWT1.DAT')
      WRITE(6,732)NM
  732 FORMAT('title=""'/'variables=Θ1,CQW,M'/'Zone t="zone 1",i=',I3,
     *',f=point')
      WRITE(6,736)(DT1X3(I),CQWX1(I),MM(I),I=0,NM)
  736 FORMAT(F5.2,'    ',F7.4,'    'F7.4)
      CLOSE(UNIT=6)
      OPEN(UNIT=6,FILE='C:\F77L\CLWOPT1.DAT')
      WRITE(6,733)NM
  733 FORMAT('title=""'/'variables=Θ1,CLWOPT1,M'/'Zone t="zone 1",i=',I3
     *,',f=point')
      WRITE(6,737)(DT1X4(I),CLWOPX1(I),MM(I),I=0,NM)
  737 FORMAT(F5.2,'    ',F7.4,'    'F7.4)
      CLOSE(UNIT=6)
      OPEN(UNIT=6,FILE='C:\F77L\COPT1T1.DAT')
      WRITE(6,738)NM
  738 FORMAT('title=""'/'variables=Θ1,COPT1,M'/'Zone t="zone 1",i=',I3,
     *',f=point')
      WRITE(6,739)(DT1X5(I),COPT1X1(I),MM(I),I=0,NM)
  739 FORMAT(F5.2,'    ',F7.4,'    'F7.4)
      CLOSE(UNIT=6)
      OPEN(UNIT=6,FILE='C:\F77L\COPT2T1.DAT')
      WRITE(6,740)NM
  740 FORMAT('title=""'/'variables=Θ1,COPT2,M'/'Zone t="zone 1",i=',I3,
     *',f=point')
      WRITE(6,741)(DT1X6(I),COPT2X1(I),MM(I),I=0,NM)
  741 FORMAT(F5.2,'    ',F7.4,'    'F7.4)
      CLOSE(UNIT=6)
      OPEN(UNIT=6,FILE='C:\F77L\COPT3T1.DAT')
```

```
      WRITE(6,742)NM
 742  FORMAT('title=""'/'variables=Θ1,COPT3,M'/'Zone t="zone 1",i=',I3,
     *',f=point')
      WRITE(6,743)(DT1X7(I),COPT3X1(I),MM(I),I=0,NM)
 743  FORMAT(F5.2,'    ',F7.4,'     'F7.4)
      CLOSE(UNIT=6)

      STOP
      END
*****************************************************************************

      SUBROUTINE MAX(D,IK,DMAX)
      DIMENSION D(1000),DMAX(100)
      INTEGER IK
C      THIS SUBROUTINE CHOOSE THE FIRST DATA IN THE DIMENSION AND CREATE
C      AN ARRAY FOR EACH TIP SPEED RATIO AND STORE THE MAXIMUM VALUE OF
c      ARRAY D1 FOR EVERY TWIST ANGLE (NT1).

      DMAX(IK)=D(1)
      RETURN
      END
*****************************************************************************

      SUBROUTINE SORT(D11,I)
      DIMENSION D11(1000)
      REAL TEMP,TEMP2,TEMP3,TEMP4,TEMP5,TEMP1
C

C      SORTING DARA IN ARRAY D1
C
      DO 20 II=1,I
      DO 20 IJ=II+1,I
      IF(D11(II).LT.D11(IJ))THEN
      TEMP=D11(II)
      D11(II)=D11(IJ)
      D11(IJ)=TEMP
      ENDIF
 20   CONTINUE
      RETURN
      END
*****************************************************************************

      SUBROUTINE SORT2(D11,D22,I)
      DIMENSION D11(100),D22(100)
      REAL TEMP,TEMP1
C

C      SORTING DARA IN ARRAY D1
C
      DO 20 II=1,I
      DO 20 IJ=II+1,I
      IF(D11(II).LT.D11(IJ))THEN
      TEMP=D11(II)
      TEMP1=D22(II)
      D11(II)=D11(IJ)
      D22(II)=D22(IJ)
```

```
      D11(IJ)=TEMP
      D22(IJ)=TEMP1

      ENDIF
 20   CONTINUE
      RETURN
      END

*****************************************************************************

      SUBROUTINE MAX2(D,D1,IK,DMAX,D1MAX)
      DIMENSION D(1000),DMAX(100),D1(1000),D1MAX(100)
      INTEGER IK
C      THIS SUBROUTINE CHOOSE THE FIRST DATA IN THE DIMENSION AND CREATE
C      AN ARRAY FOR EACH TIP SPEED RATIO AND STORE THE MAXIMUM VALUE OF
C      ARRAY D1 FOR EVERY TWIST ANGLE (NT1).

      DMAX(IK)=D(1)
      D1MAX(IK)=D1(1)
      RETURN
      END
*****************************************************************************
```

# Appendix B

**The computer program in this appendix calculates and gives the results for maximum values of windmill parameters at various tip speed ratios.**

```
      PROGRAM GC
c     MODIFIED 25.3.93
C     THIS PROGRAM CALCULATES THE ROTOR CHARACTERISTICS
C     USING GESSOW AND CRIM'S HIGH INFLOW THEORY.
      REAL M,L1,L2,K1,K2,K3,K4,K5,K6,K7,K8,K9,K10,K11,
     *     K12,K13,K14,K15,K16,K17,K18,L,LH,ACD(1000),COPT1(1000)
     *,CPW(1000),CLW(1000),DMAX1(100),DMAX2(100),DMAX3(100)
     *,DMAX4(100),DT1(25),CLWOP(1000),ALCA1D(1000),COPT2(1000)
     *,CQW(1000),COPT3(1000),MM(50),P(1000),D1MAX(100),D2MAX(100)
     *,D3MAX(100)

C     THIS PROGRAM CALCULATES MAXIMUM WINDMILL PARAMETERS SUCH AS
CPW, C    CLW,FOR TIP SPEED RATIOS BETWEEN 0.05 TO 1.75 AND WRITE THEM IN
C     A FILE. FOR ANY PARAMETERS WHICH YOU WOULD LIKE TO HAVE THE
C     RESULT JUST INPUT THE PARAMETER NAME ( e.g. CLW) IN CALL STATEMENT
C     FOR SUBROUTINES IN LINES 243, 244. THE RESULTS FILE NAME IS MAXM.DAT .

      INTEGER KLID,K,N,NT0,NT1,NCQS,NM
      CHARACTER F*20

C     NSTALL IS THE STALL LIMIT PARAMETER
      AL=13

C     DEFINE THE VALUE OF TWIST
      DO 3000 NT1=8,8
      CLOSE(UNIT=6)
      T1D=NT1

C     DEFINE THE RANGE OF TIP SPEED RATIO
      DO 3000 NM=0,50
      I=0
      M=NM*0.0025+0.05

C     DEFINE THE RANGE OF CQ/σ
      DO 1000 NCQS=0,35
      CQS=NCQS*0.000625
      DO 1000 NT0=-400,100
      T0D=NT0*0.1
      KLID=0
      CV=57.29578
      T0=T0D/CV
      T1=T1D/CV

C     INPUT THE ROTOR AND THE TETHERED SYSTEM CHARACTERISTICS
      DATA A,B,GA,S,BETAD/5.73,0.97,10.,0.05,40./
      BETA=BETAD/CV
      A0=0.0
      A1=0.0
      B1=0.0
      A2=0.0
      B2=0.0
      A0H=0.0
```

```
      LH=0.0
      K=0
      N=0
      CL=1.2
      CD=1.1
      D0=0.0087
      D1=-0.0216
      D2=0.40

C     EVALUATION OF LAMBDA FOR VARIOUS CQ/S VALUES
C     AA = COFFICIENT OF L**2.
C     BB = COFFICIENT OF L**1.
C     CC = COFFICIENT OF L**0.

      F1=T1**3*B**5/30.-T1*B**3/3.
      F2=B**2/2.-T1**2*B**4/8.
      K1=D0+D1*SIN(T0)+D2*(SIN(T0)**2)
      K7=D1*COS(T0)+D2*SIN(2.*T0)
      K8=T1*(2.*D2*COS(2.*T0)-D1*SIN(T0))
      K9=T1**2*(D1/2.*COS(T0)+D2*2.*SIN(2.*T0))

      K10=T1**3*(D1/6.*SIN(T0)-4.*D2/3.*COS(2.*T0))
      K11=T1**4*(D1/24.*COS(T0)+2.*D2/3.*SIN(2.*T0))
      K2=K7*T1
      K3=K8*T1/2.
      K4=K9*T1/3.
      K5=K10*T1/4.
      K6=K11*T1/5.
      K12=T1**5.*(4.*D2/15.*COS(2.*T0)-D1*SIN(T0)/120.)
      K13=D2*COS(T0)**2
      K14=D2*SIN(2.*T0)*T1
      K15=D2*COS(2.*T0)*T1**2
      K16=2./3.*D2*SIN(2.*T0)*T1**3
      K17=D2/3.*COS(2.*T0)*T1**4
      K18=2.*D2/15.*SIN(2.*T0)*T1**5
      G1=K13/2.-K14/3.-K15/4.+K16/5.+K17/6.-K18/7.
   54 K=K+1
      C2=M*A1*B2/2.-M*A0*B1-M/2.*B1*A2
      C3=A1**2/2.+B1**2/2.+2.*A2**2+2.*B2**2
      F3=M*M/2.*A0*A0+.375*M*M*A1*A1+.125*M*M*B1*B1-M*M/2.*A0*A2

      AA=-G1+K13/8.*M**2+A*(F1*SIN(T0)+COS(T0)*(F2-M**2/8.)
     *  -CL/8./A*(M*(1.-M/2.))**2)
      BB=-(G1*M*A1-3.*K13/16.*M**3*A1+K7/3.+K8/4.-K9/5.
     *  +K10/6.+K11/7.+K12/8.)-M**3*((K7-A*SIN(T0))/28.27
     *  -(A1*0.1875*(A*COS(T0)))-CD/28.27*(1.-M/2.))
     *  +SIN(T0)*A*(F1*M*A1+B**3/3.-B**5*T1**2/10.)
     *  +COS(T0)*A*(B**4*T1/4.-B**6*T1**3/36.+F2*M*A1)
     *  -K8*M**4/64.
      CC=A*SIN(T0)*(F1*F3+B2*(M*B)**2/8.-C2/4.*T1*B**4
     *  -C3/5.*T1*B**5)+A*COS(T0)*(F2*F3+M**2*B2*B**3*T1/12.
     *  +C2*B**3/3.+C3*(B**4/4.-T1**2*B**6/12.))-2.*CQS
     *  -(F3*G1-M**4*(K13/32.*A0**2+K1/64.+CD/128.)
     *  +K1/4.+K2/5.+K3/6.-K4/7.+K5/8.+K6/9.
     *  +M**2*(K1/4.+K2/6.+K3/8.-K4/10.+K5/12.+K6/14.)
     *  +M**2*B2*(K7/8.+K8/12.-K9/16.+K10/20.+K11/24.+K12/28.)
```

```
     *   +C2*(K13/3.-K14/4.-K15/5.+K16/6.+K17/7.-K18/8.)
     *   +C3*(K13/4.-K14/5.-K15/6. +K16/7.+K17/8.-K18/9.))

C     SOLVING FOR LAMBDA VALUES

C      THIS PART WAS MODIFIED TO GET ONLY POSITIVE VALUES OF LAMBDA AND
C      IN THE CASE THAT BOTH VALUES ARE POSITIVE GET THE RESULTS FOR BOTH
C      VALUES OF LAMBDA. (A. JABBARZADEH 18.3.93)

      IF((BB**2-4.*AA*CC).LT.0.0)GOTO 66
      L1=SQRT(BB**2-4.*AA*CC)
      L2=(L1+BB)/((-2.)*AA)
      L1=(L1-BB)/(2.*AA)
      IF((L1.LT.0.0).AND.(L2.LT.0.0))GOTO 67
      L=L1
      IF (L.LT.0.0) L=L2
      ERR= ABS(L-LH)
      IF ((ERR).LT.0.000001)GO TO 70
      LH=L
      IF(K-20)24,24,65
C     COMPARE THE RESULTS TO BE IN THE RANGE OF NONSTALL LIMIT.(αr.4,1<13)
   70 AR4=(2.5*L+T0+(0.4+M)*T1+(1.+2.5*M)*A1)*CV
      AR1=(L+T0+(1.+M)*T1+(1.+M)*A1)*CV
      IF(((AR4.LT.AL).AND.(AR1.LT.AL)).AND.((ABS(AR4-AL).LT.0.25).OR.
     *(ABS(AR1-AL).LT.0.25)))THEN
      IF(KLID.EQ.1)GOTO 24
      IF(KLID.EQ.0)GOTO 64
      ENDIF
      GOTO 1000

C     ITERATING FOR VALUES OF A0,A1,B1,A2,B2
C     Corrections to ao to b2 inserted 4/11/91

   24 N=N+1
      A0=GA/2.*(COS(T0)*(B**3*L/3.+M*M/8.*B2*B*B
     *   +0.0398*L*M**3+0.033*A1*M**4+T1*(B**5/5.+M*M/6.*B**3)
     *   -T1*T1/2.*B**5/5.*L-T1**3/42.*B**7)
     *   +SIN(T0)*(B**4/4.+(B*M)**2/4.-M**4/64.
     *   -T1*(L*B**4/4.+L*M**4/64.)
     *   -T1*T1/4.*(B**6/3.+B**4*M*M/4.)+T1**3/36.*B**6*L
     *   +T1**4/192.*B**8.)+CL*M**4./A/128.
     *   +L*L*M*M/A/8.*CD*(1.-M/2.)**2
     *   +0.0398/A*M**3*L*CL*(1.-M/2.)+0.0199/A*L*
     *   (1.-M/2.)*M**3*CD)
      B1=(COS(T0)*(M*B**5/10.*A0*T1*T1-M*B**3*A2/6.
     *   -0.05*A2*M**4-M*B**3*A0/3.)
     *   -SIN(T0)*T1*(M*B**4*A2/8.-M*B**4/4.*A0))
     *   /(SIN(T0)*(T1*B**5/5.+T1*M*M*B**3/12.
     *   -T1**3*B**7/42.)-COS(T0)*(B**4/4.
     *   +M*M*B*B/8.-T1**2/12.*B**6))
      A1=(SIN(T0)*(M*B**3*2./3.+0.0265*M**4
     *   -T1*(M*L*B**3/3.-M*B2*B**4/8.-0.0265*L*M**4)
     *   -T1*T1/5.*M*B**5)+COS(T0)*(M*L*B*B/2.
     *   -M*B**3*B2/6.-L*M**3/16.+T1*M*B**4/2.
     *   -T1*T1/8.*M*L*B**4-T1**3/18.*M*B**6)
     *   -0.01325*M**4*CL/A-0.2123*L*L*(M*(1.-M/2.))
```

```
     *   **2*CD/A-L*M**3/16.*(1.-M/2.)*CL/A-L*(1.-M/2.)
     *   /32.*M**3*CD/A)/(SIN(T0)*(M*M*T1*B**3/12.-T1*B**5/5.
     *   +T1**3*(B**7/42.-M*M*B**5/120.))
     *   +COS(T0)*(B**4/4.-(M*B)**2/8.+M**4/32.+T1*T1/2.
     *   *(M*M*B**4/16.-B**6/6.)+T1**4*B**8/192.))
      B2=GA/6.*(COS(T0)*(M*B**3*B1/3.-M*M*A0*B*B/4.
     *   -A2*B**4/2.+A2/16.*M**4+T1*T1/2.*(M*B**5/5.
     *   *B1-A2*B**6/3.))-SIN(T0)*(T1*(M*B1*B**4/4.
     *   -M*M*A0*B**3/6.-0.4*A2*B**5)))
      A2=GA/6.*(SIN(T0)*(M**4/64.-(M*B/2.)**2
     *   -T1*(M*A1*B**4/4.+2.*B2*B**5/5.)
     *   +T1*T1/16.*M*M*B**4)+COS(T0)*(M*B**3/3.*A1
     *   +B**4*B2/2.+0.0265*L*M**3+0.015*A1*M**4
     *   -T1*M*M/6.*B**3-T1*T1/2.*(M*B**5/5.*A1
     *   +B**6/3.*B2))-M**4*CL/128./A
     *   -CD/8./A*(L*M*(1.-M/2.))**2+0.0265/A*M**3*L*CL
     *   *(1.-M/2.)+0.01327/A*L*(1.-M/2.)*M**3*CD)
      IF(KLID.EQ.1)GOTO 64
      IF(ABS(A0-A0H).LT.0.000001) GOTO 54
      A0H=A0
      A1H=A1
      B1H=B1
      A2H=A2
      B2H=B2
      GOTO 24
C     CALCULATION OF THRUST COEFFICIENT,CONTROL AXIS
C     ANGLE AND WINDMILL PARAMETERS.

   64 TCTSA=SIN(T0)*(B**3/3.+M*M*B/2.-.07073*M**3
     *      -T1*(L*B**3/3.+0.03537*L*M**3)
     *      -T1*T1*(B**5/10.+M*M*B**3/12.)
     *      +T1**3*L*B**5/30.+T1**4*B**7/168.)
     *      +COS(T0)*(L*B*B/2.+M*M*B2*B/4.
     *      +M*M*L/8.+M**3*A1/16.+T1*(B**4/4.
     *      +M*M*B*B/4.-M**4/64.)+T1*T1*(M**4*L/128.
     *      -L*B**4/8.)-T1**3*(B**6/36.+M*M*B**4/48.))
     *      +CL/A*(M*M/8.*L*(1.-M/2.)+M**3/28.27)
     *      +CD/A*(M*L*L/3.142*(1.-M/2.)
     *      +M*M*L/16.)*(1.-M/2.)
      I=I+1
      CT=TCTSA/2.*S*A
      AC=ATAN(L/M+CT/2./M/(SQRT(M*M+L*L)))
      ACD(I)=AC*CV
      CQ=CQS*S

C     CALCULATION OF WINDMILL PARAMETRS
      TSR=COS(AC)/M
      CPW(I)=2.*CQ*TSR**3
      CTW=2.*CT*TSR**2
      CLW(I)=CTW*COS(A1+AC)
      COPT1(I)=CLW(I)*CPW(I)
      CLWOP(I)=CLW(I)*(1-(TAN(AC+A1))*TAN(BETA))
      ALCA1D(I)=ACD(I)+A1D
      COPT2(I)=CLWOP(I)*CPW(I)
      CQW(I)=CPW(I)*TSR
      COPT3(I)=CQW(I)*CLWOP(I)
```

```
      P(I)=T0D
      WRITE(*,*)M,T0D,NM,NCQS,L,K,I
      IF(KLID.EQ.1)GOTO 1000
      IF((L1.GT.0.0).AND.(L2.GT.0.0))THEN
      KLID=1
      L=L2
      GOTO 70
      ENDIF
      GO TO 1000
 65   WRITE(6,701)T1D,T0D,ERR,K,L
 701  FORMAT(F6.2,'  ',F6.2,'   NO CONVERGENCE  ERR=',F13.9,'   K=',I5
     *,'   L=',F7.4)
      GO TO 1000
 66   WRITE(6,702)T1D,T0D
 702  FORMAT(F6.2,'  ',F6.2,'   NO REAL SOLUTION FOR LAMBDA   AA**2-4AA*C
     *C<0  K=',I4)
      GOTO 1000
 67   WRITE(6,703)T1D,T0D
 703  FORMAT(F6.2,'  ',F6.2,'   BOTH VALUES OF LAMBDA ARE NEGATIVE')
 1000 CONTINUE

C     SORTING BASED ON FIRST PARAMETER IN THE CALL STATEMENT
      CALL SORT(CLWOP,ACD,COPT2,CPW,CLW,COPT1,CQW,COPT3,P,I)
      CALL MAX(CLWOP,ACD,P,NM,D1MAX,D2MAX,D3MAX)

      MM(NM)=M
 3000 CONTINUE
      OPEN(UNIT=6,FILE='C:\F77L\MAXM.DAT')
      NMM=NM+1
      WRITE(6,730)NMM
 730  FORMAT('title=""'/'variables=M,CLWOP'/'Zone t="zone 1",i=',I3,'
     *,f=point')

      WRITE(6,733)(MM(I),D1MAX(I),I=0,NM)
 733  FORMAT(F7.4,'     ',F7.4)
      WRITE(6,737)NMM
 737  FORMAT('Zone t="zone 2",i=',I3,',f=point')

      WRITE(6,734)(D3MAX(I),D1MAX(I),I=0,NM)
 734  FORMAT(F7.3,'     ',F7.4)
      WRITE(6,738)NMM
 738  FORMAT('Zone t="zone 3",i=',I3,',f=point')

      WRITE(6,735)(D2MAX(I),D1MAX(I),I=0,NM)
 735  FORMAT(F6.2,'     ',F7.4)

      CLOSE (UNIT=6)

      STOP
      END

*****************************************************************************
      SUBROUTINE SORT(D1,D2,D3,D4,D5,D6,D7,D8,D9,I)

C     THIS SUBROUTINE SORT VALUES IN ARRAYS D1 TO D9 BASED ON THE VALUES
IN D1
```

```
C     FROM LARGE TO SMALL.

      DIMENSION D1(1000),D2(1000),D3(1000),D4(1000),D5(1000),D6(1000)
     *,D7(1000),D8(1000),D9(1000)
      REAL TEMP,TEMP2,TEMP3,TEMP4,TEMP5,TEMP1,TEMP6,TEMP7,TEMP8

      DO 20 II=1,I
      DO 20 IJ=II+1,I
      IF(D1(II).LT.D1(IJ))THEN
      TEMP=D1(II)
      TEMP1=D2(II)
      TEMP2=D3(II)
      TEMP3=D4(II)
      TEMP4=D5(II)
      TEMP5=D6(II)
      TEMP6=D7(II)
      TEMP7=D8(II)
      TEMP8=D9(II)
      D2(II)=D2(IJ)
      D1(II)=D1(IJ)
      D3(II)=D3(IJ)
      D4(II)=D4(IJ)
      D5(II)=D5(IJ)
      D6(II)=D6(IJ)
      D7(II)=D7(IJ)
      D8(II)=D8(IJ)
      D9(II)=D9(IJ)
      D1(IJ)=TEMP
      D2(IJ)=TEMP1
      D3(IJ)=TEMP2
      D4(IJ)=TEMP3
      D5(IJ)=TEMP4
      D6(IJ)=TEMP5
      D7(IJ)=TEMP6
      D8(IJ)=TEMP7
      D9(IJ)=TEMP8
      ENDIF
 20   CONTINUE
      RETURN
      END
*******************************************************************************

      SUBROUTINE MAX(DM1,DM2,DM3,NM,D1MAX,D2MAX,D3MAX)

C     THIS SUBROUTINE STORE THE FIRST VALUE IN DM1,DM2,DM3 IN 3 OTHER
ARRAYS.

      DIMENSION DM1(1000),DM2(1000),DM3(1000),D1MAX(100),D2MAX(100)
     *,D3MAX(100)
      D1MAX(NM)=DM1(1)
      D2MAX(NM)=DM2(1)
      D3MAX(NM)=DM3(1)
      RETURN
      END
*******************************************************************************
```

# Appendix c

**The program in this appendix calculates and gives the minimum wind velocity required to remain aloft at various tip speed ratios for windmilling and autorotation states for MK3.**

```
      PROGRAM GC
c     MODIFIED 25.3.93
C     THIS PROGRAM CALCULATES THE ROTOR CHARACTERISTICS
C     USING GESSOW AND CRIM'S HIGH INFLOW THEORY.
      REAL M,L1,L2,K1,K2,K3,K4,K5,K6,K7,K8,K9,K10,K11,
     * K12,K13,K14,K15,K16,K17,K18,L,LH,ACD(1000),COPT(1000),CPW(1000),
     *CLW(1000),VMAXM(50),ACM(50),PM(50),MM(50),P(1000),ALCA1D(1000)
     *,CLWOP(1000),V(1000),SV
      INTEGER KLID,K,N,NT0,NT1,NCQS,NM
      CHARACTER F*20
C     THIS PROGRAM CALCULATES THE MINIMUM WIND VELOCITY TO REMAIN
C     ALOFT IN VARIOUS TIP SPEED RATIOS, AND ALSO GIVES THE CONTROL AXIS
C     ANGLE AT WHICH THIS OCCURS. THE RESULTS FILE NAME IS VT0.DAT.

C     NSTALL IS THE STALL LIMIT PARAMETER
      AL=13
      CLOSE(UNIT=6)
      OPEN(UNIT=6,FILE='C:\F77L\VT0.DAT')

C     INPUT TWIST IN DEGREE.
      DO 3000 NT1=0,0
      T1D=NT1
      DO 3000 NM=0,14
      NMT=NM+1
      I=1
      M=NM*0.01+0.065
      DO 1000 NCQS=0,35
      CQS=NCQS*0.000625
      DO 1000 NT0=-200,50
      T0D=NT0*0.2
      KLID=0
      CV=57.29578
      T0=T0D/CV
      T1=T1D/CV
      DATA A,B,GA,S,BETAD/5.73,0.97,10.,0.05,40./
      BETA=BETAD/CV
      A0=0.0
      A1=0.0
      B1=0.0
      A2=0.0
      B2=0.0
      A0H=0.0
      LH=0.0
      K=0
      N=0
      CL=1.2
      CD=1.1
      D0=0.0087
      D1=-0.0216
      D2=0.40
```

```
C     EVALUATION OF LAMBDA FOR VARIOUS CQ/S VALUES
C     AA = COFFICIENT OF L**2.
C     BB = COFFICIENT OF L**1.
C     CC = COFFICIENT OF L**0.

      F1=T1**3*B**5/30.-T1*B**3/3.
      F2=B**2/2.-T1**2*B**4/8.
      K1=D0+D1*SIN(T0)+D2*(SIN(T0)**2)
      K7=D1*COS(T0)+D2*SIN(2.*T0)
      K8=T1*(2.*D2*COS(2.*T0)-D1*SIN(T0))
      K9=T1**2*(D1/2.*COS(T0)+D2*2.*SIN(2.*T0))

      K10=T1**3*(D1/6.*SIN(T0)-4.*D2/3.*COS(2.*T0))
      K11=T1**4*(D1/24.*COS(T0)+2.*D2/3.*SIN(2.*T0))
      K2=K7*T1
      K3=K8*T1/2.
      K4=K9*T1/3.
      K5=K10*T1/4.
      K6=K11*T1/5.
      K12=T1**5.*(4.*D2/15.*COS(2.*T0)-D1*SIN(T0)/120.)
      K13=D2*COS(T0)**2
      K14=D2*SIN(2.*T0)*T1
      K15=D2*COS(2.*T0)*T1**2
      K16=2./3.*D2*SIN(2.*T0)*T1**3
      K17=D2/3.*COS(2.*T0)*T1**4
      K18=2.*D2/15.*SIN(2.*T0)*T1**5
      G1=K13/2.-K14/3.-K15/4.+K16/5.+K17/6.-K18/7.
   54 K=K+1
      C2=M*A1*B2/2.-M*A0*B1-M/2.*B1*A2
      C3=A1**2/2.+B1**2/2.+2.*A2**2+2.*B2**2
      F3=M*M/2.*A0*A0+.375*M*M*A1*A1+.125*M*M*B1*B1-M*M/2.*A0*A2

      AA=-G1+K13/8.*M**2+A*(F1*SIN(T0)+COS(T0)*(F2-M**2/8.)
     *  -CL/8./A*(M*(1.-M/2.))**2)
      BB=-(G1*M*A1-3.*K13/16.*M**3*A1+K7/3.+K8/4.-K9/5.
     *  +K10/6.+K11/7.+K12/8.)-M**3*((K7-A*SIN(T0))/28.27
     *  -(A1*0.1875*(A*COS(T0)))-CD/28.27*(1.-M/2.))
     *  +SIN(T0)*A*(F1*M*A1+B**3/3.-B**5*T1**2/10.)
     *  +COS(T0)*A*(B**4*T1/4.-B**6*T1**3/36.+F2*M*A1)
     *  -K8*M**4/64.
      CC=A*SIN(T0)*(F1*F3+B2*(M*B)**2/8.-C2/4.*T1*B**4
     *  -C3/5.*T1*B**5)+A*COS(T0)*(F2*F3+M**2*B2*B**3*T1/12.
     *  +C2*B**3/3.+C3*(B**4/4.-T1**2*B**6/12.))-2.*CQS
     *  -(F3*G1-M**4*(K13/32.*A0**2+K1/64.+CD/128.)
     *  +K1/4.+K2/5.+K3/6.-K4/7.+K5/8.+K6/9.
     *  +M**2*(K1/4.+K2/6.+K3/8.-K4/10.+K5/12.+K6/14.)
     *  +M**2*B2*(K7/8.+K8/12.-K9/16.+K10/20.+K11/24.+K12/28.)
     *  +C2*(K13/3.-K14/4.-K15/5.+K16/6.+K17/7.-K18/8.)
     *  +C3*(K13/4.-K14/5.-K15/6. +K16/7.+K17/8.-K18/9.))

C     SOLVING FOR LAMBDA VALUES

C     THIS PART WAS MODIFIED TO GET ONLY POSITIVE VALUES OF LAMBDA AND
C     IN THE CASE THAT BOTH VALUES ARE POSITIVE GET THE RESULTS FOR BOTH
C     VALUES OF LAMBDA. (A. JABBARZADEH 18.3.93)
```

```
      IF((BB**2-4.*AA*CC).LT.0.0)GOTO 1000
      L1=SQRT(BB**2-4.*AA*CC)
      L2=(L1+BB)/((-2.)*AA)
      L1=(L1-BB)/(2.*AA)
      IF((L1.LT.0.0).AND.(L2.LT.0.0))GOTO 1000
      L=L1
      IF (L.LT.0.0) L=L2
      ERR= ABS(L-LH)
      IF ((ERR).LT.0.000001)GO TO 70
      LH=L
      IF(K-20)24,24,65
C     COMPARE THE RESULTS TO BE IN THE RANGE OF NONSTALL LIMIT.(αr.4,1<13)
   70 AR4=(2.5*L+T0+(0.4+M)*T1+(1.+2.5*M)*A1)*CV
      AR1=(L+T0+(1.+M)*T1+(1.+M)*A1)*CV
      IF(((AR4.LT.AL).AND.(AR1.LT.AL)).AND.((ABS(AR4-AL).LT.0.25).OR.
     *(ABS(AR1-AL).LT.0.25)))THEN
      IF(KLID.EQ.1)GOTO 24
      IF(KLID.EQ.0)GOTO 64
      ENDIF
      GOTO 1000
C     ITERATING FOR VALUES OF A0,A1,B1,A2,B2
C     Corrections to ao to b2 inserted 4/11/91

   24 N=N+1
      A0=GA/2.*(COS(T0)*(B**3*L/3.+M*M/8.*B2*B*B
     *  +0.0398*L*M**3+0.033*A1*M**4+T1*(B**5/5.+M*M/6.*B**3)
     *  -T1*T1/2.*B**5/5.*L-T1**3/42.*B**7)
     *  +SIN(T0)*(B**4/4.+(B*M)**2/4.-M**4/64.
     *  -T1*(L*B**4/4.+L*M**4/64.)
     *  -T1*T1/4.*(B**6/3.+B**4*M*M/4.)+T1**3/36.*B**6*L
     *  +T1**4/192.*B**8.)+CL*M**4./A/128.
     *  +L*L*M*M/A/8.*CD*(1.-M/2.)**2
     *  +0.0398/A*M**3*L*CL*(1.-M/2.)+0.0199/A*L*
     *  (1.-M/2.)*M**3*CD)
      B1=(COS(T0)*(M*B**5/10.*A0*T1*T1-M*B**3*A2/6.
     *  -0.05*A2*M**4-M*B**3*A0/3.)
     *  -SIN(T0)*T1*(M*B**4*A2/8.-M*B**4/4.*A0))
     *  /(SIN(T0)*(T1*B**5/5.+T1*M*M*B**3/12.
     *  -T1**3*B**7/42.)-COS(T0)*(B**4/4.
     *  +M*M*B*B/8.-T1**2/12.*B**6))
      A1=(SIN(T0)*(M*B**3*2./3.+0.0265*M**4
     *  -T1*(M*L*B**3/3.-M*B2*B**4/8.-0.0265*L*M**4)
     *  -T1*T1/5.*M*B**5)+COS(T0)*(M*L*B*B/2.
     *  -M*B**3*B2/6.-L*M**3/16.+T1*M*B**4/2.
     *  -T1*T1/8.*M*L*B**4-T1**3/18.*M*B**6)
     *  -0.01325*M**4*CL/A-0.2123*L*L*(M*(1.-M/2.))
     *  **2*CD/A-L*M**3/16.*(1.-M/2.)*CL/A-L*(1.-M/2.)
     *  /32.*M**3*CD/A)/(SIN(T0)*(M*M*T1*B**3/12.-T1*B**5/5.
     *  +T1**3*(B**7/42.-M*M*B**5/120.))
     *  +COS(T0)*(B**4/4.-(M*B)**2/8.+M**4/32.+T1*T1/2.
     *  *(M*M*B**4/16.-B**6/6.)+T1**4*B**8/192.))
      B2=GA/6.*(COS(T0)*(M*B**3*B1/3.-M*M*A0*B*B/4.
     *  -A2*B**4/2.+A2/16.*M**4+T1*T1/2.*(M*B**5/5.
     *  *B1-A2*B**6/3.))-SIN(T0)*(T1*(M*B1*B**4/4.
     *  -M*M*A0*B**3/6.-0.4*A2*B**5)))
      A2=GA/6.*(SIN(T0)*(M**4/64.-(M*B/2.)**2
```

```
     *   -T1*(M*A1*B**4/4.+2.*B2*B**5/5.)
     *   +T1*T1/16.*M*M*B**4)+COS(T0)*(M*B**3/3.*A1
     *   +B**4*B2/2.+0.0265*L*M**3+0.015*A1*M**4
     *   -T1*M*M/6.*B**3-T1*T1/2.*(M*B**5/5.*A1
     *   +B**6/3.*B2))-M**4*CL/128./A
     *   -CD/8./A*(L*M*(1.-M/2.))**2+0.0265/A*M**3*L*CL
     *   *(1.-M/2.)+0.01327/A*L*(1.-M/2.)*M**3*CD)
      IF(KLID.EQ.1)GOTO 64
      IF(ABS(A0-A0H).LT.0.000001) GOTO 54
      A0H=A0
      A1H=A1
      B1H=B1
      A2H=A2
      B2H=B2
      GOTO 24
C     CALCULATION OF THRUST COEFFICIENT,CONTROL AXIS
C     ANGLE AND WINDMILL PARAMETERS.

   64 TCTSA=SIN(T0)*(B**3/3.+M*M*B/2.-.07073*M**3
     *     -T1*(L*B**3/3.+0.03537*L*M**3)
     *     -T1*T1*(B**5/10.+M*M*B**3/12.)
     *     +T1**3*L*B**5/30.+T1**4*B**7/168.)
     *     +COS(T0)*(L*B*B/2.+M*M*B2*B/4.
     *     +M*M*L/8.+M**3*A1/16.+T1*(B**4/4.
     *     +M*M*B*B/4.-M**4/64.)+T1*T1*(M**4*L/128.
     *     -L*B**4/8.)-T1**3*(B**6/36.+M*M*B**4/48.))
     *     +CL/A*(M*M/8.*L*(1.-M/2.)+M**3/28.27)
     *     +CD/A*(M*L*L/3.142*(1.-M/2.)
     *     +M*M*L/16.)*(1.-M/2.)
      CT=TCTSA/2.*S*A
      AC=ATAN(L/M+CT/2./M/(SQRT(M*M+L*L)))
      ACD(I)=AC*CV
      A1D=A1*CV
      CQ=CQS*S

C     CALCULATION OF WINDMILL PARAMETRS
      TSR=COS(AC)/M
      CPW(I)=2.*CQ*TSR**3
      CTW=2.*CT*TSR**2
      CLW(I)=CTW*COS(A1+AC)
      COPT(I)=CLW(I)*CPW(I)
      CLWOP(I)=CLW(I)*(1.-(TAN(AC+A1))*TAN(BETA))
      ALCA1D(I)=ACD(I)+A1D
      P(I)=T0D
      IF(CLWOP(I).EQ.0.)THEN
      CLWOP(I)=0.000000001
      ENDIF
      SV=42.4/(CLWOP(I)*1.225)
      IF(CLWOP(I).LT.0.)GOTO 1000
      V(I)=SQRT(SV)*3.6
      WRITE(*,*)M,I,clwop(I),V(I),ACD(I)
      I=I+1
      IF(KLID.EQ.1)GOTO 1000
      IF((L1.GT.0.0).AND.(L2.GT.0.0))THEN
      KLID=1
      L=L2
```

```
      GOTO 70
      ENDIF
      GO TO 1000
 65   WRITE(6,701)T1D,T0D,ERR,K,L
 701  FORMAT(F6.2,'  ',F6.2,'  NO CONVERGENCE  ERR=',F13.9,'  K=',I5
     *,'  L=',F7.4)
      GO TO 1000
 66   WRITE(6,702)T1D,T0D
 702  FORMAT(F6.2,'  ',F6.2,'  NO REAL SOLUTION FOR LAMBDA   AA**2-4AA*C
     *C<0  K=',I4)
      GOTO 1000
 67   WRITE(6,703)T1D,T0D
 703  FORMAT(F6.2,'  ',F6.2,'  BOTH VALUES OF LAMBDA ARE NEGATIVE')
 1000 CONTINUE
C     SORTING RESULTS BASED ON THE CONTROL AXIS ANGLE VALUE
C
      DO 20 II=1,I-1
      DO 20 IJ=II+1,I-1
      IF(ACD(II).LT.ACD(IJ))THEN
      TEMP=ACD(II)
      TEMP1=V(II)
      ACD(II)=ACD(IJ)
      V(II)=V(IJ)
      ACD(IJ)=TEMP
      V(IJ)=TEMP1
      ENDIF
 20   CONTINUE
      IF(NMT.EQ.1)THEN
      WRITE(6,800)NMT,I
 800  FORMAT('title=""'/'variables=αc,V'/'Zone t="zone',I2,'",i=',I3
     *,',f=point')
      ELSE
      WRITE(6,900)NMT,I-1
 900  FORMAT('Zone t="zone',I2,'",i=',I3,',f=point')
      ENDIF
      WRITE(6,700)(ACD(I),V(I),I=1,I-1)
 700  FORMAT(F8.3,'    ',F8.3)

C     DETERMINING THE AUTOROTATIVE WIND VELOCITY AND THE COLLECTIVE
C     PITCH AND THE CONTROL AXIS ANGLE AT WHICH IT OCCURS.THE RESULTS
C     FILE NAME IS VMIN.DAT .

C     SORTING RESULTS BASED ON THE V  VALUE FROM SMALL TO GREAT

      DO 21 II=1,I-1
      DO 21 IJ=II+1,I-1
      IF(V(II).GT.V(IJ))THEN
      TEMP=ACD(II)
      TEMP1=V(II)
      TEMP2=P(II)
      ACD(II)=ACD(IJ)
      V(II)=V(IJ)
      P(II)=P(IJ)
      ACD(IJ)=TEMP
      V(IJ)=TEMP1
      P(IJ)=TEMP2
```

```
      ENDIF
21    CONTINUE
      VMAXM(NM)=V(1)
      ACM(NM)=ACD(1)
      PM(NM)=P(1)
      MM(NM)=M
3000  CONTINUE
      CLOSE(UNIT=6)
      OPEN(UNIT=6,FILE='C:\F77L\VMIN.DAT')
      NMM=NM+1
      WRITE(6,730)NMM
730   FORMAT('title=""'/'variables=M,V,'/'Zone t="zone 1",i=',I3,'
     *,f=point')

      WRITE(6,733)(MM(I),VMAXM(I),I=0,NM)
733   FORMAT(F7.3,'     ',F8.5)
      WRITE(6,737)NMM
737   FORMAT('Zone t="zone 2",i=',I3,',f=point')

      WRITE(6,734)(PM(I),VMAXM(I),I=0,NM)
734   FORMAT(F7.3,'     ',F8.5)
      WRITE(6,738)NMM
738   FORMAT('Zone t="zone 3",i=',I3,',f=point')

      WRITE(6,735)(ACM(I),VMAXM(I),I=0,NM)
735   FORMAT(F7.3,'     ',F8.5)

      CLOSE (UNIT=6)

      STOP
      END
```

UNIVERSITY OF SYDNEY LIBRARY
0000000602602714

Allbook Bindery
91 Ryedale Road
West Ryde 2114
Phone: 807 6025